

Forbedret Duktilitet av LWAC ved Bruk av Stål Fiber

Trykk

Tor Jørgen Larsen

Bygg- og miljøteknikk (2-årig)

Innlevert: juni 2014

Hovedveileder: Jan Arve Øverli, KT

Norges teknisk-naturvitenskapelige universitet
Institutt for konstruksjonsteknikk

PREFACE

This Master thesis; “Enhanced Ductility of LWAC by the Inclusion of Steel Fibres”, is the result of 20 weeks of work through the winter and spring of 2014 at the Department of Structural Engineering at the Norwegian University of Science and Technology, (Ntnu). The work carried out during the process of making this thesis have been performed by Tor Jørgen Larsen.

It was originally Kværner that several years ago were curious of the effect that steel fibre inclusion might have on the poor ductility of LWAC. Sintef and Ntnu were assigned to do the research and hence are the work and results of this thesis a consequence of the cooperation between Ntnu, Sintef and myself, Tor Jørgen Larsen.

I have found the process of making this thesis very interesting and rich in terms of more personal knowledge and understanding of the field of concrete and especially Light weight aggregate concrete. I am however left with more questions now as I am rounding of this thesis, than I was at the very beginning of the process.

During this relatively long and unison period of a Master-time I have learned to appreciate the importance of a good companionship amongst colleagues, who are eager to participate in discussions both on but most of all off topic, and would give you a pat on the back when the laboratory tests are postponed for the fourth time.

The most memorable experience from these 20 weeks are the feeling and stress relief you get from shearing a mug of really strong coffee, half a kilo of chocolate or a pizza together with good friends.

Tor Jørgen Larsen

Trondheim, 10.06.2014

AKNOWLEDGEMENTS

The research work presented in this thesis have been performed at the Department of Structural engineering at the Norwegian University of Science and Technology, (Ntnu), in Trondheim,

I would like to start by thanking my two Supervisors; Associate Professor Jan Arve Øverli and Associate Professor Håvard Nedrelid for being kind enough to take their time to give answers to all of my questions and to shear with me from their own knowledge. They have also been very helpful in the pursuit of relevant literature and have been kind enough to lend me some of their personal literature.

I have to thank Håvard in especial for being willing to participate in countless discussions, and for keeping me more or less on the right track through the process.

The laboratory work was carried out under strict supervision and by careful guidance of the laboratory crew. I have to especially thank Principal Engineer Ove Loraas, Engineer Steinar Seehuus and Principal Engineer Gøran Loraas for taking their valuable time to help me with my work and for offering good guidance. Not only where they helpfull with the practical work, but they were also kind enough to shear with me from their experiences and knowledge and were more than willing to endure in discussion.

This thesis have been performed in cooperation with Sintef as well,

I would hence like to thank Helge Braa for being the involved supervisor from Sintef, shearing his knowledge and experience with me.

I would also like to thank Gunnrid Kjellmark, from Sintef for being very helpful with determining the composition of the matrixes.

Two separate groups were performing the exact same tests, one of whom was I. Because of practicalities were all laboratory work done in cooperation with the other group.

The other group contained of Daniel Jettli and Gøran Sæther. I am of great gratitude towards the members of the other group for being helpful and willing to share their knowledge and experiences with me.

Last but not least, I have to thank Bendik Male Kolberg, Fredrik Jenseg Eriksen, Kenth Daniel Solheim and Olav Kristoffer Mork, my office companions, for all motivation, computer guidance, discussion of hypothesis and for being a great company through the past 20 weeks!

SUMMARY AND CONCLUSION

This research work has been performed as a part of the pursuit on finding the best actions to enhance the poor ductility of Light Weight Aggregate Concrete. In this specific work the effect of steel fibre inclusion have been studied.

The reason for this research to have been performed is due to the desire of improving the poor ductility for Light Weight Aggregate Concrete. Why a LWAC with enhanced mechanical behaviour would be of any interest is because of the larger scale of structures for which concrete could be applied, due to a considerable reduction of deadweight while still behaving in an adequately good mechanical manner.

To research the effect of steel fibre inclusion to LWAC there were performed uniaxial compression tests on LWAC prisms with different dosages of fibres, both in centric and eccentric compression. Similar tests on NDC prisms were also performed, while mostly for the purpose of comparison between the different behaviour from the two concrete types.

The eccentric compression tests were performed so that it would be possible to also study the effect of steel fibre inclusion on a LWAC structure exposed to a strain gradient, which e.g. would be highly present in a beam or floor deck in bending.

The prisms were compressed until failure. In combination with the recorded displacements a description of the mechanical behaviour for the prisms could be established and evaluated.

From the results of the research it is obvious that the inclusion of steel fibres have a positive effect on the ductility for LWAC in compression. The effect was especially pronounced when a strain gradient was present across the prisms.

For the centric compression tests, fibres in the amount of 0,5% reported best effects, rather than the 1,0%.

For the eccentric tests however the effect of steel fibres on the mechanical behaviour proved to be improving with increasing amount of fibres.

SAMMENDRAG OG KONKLUSJON

Dette arbeidet har blitt gjort er en del av jakten på å finne de beste handlingene for å forbedre den dårlige duktiliteten til betong med lett-tilslag. I dette spesifikke arbeidet har effekten av å tilsette stålfibrer blitt undersøkt.

Grunnen til at dette arbeidet har blitt gjennomført er på grunn av ønsket om å forbedre den dårlige duktiliteten til betong med lett-tilslag. Hvorfor betong med lett-tilslag med forbedrede mekaniske egenskaper er av interesse er på grunn av en større mengde konstruksjoner for hvor betong kunne bli benyttet på grunn av en ganske mye lettere egenvekt, samtidig som styrken og de mekaniske egenskapene var gode.

For å undersøke effekten av stål fiber i betong med lett-tilslag ble det gjennomført enaksielle trykkteste tester på prismer av betong med lett-tilslag med forskjellige doser av stål fibrer, både under sentrisk og eksentrisk trykk. Det ble også gjort like tester på prismer av normal betong, men det var mer av et formål for sammenligning av mekanisk oppførsel mellom de to betongtypene.

Den eksentriske trykktesten ble gjennomført for å se på effekten av stål fibrer på betong med lett-tilslag under trykk, men som samtidig er påvirket av en tøyning gradient, som vil være aktuelt i bjelker og gulv under bøyning.

Prismene ble komprimert helt til brudd. I kombinasjon med de målte forskyvningene kunne en beskrivelse av den mekaniske oppførselen under trykk bli etablert og vurdert.

Ut ifra resultatene funne gjennom arbeidet er det helt klart at stål fibrer har en positiv effekt på duktiliteten til betong med lett-tilslag under trykk. Spesielt var effekten av stålfibrer veldig bra for testene påvirket av en tøyning gradient.

Fra de sentriske trykktestene ble det erfart at stålfibrer ved en mengde på 0,5% har større positiv effekt på forbedringen av de mekaniske egenskapene for betong av lett-tilslag enn stålfibrer ved en mengde på 1,0%.

For de eksentriske testene viste det seg at effekten av forbedrede mekaniske egenskaper var stigende med stigende grad av stålfibre.

Table of Contents

PREFACE.....	I
AKNOWLEDGEMENTS.....	III
SUMMARY AND CONCLUSION.....	V
SAMMENDRAG OG KONKLUSJON.....	VII
TABLE OF CONTENTS.....	X
LIST OF FIGURES.....	XII
1.1 LIST OF TABLES.....	XIV
1 INTRODUCTION.....	2
1.1 GENERAL.....	2
1.2 OBJECTIVES OF STUDY.....	3
1.3 OUTLINES OF THE THESIS.....	4
1.4 LIMITATIONS.....	5
2 THEORY STUDIES.....	6
2.1 INTRODUCTION.....	6
2.2 NORMAL DENSITY CONCRETE.....	6
2.3 LIGHTWEIGHT AGGREGATE CONCRETE.....	8
2.3.1 <i>Fundamental understanding of Lightweight Aggregate Concrete</i>	8
2.3.2 <i>Light Weight Aggregate</i>	9
2.3.3 <i>Brittleness in LWAC</i>	11
2.3.4 <i>Steel fibre induction</i>	12
2.3.5 <i>Strain gradient</i>	15
2.3.6 <i>Failure mechanisms</i>	16
2.3.7 <i>Rotation capacity</i>	18
2.3.8 <i>Size and boundary effects</i>	18
3 PREPARING WORK FOR LABORATORY TEST.....	20
3.1 INTRODUCTION.....	20

3.2	MATERIALS	21
3.2.1	Concrete matrixes.....	21
3.2.2	Aggregates.....	22
3.2.3	Cement.....	24
3.2.4	Additive materials.....	24
3.2.5	Steel fibres.....	25
3.2.6	Superplasticizer.....	25
3.3	PHYSICAL SIZE AND GEOMETRY	26
3.4	FORMWORK AND CONCRETE CASTING	27
3.5	PREPARATION OF TEST SPECIMEN	30
3.6	TEST MACHINE AND TEST SETUP.....	31
3.7	RECORDING OF TEST RESULTS	32
4	TEST RESULTS.....	38
4.1	INTRODUCTION.....	38
4.2	CYLINDER COMPRESSION TESTS.....	38
4.3	PRISM TESTS	40
4.3.1	Age at testing.....	40
4.3.2	Introduction to diagrams	40
4.3.3	Stress - Strain and Load – Strain diagrams for LWAC prisms in compression.....	44
4.3.4	Diagrams for NDC prisms in compression.....	47
4.3.5	Comments on the prism test results.....	50
5	DISCUSSION OF RESULTS	68
5.1	LWAC PRISMS IN CENTRIC COMPRESSION	68
5.2	LWAC PRISMS IN ECCENTRIC COMPRESSION.....	72
5.3	NDC PRISMS IN CENTRIC COMPRESSION.....	74
5.4	NDC PRISMS IN ECCENTRIC COMPRESSION	74
5.5	GENERAL OBSERVATIONS.....	75
6	CONCLUSION AND SUGGESTION TO FURTHER WORK.....	80
6.1	CONCLUSION	80
6.2	SUGGESTION TO FURTHER WORK.....	81
7	SITERTE VERK.....	84
A.	APPENDIX WATER ABSORPTION OF AGGREGATE	89
B.	APPENDIX MATRIXES	95
C.	APPENDIX TEST RESULTS.....	120

LIST OF FIGURES

Figure 2.1	Microcrack initiation at Aggregates, Figure inspired by Markeseth [25]	7
Figure 2.2	LECA aggregate.....	9
Figure 2.3	Brittleness failure in column.....	11
Figure 2.4	Toughness and Ductility.....	14
Figure 2.5	Failure modes. Shear failure due to forming of shear band to the left, and failure due to lateral expansion to the right.....	17
<i>Figure 3.1</i>	<i>Dramix 65/60</i>	25
Figure 3.2	Prism dimensions in 3-Dimensional perspective	26
Figure 3.3	Formwork for prisms and cylinders.....	28
<i>Figure 3.4</i>	<i>Cone for workability measuring</i>	29
<i>Figure 3.5</i>	<i>Casting of unreinforced LWAC prisms and cylinders</i>	29
<i>Figure 3.6</i>	<i>Compression device</i>	32
<i>Figure 3.7</i>	<i>Spherical ball bearing</i>	32
<i>Figure 3.8</i>	<i>Eccentricity at bottom</i>	33
<i>Figure 3.9</i>	<i>Eccentricity at top</i>	33
Figure 3.10	Eccentrically and eccentrically prism set up.....	34
Figure 3.11	Location of LVDTs. The drawing to the left shows the prism from south side, the drawing to the right shows the prism from the top. “1” refers to the vertical 30cm LVDT, “2” refers to the vertical 20cm LVDT and “3” refers to the transversal LVDT	35
<i>Figure 3.12</i>	<i>Location of LVDTs on North face</i>	35
Figure 4.1	Stress-strain relationships for centrally compressed LWAC prisms without any steel fibres per volume fraction	44
Figure 4.2	Load-strain relationships for eccentrically compressed LWAC prisms containing 0,0% steel fibres per volume fraction.....	44
Figure 4.3	Stress-strain relationships for centrally compressed LWAC prisms containing 0,5% steel fibres per volume fraction.....	45

Figure 4.4	Load-strain relationships for eccentrically compressed LWAC prisms containing 0,5% steel fibres per volume fraction.....	45
Figure 4.5	Stress-strain relationships for centrally compressed LWAC prism containing 1,0% steel fibres per volume fraction.....	46
Figure 4.6	Load-strain relationships for eccentrically compressed LWAC prisms containing 1,0% steel fibres per volume fraction.....	46
Figure 4.7	Load-strain relationships for one eccentrically compressed NDC prism containing 0,0% steel fibres per volume fraction.....	47
Figure 4.8	Stress-strain relationships for one centrally compressed NDC prism containing 0,5% steel fibres per volume fraction.....	48
Figure 4.9	Load-strain relationships for eccentrically compressed NDC prisms containing 0,5% steel fibres per volume fraction.....	48
Figure 4.10	Load-strain relationships for eccentrically compressed NDC prisms containing 1,0% steel fibres per volume fraction.....	49
Figure 4.11	Young's Modulus for the centrally compressed LWAC prism B2 with 1,0% steel fibres per volume fraction.....	53
Figure 4.12	Poisson's Ratio for the centrally compressed LWAC B1 prism with 0,5% steel fibres per volume fraction.....	54
Figure 4.13	LWAC 0,0% B2 centric	55
Figure 4.14	LWAC 0,0% B1 centric	55
Figure 4.15	LWAC 0,5% B2 centric, South and East face.....	56
Figure 4.16	LWAC 0,5% B1 centric, Close up of shear band on North face.....	56
Figure 4.17	<i>LWAC 0,0% B3 eccentric, North face</i>	<i>59</i>
Figure 4.18	<i>LWAC 0,0% B4 eccentric, North and West face.....</i>	<i>59</i>
Figure 4.19	<i>LWAC 0,5% B4 eccentric, East and North face.....</i>	<i>60</i>
Figure 4.20	<i>LWAC 0,5% B4 eccentric, West face</i>	<i>60</i>
Figure 4.21	<i>LWAC 1,0% B4 eccentric, West face</i>	<i>60</i>
Figure 4.22	<i>LWAC 1,0% B3 eccentric, North and West face.....</i>	<i>60</i>
Figure 4.23	NDC 0,0% B3 eccentric, Fraction of the prisms.....	66
Figure 4.24	NDC 1,0% B4 eccentric, West face.....	66
Figure 4.25	NDC 1,0% B4 eccentric, North and West face	66
Figure 4.26	NDC 0,0% B3 eccentric, Fraction of prism.....	66

LIST OF TABLES

Table 3.1	Number of different prisms	20
Table 3.2	Number of different beams.....	21
Table 3.3	Number of different cylinders	21
Table 3.4	Constituents of different matrixes	22
Table 3.5	Particle density, stored humidity and water absorption for different ag.....	24
Table 3.6	Physical dimensions of different structures	27
Table 3.7	Mixing order	28
Table 3.8	Sink Value, Slump Value, Air content and Density.....	29
Table 3.9	Time of casting.....	30
Table 4.1	Height, weight, and cylinder compression strength f_{cp} for LWAC cylinders. (All cylinders ¹ were tested at approximately 58 days of age after casting)	39
Table 4.2	Height , weight, and cylinder compression strength f_{cp} for NDC cylinders. (All cylinders ¹ were tested at approximately 72 days of age after casting)	39
Table 4.3	Concrete age at prism testing [days].....	40
Table 4.4	Maximum load P_{max} , prism compression strength f_{cp} and load at failure P_{fail} for LWAC prisms in centric compression	51
Table 4.5	Longitudinal ϵ_l - and cross sectional ϵ_c strains at peak stress and at failure, plus change of strains from peak state to failure for LWAC prisms in centric compression	51
Table 4.6	Final averaged values of maximum load P_{max} , load at failure P_{fail} , prism compression strength f_{cp} , longitudinal strain at peak load ϵ_{lpeak} and longitudinal strain at failure ϵ_{lfail} for LWAC prisms in centric compression	52
Table 4.7	Maximum load P_{max} and load at failure P_{fail} for each LWAC prism in eccentric compression	57
Table 4.8	Final averaged values for maximum load P_{max} , load at failure P_{fail} and change of load from peak state to failure P_{change} , for LWAC prisms in eccentric compression.....	57
Table 4.9	Final averaged strains for LWAC Prisms in Eccentric Compression	58
Table 4.10	Maximum load P_{max} , prism compression strength f_{cp} and load at failure P_{fail} for NDC prisms in centric compression.....	61

Table 4.11	Longitudinal ϵ_l and cross sectional ϵ_c strains at peak stress and at failure, plus change of strains ϵ_{change} from state of maximum load to failure, for NDC prisms in centric compression	62
Table 4.12	Maximum load P_{max} and load at failure P_{fail} for each NDC prism in eccentric compression	63
Table 4.13	Final averaged values for maximum load P_{max} , load at failure P_{fail} and change in load from peak state to failure P_{change} , for NDC prisms in eccentric compression	63
Table 4.14	Averaged strains for NDC Prisms in Eccentric loading	64

2

1 Introduction

1.1 General

Concrete is roughly put a composite material composed of sand, coarse granular materials, cement and water. When the different constituents are mixed together, water and cement react and turn into a strong glue which ties the different components of the matrix together in moulds of desired shape and size.

The use of concrete goes long back. Both the Egyptians (3000 BC), the Chinese and the Greeks (800BC) all made use of cementitious materials. The Ancient Romans were the first large-scale users of concrete technology. Their concrete was made from quicklime, pozzolana and aggregates of pumice. In the years between 300 BC and 476 AD they built concrete structures such as the Colloseum, Pantheon and the aqueducts. [1]

After the fall of the Roman Empire the use of concrete was greatly reduced until the technique was all forgotten between 500 AD and the 1300s. From the 12th century and up till the 1700s the concrete gradually returned as a construction material. A method of producing Portland cement was patented by Joseph Aspin in 1824 and the first reinforced concrete structure were made in 1849.

Today, concrete is often the building material of choice. In fact twice as much concrete, ton for ton, is used in construction around the world than the total of all other building materials, including wood, steel, plastic and aluminum. [2]

Despite the great use, normal density concrete (NDC) has a large disadvantage. Compared to for instance steel, NDC has a low strength-to-weight ratio which makes it less appropriate for use in e.g. tall buildings, long-span bridges, long span roofs/floors etc. For cases like this it is therefore still preferable to use steel instead of concrete.

However, there is to a certain degree possible to improve the poor strength-to-weight ratio for NDC. One option is to increase the concrete strength, making it a so-called high-strength concrete (HSC). Another way to improve the strength-to-weight ratio is to

reduce the density of the concrete. The weight reduction is accomplished by making use of lighter aggregates instead of, or combined with, ordinary aggregates used in NDC. This lighter concrete is called a lightweight aggregate concrete (LWAC).

A third alternative is to combine the two options mentioned above, making a high-strength lightweight aggregate concrete (HSLWAC).

In hardened ordinary concrete the volume of the aggregate is typically about 70%. The remaining 30% is hardened cement paste, pores and water.

For fully utilization of the cement, the lowest water-cement ratio needed is according to theory 0,25. In practice however, to ensure that all of the cement particles will react it is therefore necessary to use some more water than what is theoretically needed. The excess water that does not react with cement will evaporate during hardening, leaving behind pores. The pores in the cement paste weaken the concrete strength and are seen as a direct correlation to the water-cement ratio. More water gives a higher water-cement ratio and more pores, which results in a lower concrete strength.

For normal strength concrete with any density the water-cement ratio is typically from 0.40 to 0.60. High strength concrete however, have reportedly been made with a water-cement ratio as low as 0.21, achieved by making use of water reducing chemical admixtures [3].

1.2 Objectives of study

The main objective of this thesis has been to confirm theory on the field of improved ductility of lightweight aggregate concrete under compression by inclusion of steel fibres.

Because of uncertainties regarding the material parameters for LWAC, numerical simulations would probably have given poor and unsatisfying results.

This Master thesis does therefore consist of two parts: theory studies and a physical test-part.

The plan was to cast a number of concrete prisms, made of both NDC and LWAC and also both with and without steel fibres. The prisms were then to be uniaxially compressed

until failure and beyond. The results from the tests should then be compared to theories on the field of steel fibre reinforced LWAC structures.

(Some of the most interesting aspects that were up for discussion were: effect of lightweight aggregates -lack of strength and change in density, confinement from steel fibres both in tension and in compression, difference in both strength and ductility with increasing dosages of fibres, strain gradient, rotational capacity, localization of forces prior to failure, different failures and shape of failure and most importantly: improved ductility.)

1.3 Outlines of the thesis

Chapter 2: A study of existing theory that is important and in relation to the research that is performed in this thesis. Such as aspects around LWAC, the effect of using steel fibre reinforcement, rotational capacity, localization of forces, shape- and size effect, crack propagation, failure shapes, improved ductility, etc.

Chapter 3: Preparation of laboratory test. (Short presentation of what is wanted and expected from the test, a working hypothesis by other means.) Thorough description of the laboratory work, taking into account: building of formwork, number of different specimens, shape and size of specimens, mixing of concrete, amounts and characteristics of constituents, time from casting until testing, test setup, the reason for why certain choices and actions are made and observations done during different stages of laboratory work.

Chapter 4: Presentation and comparing of the test results. Comments on observations done during testing and comparing of experimental behaviour and working hypothesis. Discussion of results.

Chapter 5: Discussion of test results

Chapter 6: The thesis is summarized, conclusions are drawn and suggestions for further research are made.

1.4 Limitations

In early days, one had the impression of a homogenous material with homogenous mechanical behaviour throughout an entire concrete structure. Now days, the fact that concrete does not behave homogeneously at all is a commonly shared theory.

Not only is concrete now seen as a composite material, but the mechanical behaviour of a concrete structure is rather shape- and size dependent as well. Material properties for different concrete strengths given in e.g. the Euro code, have therefore been measured and averaged for a certain geometry of concrete.

In the way the laboratory test is to be carried out and the way that the results are recorded, there is chance that if a localized zone of forces (localized failure) occurs, the localization will not be registered.

The test machine has been manually put together and adjusted. There is therefore a reasonably good reason for assuming that the machine is slightly out of the ideal position.

Not only may the recording of the test results be inaccurate, but also the upset of the testing machine and how the specimen is tested, will most certainly affect the test results in some way. Like the lack of ability to rotate when the specimen is tested eccentrically, or boundary constraints from horizontal friction forces between the concrete specimen and the testing rig.

2 Theory studies

2.1 Introduction

Concrete is by far the most used building material ton for ton around the world today. The great use of concrete reflects its versatility. However, the low strength-to-weight ratio for normal density concrete makes it less adequate for use in certain structures such as tall buildings, long span constructions, etc.

Making the strength-to-weight ratio better would result in a more versatile concrete which could be used in an even larger scale.

(In this chapter previous research and established knowledge on LWAC and related aspects that are interesting to this thesis will be studied and commented on in a best possible way)

2.2 Normal density concrete

Conventionally used concrete, also called Normal Density Concrete (NDC), has a density of about 2400kg/m^3 [4] and are basically composed of water, cement, sand and coarse, rigid aggregates. NDC has a rather poor strength-to-weight ratio compared to steel, which may prevent it from being used in certain types of structures. Nonetheless, there are several possibilities on how to make the strength-to-weight ratio better. One of which is to increase the concrete strength while keeping the same weight.

The concrete strength depends on several different factors such as: water/cement ratio, size and type of aggregate, bond strength in the mortar-aggregate interface, additives, etc. and varies from some few MPA (Low Strength Concrete, in compression), to well above 100MPA (High Strength Concrete, in compression).

The increase of strength at the same density yields a better strength-to-weight ratio, which indicates that the concrete is to a larger degree fit for use in structures where it has earlier been excluded.

However, the rise in concrete strength comes with some disadvantages. Increasing the strength of concrete yields a more brittle mechanical behaviour. The increase in brittleness can be explained by the more homogenous material behaviour, due to more similar rigidity of mortar and aggregates and also of increased bond strength between aggregates and mortar.

When a HSC-specimen is loaded in compression, the difference in internal strains of mortar and aggregate will be smaller than for medium- and low strength concrete. Hence, the forming of micro cracks around the aggregates will not take place until at a high relative load level compared to concretes of lower strength. Then, as the micro cracks initiate they will rapidly propagate to end in a sudden and brittle failure.

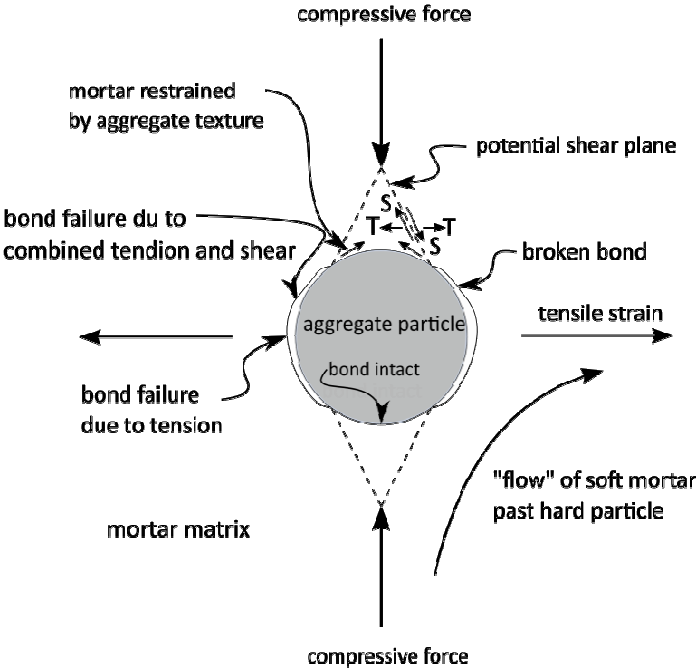


Figure 2.1 Microcrack initiation at Aggregates, Figure inspired by Markeseth [25]

For NDC exposed to uniaxial compression, the lateral tension due to the Poisson effect and the big difference in rigidity between aggregate and mortar makes microcracks occur

around in the interface between aggregate and hardened paste. For NDC with up to “medium” strength, this happens at a relative load level of about 40%.

Even if cracks occur, the concrete will not fail with no further notice. To a certain load point, loads will be carried on by the aggregates and stresses redistributed by the microcracking of concrete. The cracks will develop in length and width with increasing load, before the structure finally breaks after having endured considerable deformations.

Stress-strain relationships for concrete have been well-researched through the modern history of concrete. The research has stated that there is no such thing as a standard stress strain curve for concrete. The stress-strain behaviour of concrete is first of all dependent on whether the concrete specimen is subjected to tension- or compression, then the actual shape, size, strength and possible local weak points have a great impact on the stress-strain relation.

Nevertheless, the shape of the curves is more or less alike for the same type of concrete.

2.3 Lightweight Aggregate Concrete

2.3.1 Fundamental understanding of Lightweight Aggregate Concrete

The other way to improve the poor strength-to-weight ratio for concrete is to decrease the dead weight. The weight reduction is accomplished by making use of lightweight aggregates (LWA) as a substitute for some- or all of the coarse aggregates.

The Lightweight aggregates, like for instance Leca Pebbles, are filling out the same volume as the replaced aggregates would have done, while the weight of the LWAs are far less than for ordinary aggregates. This gives a concrete with a considerably low weight, compared to NDC.

The density of LWAC depends on multiple factors and varies over a wide range. Richard Dorf [4] states that a density of about 1700kg/m³ is quite common for LWAC.

The lighter concrete will be beneficial for use in several situations where NDC have proved to be too heavy. However, just as for HSC the mechanical behaviour of the LWAC

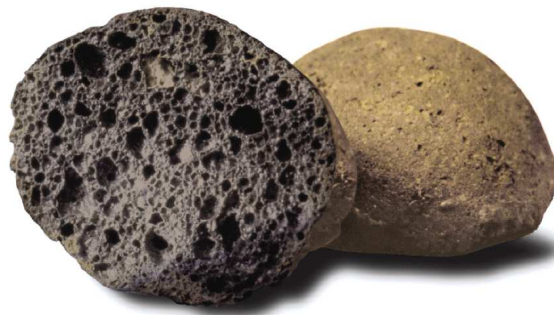
has shown to be very brittle, preventing it from utilizing its potential as a lighter, but still strong material.

Researchers have showed that inclusion of fibres into LWAC is an appropriate solution to overcome some of the brittleness problems. [5], [6]. (Failure mode) fraction goes through aggregates, most likely)

2.3.2 Light Weight Aggregate

Lightweight aggregates are pellets with lower weight, lower strength and lower rigidity compared to ordinary aggregates. There are several different types of LWAs. Some come naturally from the nature, while others have to be processed. (LWAs are different in size, shape, density, rigidity, etc. just like conventional aggregates. This yields different material behaviour for the different aggregates.)

The LWAs used in this thesis are LECA pellets. LECA = Lightweight expanded clay aggregate. LECA pellets are a pure natural recourse produced of expanded clay and burned in a rotary furnace at about 1200°C. The pellets come out in sizes between 0-32mm and are sorted in different fractions [7].



*Figure 2.2 LECA aggregate.
Picture copied from Wikipedia*

Conventionally used aggregates, like for instance pebbles of quartz or granite, have a high rigidity and compression strength, ranging well above most hardened cement paste.

The high porosity of the LWAs leads to a great reduction in the compression capacity and rigidity compared to ordinary aggregates.

Not only is there a difference in the compressive capacity and rigidity between different aggregates, but the shape of the aggregates play a rather big role in the concrete behaviour as well. A more edgy and rough aggregate surface will to a certain level prevent the aggregates from “slipping” relative to the mortar, ensuring better structural results. This slip is called “bond slipping”. The round shape of the Leca aggregates should therefore indicate that it would slip relatively easy. However, the great porosity and the porous surface of the Leca pellets allow the cement paste to “penetrate” into aggregates, making the transition zone between paste and aggregate more or less not-existing. In addition to that, the LWAs have a pretty similar rigidity as the mortar, thus there will not be no considerable difference in strains over the aggregate-mortar intersection. The LWAs will therefore probably not slip relative to the mortar.

No bond slipping leads to no micro cracks, which again leads to a sudden and brittle failure due the very homogenous composite.

2.3.3 Brittleness in LWAC

Even though concrete is by far the most used building material around the world, it is known to be a brittle material. What characterises a brittle material is the absent ability to redistribute high local stresses. This redistribution of stresses in concrete is due to microcracking [8]. The lack of ability to redistribute local stresses, or the lack of ability to absorb energy during loading, will lead to a sudden and explosive failure [9].

As mentioned, by increasing the strength of NDC, the already brittle concrete becomes even more brittle [10] [6, p. 453]. The same increase in brittleness is experienced for LWAC and is the reason to why it has not been used in a larger scale in structures with a certain demand to ductile mechanical properties.

The reason to why the LWAC is more brittle than NDC can be explained by the more homogenous concrete behaviour. The reason to the more homogenous material behaviour is at least twofold. 1: Relatively little difference in rigidity of mortar and aggregates. 2: Improved bond strength between aggregates and mortar caused by cement paste penetrating into the LWA. [8]



Figure 2.3 Brittleness failure in column.

Picture have been copied from The University of Michigan's website [47]

For the sake of LWAC in uniaxial compression, the much more homogenous material behaviour and the improved bond strength leads to reduced tendency of microcracking

at an early stage. In fact, researches have shown that the occurrence of microcracks will not happen before at a relative load level of close to 90%. This homogenous material behaviour can be seen from the linear shape of the stress-strain curve of LWAC. The late occurrence of microcracks for LWAC results in a more sudden failure, due to the reduced ability to redistribute stresses.

2.3.4 Steel fibre induction

2.3.4.1 Fibres

LWAC behaves in a very brittle manner when compressed, which has prevented it from being used for certain structural purposes. To improve the poor material behaviour of LWAC, considerable work on the effect of fibre inclusion into concrete has been performed.

Fibres are categorized as polymeric, natural and metallic. [11] Tests on different fibres in material, shape and size have been performed to find the combination that yields the best effect. The type of fibre used and the amount of it has shown to have a great impact on the behaviour of fibre reinforced concrete.

Both for the sake of NDC and LWAC steel fibres have been reported to give the best improvement of ductility [6].

Fibre reinforced structures are classified by their fibre volume fraction. Less than 1% fibre volume fraction = low, 1-2% fibre volume fraction = medium, and above 2% fibre volume fraction = high. [12].

The fibres don't affect on the mechanical behaviour until cracks are forming. Due to the typical linearity of the stress-strain curve of most LWACs, Domagala et al. [13] [14] showed that the initiation of cracking does not happen until the relative compressive load level approaches about 90%. As soon as the microcracks have appeared the fibres prevents the crack from further propagation, and act as a load carrier across the cracks. Due to the fibres, the cracks are slimmer in width, while the number of cracks is larger.

2.3.4.2 Workability

The inclusion of steel fibres to improve the engineering properties of LWAC does not only affect the concrete in a positive manner. For certain concrete-casting situations it is

crucial that the concrete has the ability to fill out the entire formwork and to fully enclose around the ordinary reinforcement as required, without the use of a vibration tool. It is therefore essential that the concrete has a good slump value. The slump value is a measure of workability and the ability for the concrete to be self compacting. Even for a quite low volume fraction of steel fibres added to the LWAC under mixing, the workability of the fresh concrete gets poorer [13]. The work of e.g. Topcu et al. [15] and Koksall et al. [16] shows a remarkable decrease in workability for increasing fibre volume fraction. The decrease in workability for the fresh concrete depends on the type and volume of the fibre used, where steel fibres have a reportedly particular negative impact. One way to ensure an acceptable level of workability for fibre reinforced concrete, is to make use of superplasticizers. The superplasticizer increases the workability and also reduces the effect of balling for high dosages of fibres. [17]. Campione et al. [18] reported good workability for their fresh steel fibre reinforced LWACs with fibre volume fraction of up to 2%, fibre length of 30mm and aspect ratio of 60, by adding 1,5% superplasticizer by cement weight.

Another aspect to consider is the “floating” of coarse lightweight aggregates and “sinking” of the heavier mortar and ordinary aggregates within the concrete mix for the LWACs with high slump values. ACI 213R-87 [19] therefore suggests a maximum slump value of 100mm to obtain an even mix for LWAC.

In the other end of the scale, Mehta and Monterio [12] have reported that LWACs with slump values between 50-75mm should have sufficiently good workability.

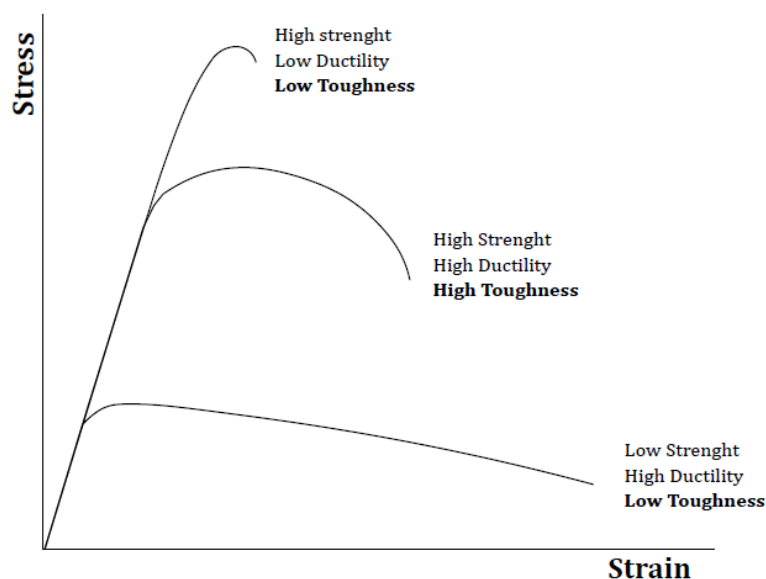
2.3.4.3 Confinement

It is mainly the enhanced confinement, due to steel fibre inclusion that is the reason to the improved mechanical behaviour for LWAC. The increased confinement has several different effects on the concrete: Enhanced confinement will prevent the outer most concrete of ordinary reinforced members from spalling at loads approaching peak load. Another effect of increased confinement is that the fibres ensure a better correlation between concrete and the reinforcement [20]. In the special case of LWAC, the inclusion of steel fibre reinforcement has some other more important and pronounced effects on the material behaviour. Improved flexural strength, ductility and toughness is some of the most important effects.

2.3.4.4 Ductility, Toughness and flexural stiffness

A great deal of work has been done in the mission on improving the structural behaviour of LWAC. The researches have reported on enhanced compressive strength, larger strains at peak load and larger tensile splitting strength, by adding fibres in small volume fractions to the LWAC. [21] [20]. More importantly, the studies have shown that the inclusion of steel fibres have led to improved ductility, toughness and flexural strength.

Ductility is described as the ability to sustain considerable inelastic deformations, both prior to maximum load, but most of all in the postpeak region, without a significant drop in load bearing capacity [22]. Toughness however, is the ability of a specimen to carry high loads even if it is cracked. Expressed in other words; the ability of a material to absorb energy and plastically deform without fracturing. [23] The two phenomenon toughness and ductility are as can be seen closely related and have often been confusingly mixed about each other.



*Figure 2.4 Toughness and Ductility
Inspired by picture from etomica.org*

The figure may possibly describe the difference between toughness and ductility in a good and manner. Nonetheless, this thesis is mostly focusing on the ductility, due to the impact that improved ductility will have on the use of LWAC.

Because of the focus on compressive strength of concrete, researchers are using the stress-strain curves for concrete in compression and the ratio of elastic and inelastic strains at ultimate strain, to define the ductility D_c . [22] [8],

$$D_c = \frac{\epsilon_u - \epsilon_c}{\epsilon_c} = \frac{\epsilon_{pl}}{\epsilon_c}$$

where ϵ_u is the ultimate strain, ϵ_c is the elastic strain and ϵ_{pl} is the inelastic strain. Toughness however is the sum of the absorbed energy through loading, and are estimated as the sum of the area under the stress – strain curve. [23] [20]. Mehta and Monterio [12] claimed that the greatest advantage of making use of steel fibres in concrete were the great increase of flexural toughness. The research performed by Libre et al [24] showed that by adding 1% volume fraction of fibre into LWAC, the toughness got 78 times better, while the flexural strength got three times better. Øverli and Jensen [22] reported a great improvement of ductility for LWAC by addig steel fibres in 1% fibre volume fraction. The results from e.g. Øverli and Jensen [22] and [20] proved that the sought-for improved ductility, led to some important enhancements on the mechanical behaviour for LWACs: Considerable improvement in impact strength and ability to resist seismic loads, were some of the important reported positive changes that steel fibre reinforcement have on LWAC. (This has however no importance for thi thesis=

2.3.5 Strain gradient

The strain gradient affects the stress-strain curve for a specimen in loading both by increasing the compressive strength, increasing the strain and improving the ductility. Markeset [25] reported an increase in ultimate compressive stress of 10-30%, due to the effect of a strain gradient. The reason for the enhanced mechanical behaviour is due to the enhanced confinement, which partly is caused by the difference in deformation between different concrete fibres, while the other reason to the improved confinement is because of steel fibres. Nonetheless, the lateral deformation of the most stressed fibre is counteracted by less stressed fibres, causing a compressive confinement on the most stressed fibre. [25] Experimental investigations from the same Phd by Markeset [26] on

concrete prisms with eccentrically loading in compression show an increase of compressive strain in the most extreme fibre with increasing eccentricity. This gradient effect can be explained by the non-unique relationship between stress and strains on the descending branch of a stress-strain curve for concrete in compression. Schumacher [27] confirmed the work of Markeset, and said that for a higher strain gradient, the fracture zone becomes shorter and the confinement over the width increases.

2.3.6 Failure mechanisms

There are mainly two different types of failure modes for concrete in uniaxial compression, shear failure and lateral tension failure. Both failure modes can be described at several levels

Especially for NDC the heterogeneity of a specimen is basically due to two reasons: One; difference in rigidity between the mortar and aggregates, and two; uneven dispersion of different constituents. The uneven dispersion leads to a non-uniform distribution of strains over the length and width of the specimen.

Due to the heterogeneity of concrete, one point within the specimen will be the weakest, or the strains and stresses will be at its highest at this point. At this specific point, the first microcracks will initiate.

The forming of microcracks around the aggregates as bond cracks along the vertical sides of the aggregate, is due to a combination of large shear stresses and lateral tensile forces. Radial compressive stresses on the more horizontal surfaces of the aggregate prevents the bond crack from developing, only allowing intersection bond crack surfaces to slide relative to each other [25].

As the inclined bond crack faces slide relative to each other, lateral tension stresses leads to further growth of the bond cracking. At a certain load level, about 40% of peak load, the cracks will grow into the mortar. The microcracks propagate into axial and inclined macrocracks with increasing load, leading to a combined lateral tension shear band failure.

Sliding mode of failure occurs when the inclined microcracks coalesce to form incline localized shear bands.

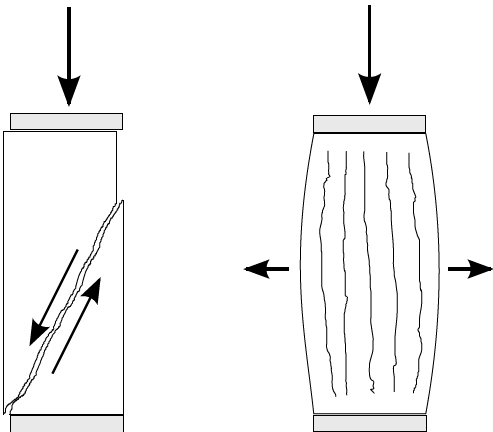


Figure 2.5 Failure modes. Shear failure due to forming of shear band to the left, and failure due to lateral expansion to the right

Tensile mode failure occurs when a critical lateral deformation is exceeded. Microcracking in Lightweight aggregate concrete does occur due to large local lateral tension stresses at the top and bottom of the aggregates. Because of the relatively low rigidity of LWAs, combined with the improved bond strength between aggregate and mortar, the microcracks of LWAC will go through the aggregate or/and the mortar, preceding the formation of a bond crack. However, the microcracks do not form until at a very high relative load level for LWAC. This is due to the increased homogeneity of the concrete, due to more similar rigidities between mortar and aggregate. However, uncertainties around the failure of LWAC are pronounced. Suggestions of that shear bands will not form due to the high tensile lateral tensions at the top and bottom of the aggregates, which might indicate that microcracks will form vertically through the aggregate, leading to a tensile splitting failure. However, if a localized shear band should form it has to be because of the aggregate interlocked by the mortar, or the frictional restraint in the shear band is smaller than for normal density concrete.

2.3.7 Rotation capacity

The rotation capacity has yet to be clearly defined in literature. However, in general, the total rotation of a specimen in loading and bending is subdivided into elastic- and plastic rotation, whereas the plastic rotation is defined as the rotation capacity. In order to the redistribution of stresses (ductility) in a loaded specimen, it is of great importance that the rotation capacity is large enough to avoid a brittle failure. The rotation capacity is influenced by a great number of different factors, to which their specific influence have been difficult to establish, due to the large scatter in experimentally derived values on the research of rotation capacity. Amongst others; Langer [28], Graubner [29] and Bigaj [30] performed specific research on the effect of different factors on the rotation capacity of reinforced concrete specimens. The results can be red in table 2.1 in the work of Schumacher [31]. According to Schumacher is not possible to state the effect of steel fibres on the rotation capacity, of an ordinary reinforced concrete member, in a straightforwardly manner [32]. That is due to the addition of steel fibres and their effect on the factors that affect the rotation capacity, may have contradictional effects. Work done by e.g. Grübl et al. [33], Bigaj-van Vliet et al. [34] and Mitchell et al. [35] shows that the improvement of ductility in compression and tension due to the inclusion of steel fibres have a positive effect on the rotation capacity for ordinary reinforced NDC members. It is necessary to mention that the research of Petra Schumacher, which this entire paragraph has been based on, has been performed on ordinary reinforced NDC, both with and without steel fibres. She also states that for structures that are only reinforced by steel fibres, the inclusion of steel fibres increases the rotation capacity due to increased ductility. Based on the brittle behaviour of LWAC, it is fairly safe to state that the effect on rotation capacity of LWAC becomes drastically better by the inclusion of steel fibres.

2.3.8 Size and boundary effects:

The shape, size and boundary conditions of a concrete member affects the mechanical behaviour for structures in compression. Comparing a cylinder of the “same” dimentions to a prism, the cylinder would yield better results in form of compression capacity than the prism. This is du the effect of more exposed edges of the prism.

The size effect have been thoroughly studied by e.g. Balendran et al. [5] have shown that the slenderness of a compressed specimen is of great influence for the post peak behaviour. For slenderness ratios above 2,0, the strength was about the same, while the curve of the descending branched varied quite a lot. [36]. The flexural strength of concrete decreases as the slenderness increases.

Kotsovos [37] claimed that concrete would lose all its load bearing capacity as soon as it had reached peak load, and that it was due to the boundary constraints that the test showed otherwise. This statement however, seem to be a little too extreme.

The work of e.g. Sangha and Dühr [36] has shown that with a slenderness above 2,5, the boundary constraints will not effect on the post peak behaviour of a member in uniaxially compression.

The size effect is more pronounced for brittle materials. This implies that the size effect should be even larger for the LWAC compared to the NDC. The size effect is however assumed to be less for the steel fibre reinforced LWAC, since this most likely has a more ductile mechanical behaviour.

3 Preparing work for laboratory test

3.1 Introduction

The objective of doing this thesis is mainly to confirm the knowledge around the effect that inclusion of steel fibre reinforcement have on the poor structural behaviour of LWAC in compression. Chapter two and three will describe the physical tests done in this thesis to complement previous research.

The main tests were performed on concrete prisms in compression until failure. Both with centric and eccentric load, both with NDC and LWAC and both with and without steel fibre reinforcement.

Table 3.1 Number of different prisms

Fibre volume fraction	NDC		LWAC	
	Centric	Eccentric	Centric	Eccentric
0,0%	2	2	2	2
0,5%	2	2	2	2
1,0%	2	2	2	2

The reason for why there were performed tests on NDC, was for the case of comparison of mechanical behaviour to LWAC. The reason for why the prisms were tested eccentrically as well as centrically was in the sake of checking out the effect of strain gradients on the specimen. In addition to prisms tests there were also casted a number of cylinders and beams with predetermined shape and size. The beams had not really nothing to do with this thesis, but were casted out of the same batches as the prisms, and were done as a favour for Terje Kanstad, which have an ongoing research on fibre reinforced concrete beams. The work performed on the beams will therefore not be further commented in this thesis.

Table 3.2 Number of different beams

Fibre volume fraction	NDC	LWAC
0,0%	-	-
0,5%	3	3
1,0%	3	3

The cylinders, which were also made by the same concretes recipes, were to be used as reference values for the measurements of prisms and beams in the sake of age of concrete at the time of testing. There were only made three cylinders each for both NDC and LWAC with 0,0% volume fraction of steel fibres. This is due to the fact that there were made no beams with steel fibre content of 0,0%. No prisms with 0,0% steel fibre reinforcement were therefore naturally not needed for comparing the strength of the beams.

Table 3.3 Number of different cylinders

Fibre volume fraction	NDC	LWAC
0,0%	3	3
0,5%	6	6
1,0%	6	6

3.2 Materials

3.2.1 Concrete matrixes

Uniaxially compression tests were supposed to be performed on LWAC- and NDC prisms, both with non- and different dosages of steel fibres included in the concrete mix. Six different matrixes were used, three of which were for NDC and the remaining three for LWAC. The matrixes used in this research had been composed and handed over by Gunrid Kjellmark from SINTEF and had proven to be adequately good for the purpose of this thesis in previous research.

The different materials used in the recipes are roughly presented in the table below:

Table 3.4 Constituents of different matrixes

Constituents [kg/m ³] ¹⁾	NDC			LWAC		
	0,0%	0,5%	1,0%	0,0%	0,5%	1,0%
NStandard FA	301,1	302,6	302,0	-	-	-
N. Standard	-	-	-	454,3	454,7	455,0
Silica Fume	30,1	30,2	20,2	45,4	45,5	45,5
Fly Ash	45,2	45,2	45,3	-	-	-
Lime Stone	-	-	-	4,5	4,5	4,5
Årdal 0-2mm	594,2	589,1	584,0	269,6	267,2	264,9
Årdal 0-8mm	1100,3	1090,8	1081,3	431,3	427,6	423,9
LECA 2-4mm	-	-	-	119,2	118,2	117,2
LECA 4-8mm	-	-	-	230,7	228,7	226,7
Silaica Damp.	0,3	0,3	0,3	-	-	-
Free Water	206,0	206,3	206,6	207,2	207,3	207,5
Abs. Water	6,7	6,6	6,6	20,7	20,4	30,1
Superplast.	4,5	4,5	4,5	8,2	8,2	8,2
Steel fibres	-	39,0	78,0	-	39,0	78,0
W/(c+s)	0,57	0,57	0,57	0,38	0,38	0,38

¹⁾The amounts given in the table are for a matrix volume of 1 m³. In the case of this work wehre each matrix should be exactly 0,1m³, the amount of the different constituents that is supposed to be used are exactly 10% of the amounts in the recipe.

The complete recipes on the matrixes, with proportioning, dosages, aggregate fractions and more, can be found in Appendix B.

3.2.2 Aggregates

Prior to the making of the concrete matrix recipes, there were performed some tests to establish the stored humidity and water absorption of the different aggregates.

It is of great importance to know the amount of water stored in the aggregates and how much water the aggregates will absorb when soaked in water, so that the exact amount of water needed to be added to obtain the wanted viscosity is known.

The procedure of the water-absorptions test is presented in Appendix A.a. while the results are presented in Table 3.5 and in Appendix A.b.

3.2.2.1 Coarse Aggregates

The coarse ordinary aggregate used in this thesis is “Årdal 0-8mm (A-3995)”. The term “coarse” does not really describe this aggregate type in an ideal way, due to the wide dispersion of different aggregate sizes within. However, the even dispersion over the entire range (0-8mm), with a dispersion module of 3,3 (Annex B) has a positive effect on e.g. the flexural strength of the hardened concrete. The compressive strength and secant modulus for the aggregates was not measured nor given, but it is assumed to range well above the values for hardened mortar. The amount of stored water, water absorption and particle density for this particular aggregate are presented in Table 3.5 and in Annex B.

3.2.2.2 Fine Aggregates/ Sand

The sand used in this work is of the type “Årdal 0-2mm (A-3726)”. The results from the stored water- and water absorption test as well as particle density for the fine aggregate are presented in Table 3.5 as well as in Annex B.

3.2.2.3 Lightweight Aggregates

LECA pellets in two different fractions, 2-4mm and 4-8mm, have been used as LWAs in this work. The LWAs replaced about 60% of the ordinary aggregates in the LWAC compared to the NDCs. The pellets of the smallest fraction have a bulk density of about 590kg/m³, while the pellets in the range of 4-8mm have a bulk density of 800kg/m³. The particle density however, is quite a bit higher, Table 3.5.

The porosity of the LWAs does not only affect the weight of the aggregates, but it also have a pronounced negative effect on the compressive strength, tensile strength and stiffness. The LECA pellets have a round and quite regular shape, with visible pores on the surfaces.

The results from the water absorption test performed on the Leac pellets can be found in Annex A.b, while other information about the LWA can be found in Annex B.

Table 3.5 Particle density, stored humidity and water absorption for different aggregates

	Årdal		LECA	
	0-2mm	0-8mm	2-4mm	4-8mm
Bulk dens. [kg/m ³]	2650	2650	380 ¹	800
Part. dens. ² [kg/m ³]	2650	2650	530	1600
Hum., storage ³ [%]	1,00	2,60	0,75	13,93
Water absorption ⁴ [%]	0,30	0,30	17,91	3,12

¹ The values given in the table for LECA are values found from the top layer of stored aggregates

² Particle density at storage

³ The humidity of the particles at storage has been calculated by comparing to oven dry particles

⁴ The water absorption presented in the table represents the absorption from the humidity-state at storage

3.2.3 Cement

Norcem Standard FA cement was used in the NDC-matrixes, while Norcem Standard cement was used in the LWAC-matrixes. The difference between the two different types of cement is that there have been added 20% Fly Ash to the Standard FA cement [38], which makes the concrete durable even if alkali reactive aggregates are used [39]. The two different cements types are made in Norway, and are applicable for use in all exposure-, durability- and strength classes.

3.2.4 Additive materials

3.2.4.1 Silica Fume, Fly Ash and Limestone

Elkem Microsilica 940 U(A-4066) and Fly Ash were used in the concrete mix as filler materials. Both the Silica Fume and the Fly Ash are bi- or even waste products from the production of the metal ferrosilicium and electricity and heat from coal-crafted energy production plants, respectively [38], [40]. The two bi-products are so-called pozzolanic materials, which are used as replacement of some of the cement. The pozzolanic materials react with limestone powder, which is also an additive material, and water to create a cementitious effect. The use of pozzolanic materials in concrete increases bond

strength(filler) reduces the economical costs, reduces the environmental costs and enhances the durability, due to the reduction of possible alkali-reactions [41], [40], [38].

3.2.5 Steel fibres

For those matrixes where fibre reinforcement was induced, straight steel fibres with cramped ends, named “Dramix 65/60 3D”, were used. The fibres are 60mm long and have a “radius” of 0,9mm, giving it an Aspect Ratio of 65.



Figure 3.1 Dramix 65/60

The tensile strength of the steel fibres is about 1200 MPa [42], and due to the cramped ends, the fibres have good anchorage strength. The steel used in the fibres were “ordinary” steel with a density of 7,800kg/m³ and a Young’s modulus “E” of 210,000MPa. The fibres were added to the matrix in dosages of 0,5% and 1,0% volume fractions.

3.2.6 Superplasticizer

The superplasticizing material Dynamon SX-N was used in the concrete matrix so that the original amount of water could be reduced to increase the concrete strength (lower water/cement relation), at the same time as a good workability and a good slump value of the fresh concrete were obtained.

3.3 Physical size and geometry

The size and geometry of the cylinders and beams were predetermined. The beams had sizes of 150x150x550mm, while the cylinders had a diameter of 100mm and height of 200mm. These sizes gave each a volume of 12.375l and 1.571l, respectively.

For the choice of physical size of the prisms, several concerns had to be taken into account. 1: The prism had to be of suitable size to fit in the available testing machines. 2: the cross section of the specimen should not be too large due to limited compression capacity for the test machine. It is essential for the test that the specimen will be loaded until failure. 3: For a too slender prism the effect of buckling could affect the results. A maximum slenderness of 4,0 have been proposed to avoid this effect. 4: For an axially compressed prism with a too low slenderness, the restraints from the interfaces between test rig and concrete specimen would affect the test results. From calculations on the damage zone by e.g. Kotsovos [37], researchers have stated that failure occurs within a length 2.5 times the width of the specimen for prisms in compression. This gives an absolute minimum slenderness of 2.5 for the prisms.

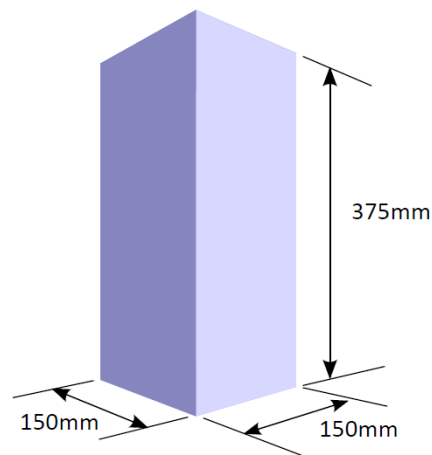


Figure 3.2 Prism dimensions in 3-Dimensional perspective

The physical size of the prisms was set to be 150x150x375mm based on the anticipated concrete compression strength and the reasons mentioned above. This geometry gives a volume of 8.4375l and a slenderness of 2.5.

The compression strength of the NDC was assumed to be about 45MPa, yielding an anticipated compressive load at failure of about 1000kN.

Table 3.6 Physical dimensions of different structures

	Length [mm]	Width [mm]	Height [mm]	Diameter [mm]	Volume pr. Specim. [dm ³]
Prisms	150	150	375	-	8.438
Beams	550	150	150	-	12.375
Cylinders	-	-	200	100	1.571

3.4 Formwork and Concrete casting

Before the concrete mixing could start, the formwork had to be prepared. For the case of the cylinders and beams, the formwork did already exist due to standard sizes. Hence, all that had to be done prior to casting was to apply oil to the surfaces. This treatment had to be done to ensure that the concrete would not stick to the formwork when dismantled.

For the prisms, however, the formwork had to be built from scratch. Thanks to experienced laboratory workers, the construction of the formwork was easily put together and disassembled, making it easy to use over again. The same oil treatment had to be performed on the formwork of the prisms as well.



Figure 3.3 Formwork for prisms and cylinders

With the formwork assembled and prepared for use, the weighing and measuring of the different constituents of the matrixes could start. To satisfy the desired volume to fill all the formwork, each concrete batch should have a total volume of 100l.

After having measured and prepared all the different materials, they were added to a concrete mixer in a specific order, with a specific time interval for each new additive.

Table 3.7 Mixing order

Constituents	Comments
1. Addition of Fine- and Coarse aggregate	
2. Addition of Leca 800, 4-8mm	(In the case of LWAC)
3. Addition of Leca, 2-4mm	(In the case of LWAC)
4. Addition of cement and additives	(Pozzolanic materials and lime stone)
5. Dry-mixing for 1 min	
6. Addition of water	
7. Addition of Superplasticizer (SP)	
8. Wet-mixing for 2-4 min.	Depending on how the concrete looks
9. Letting the matrix “rest” for 2 min	
10. Adjusting the consistency by add. SP	
11. Remixing for one minute	
12. “Gentle” addition of fibres	(For fiber reinforced concrete)
13. Adjusting the consistency by add. SP	(If required)

As the mixing procedure was finished, tests to establish the consistency properties of the fresh concrete were done. T-50 sink- and slump values, air content and density were measured for each concrete matrix.



Figure 3.4 Cone for workability measuring



Figure 3.5 Casting of unreinforced LWAC prisms and cylinders

Table 3.8 Sink Value, Slump Value, Air content and Density

Concrete type	Fibre fract. [%]	T-50 Sink ¹ [s]	Slump ² Value [mm]	Air Content [%]	Density [kg/m ³]
NDC	0.0	4.88	660	3.5	2267.3
	0.5	5.00	640	2.7	2298.1
	1.0	7.00	600	2.5	2326.5
LWAC	0.0	1.88	590	7.0	1696.7
	0.5	1.97	570	5.8	1774.9
	1.0	2.88	560	5.6	1726.0

¹ A measure of how long time it takes for the concrete kept in a cone, to spread to a diameter of 50cm.

² A measure of the total spread for the same concrete

The recipes on the matrixes led to concretes with a fairly good slump, close to the range of self-compacting concrete. For some of the matrixes it was necessary to add more Superplasticizing fluids than what was originally given in the recipe to obtain the desired consistency. A good consistency is of great importance for several reasons: 1:

The concrete must have sufficient viscosity to be able to fill out all the voids of the formwork, more or less by the work of nothing but its own weight. 2: Fresh concretes with a poor viscosity; fibre concretes in especial, have a poor grade of workability.

All three matrixes of NDC were mixed and casted at the same day. About 24 hours after casting, the formwork was dismantled, cleaned, and put back together. The same procedure was followed for the casting of LWAC;

Table 3.9 Time of casting

Concrete type	Fibre fraction [%]	Day	Time of day
	0.0		10.00
NDC	0.5	10.02.2014	12.00
	1.0		14.30
	0.0		10.00
LWAC	0.5	12.02.2014	12.00
	1.0		14.30

After casting, the fresh concrete laying in it’s formwork, was covered in plastic sheets, keeping the water from evaporating, sustaining a humid environment for best possible hardening conditions. The concrete were kept in the formwork for about 24 hours before it was transferred to a water tank, for further storage and hardening under optimal conditions.

3.5 Preparation of test specimen

Prior to the compression tests, the specimens had to be prepared and adapted to fit the test rigs. The formwork of the prisms was constructed in such a way that the concrete was pored into the form from the side. Hence, the two sides that were supposed to be in contact with the test rig were more or less perfectly aligned, thus the prisms needed no more adapting.

Due to uneven casting surfaces on the top of the cylinders, the top and bottom had to be smoothed and aligned with the help of a sanding machine, to ensure even and reliable interfaces between the test machine and the specimen.

For the beams, which were going to be tested in bending in a three- or four point testing procedure, it did not really matter if the concrete casting surfaces were smooth or not. However, there were sawed a notch, about 25 mm deep into the “thickness” of the beams, to predetermine where the fatal crack would be located.

3.6 Test machine and test setup

Due to several different reasons, the only available testing machine that suited to the prisms was one with a load capacity of 1000kN. According to the calculations done in the process on establishing the size and geometry of the prisms, the capacity of the rig could in case of an extra strong specimen be a little too poor.

Nevertheless, due to lack of time the prism tests had to be performed in this rig.

Promises were given by the responsible laboratory guys, that by adjusting the hydraulic pressure, one could over-load the rig with another 20% in addition, making the final load capacity 1200kN. This high theoretical loading should surely be large enough to brake the prism.

The rig was an electro-hydraulic servo-controlled displacement machine.

A spherical ball bearing was used between the top of the prism and the test machine during centric loading to ensure a good grade of free rotation. The two interfacial surfaces of the bearing were thoroughly lubricated to avoid as much friction as possible.

Ideally there should have been used spherical ball bearings both above and underneath the prism, both for centric and eccentric loading. But due to a large risk of the prism to pop out of the testing machine, causing harm, this was prohibited.



Figure 3.7 Spherical ball bearing



Figure 3.6 Compression device

When bearings were used, they were manually centred on the top of a two cm thick steel plate with the same dimensions as the cross section of the prism, which again was placed on the top of the prism. The purpose of the steel plate was to spread the load, so that the entire cross section was used as a load carrier. There were also used a similar steel plates between the bottom of the prism and the testing machine.

In the case where prisms were loaded eccentrically, a 2x2x15 cm steel part was welded onto another 2cm thick and 15x15cm large steel plate. This part was placed, bulk pointing down, on top of the steel plate that was resting on top of the prism, and positioned in such a way, that the load would be eccentric by $h/6$ on the prism.

3.7 Recording of test results

To be able to monitor the strain development in the prisms in a best possible way, the position and length of LVDTs were thoroughly discusses. Previous quite similar work were studied to find good reasons to where to place the LVDTs. Base on this, it was decided that there should in total be used six LVDTs per prism, three on the north face and three on the south face. One LVDT should be 300mm of length in a vertical direction, one should be 200mm of length, vertically and the final LVDT should be 100mm, mounted horizontally, and vertically centred on the prism.

LVDT is short for Linear Variable Displacement Transducer. The LVDT consists of a number of parts, but simply put, there are two ends that are fastened with a certain space to the surface of the test object. Between the two ends, there is a thin and stiff rod

which is mounted to be rigid at one end, while the other end is free to axially move forth and back inside a certain device which is constantly recording the axial displacements. The LVDTs are connected to a computer which plots the displacements in correlation to the load applied to the test specimen, drawing a displacement-load graph for each LVDT. There were several reasons to why there were chosen to only record the strains on two faces: 1. In the case of centric loading, recordings towards the sides of two opposite faces would be adequate to reflect the strains of the prisms. 2: In the case of eccentric loading it was mainly the strains on the most and least strained faces that were of any interest. The most and least strained sides would be those normal to the direction that the load had been moved to become eccentric.



Figure 3.9 Eccentricity at top



Figure 3.8 Eccentricity at bottom

To create eccentric load, the prisms were moved by $h/6$, h being the height of the prism cross section, from the centric position towards the south. Due to this movement it will according to Markeseth now be large compressive strains at the north face, while the south face will be unstrained. The assumption of zero strains and stresses on the least stressed side has been based on the assumption of a linear stress dispersion over the cross section. This however is not correct, as concrete is nothing but homogenous. The strains at the south side will however be quite close to zero, depending on the exact position of the load and the on irregularity of the dispread constituents of the concrete specimen.

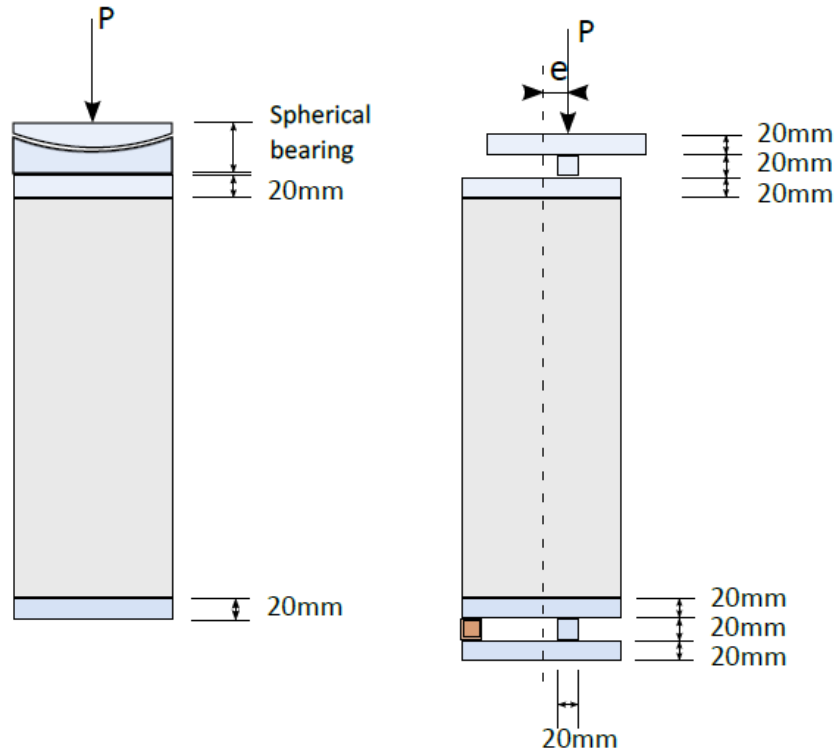


Figure 3.10 Eccentrically and eccentrically prism set up

During the testing, the casting surface of the prism was always faced towards east.

The reason to why there were mounted two vertical LVDTs with different lengths on each side, was to see if any signs of localization of strains just prior to failure or the effect of strain softening could be recorded.

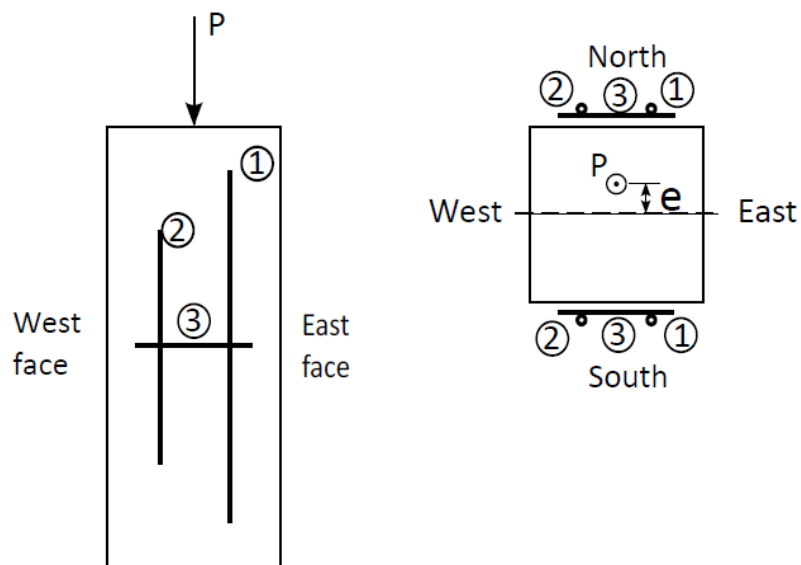


Figure 3.11 Location of LVDTs. The drawing to the left shows the prism from south side, the drawing to the right shows the prism from the top. "1" refers to the vertical 30cm LVDT, "2" refers to the vertical 20cm LVDT and "3" refers to the transversal LVDT

The purpose of the horizontal LVDT was to measure the horizontal strains due to the effect of Poisson or as the effect of tensile splitting strains. There are no certainties that the maximum horizontal deformation will take place at the location of the horizontal LVDT, i.e. at the midpoint. It is however likely to assume that it will record most of the lateral displacements anyhow, due to the length of the failure zone.



Figure 3.12 Location of LVDTs on North face

During the test, it was experienced that some of the LVDT reported uneven or sometimes no results at all. The poor recordings were mor often than not due to faults on the connection between computer and LWDT. This poor or largely deviating results were excluded from the results presented later on.

Stiffness of testing machine, load rate, load intervals, etc.

4 Test results

4.1 Introduction

The poor mechanical behavior of LWAC in terms of high brittleness is loudly pronounced and has kept it from being used in structures where strong building materials of low weight is needed. Different reasons to the problem and actions that might improve the behavior have been studied and looked into. The goal of this thesis have been to try to verify some of the results from previous studies done in the pursuit of making a LWAC with improved mechanical behavior, due to inclusion of steel fibres. Laboratory tests were performed on LWAC- and NDC prisms in compression, both with and without steel fibres, to see if the results from the work of this thesis could be compared and set in relation to previously performed tests on the actual field.

4.2 Cylinder compression tests

Due to the possibility of wide dispersion in time of the prism tests there were made a certain number of cylinders from the same concrete batches as for the prisms, ref. Table 3.3. The cylinders were supposed to be tested at the same age as the prisms at the time of prism test. The reason for these cylinder tests to be performed is due to the constant rise in concrete strength when maturing. If the different prism tests for the same type of concrete should turn out to be performed not at the same time at all, one could then use the results from the cylinder tests to adjust the strength, so that one could properly compare the prism results.

Table 4.1 Height, weight, and cylinder compression strength f_{cp} for LWAC cylinders. (All cylinders¹ were tested at approximately 58 days of age after casting)

LWAC cylinders				
Fibre volume [%]	Cylinder identity	Height [mm]	Weight [g]	f_{cp} [MPa]
0,0	1	195	2720,0	46,06
	2	195	2749,9	47,07
	3	197	2716,9	43,81
0,5	1	194	2747,1	44,61
	2	- ¹	-	-
	3	197	2746,7	45,2
1,0	1	195	3171,7 ²	61,46 ²
	2	198	2764,8	38,14 ³
	3	199	2808	46,51

¹ The cylinder was tested at an early stage (30 days after casting) to predict a needed compressive capacity of a test machine.

² These values are hardly correct. The weight doesn't fit to neither the other LWAC prisms, nor the NDC prisms. The compressive strength f_{cp} however seems to be taken from the recordings of NDC.

Table 4.2 Height, weight, and cylinder compression strength f_{cp} for NDC cylinders. (All cylinders¹ were tested at approximately 72 days of age after casting)

NDC cylinders				
Fibre volume [%]	Cylinder identity	Height [mm]	Weight [g]	f_{cp} [MPa]
0,0	1	195	3467,7	61,85
	2	195	3475,0	62,30
	3	193	3416,9	60,10
0,5	1	194	3501,2	63,49
	2	196	3595,0	65,73
	3	- ¹	-	58,29 ¹
1,0	1	195	3586,5	69,34
	2	196	3569,6	68,88
	3	199	3620,6	68,38

¹ The cylinders were tested at an early state (28 days after casting) to try to predict which test machine was needed to have sufficient compressive capacity.

As it turned out, because of a delay in the laboratory, all prism tests were performed at a late stadium, at approximately 58- and 72 days after casting for the LWAC- and NDC

prisms respectively. Due the already high relative load at this late time of testing, a couple of days in difference nearly make no difference to the compressive strength.

4.3 Prism tests

4.3.1 Age at testing

The age of the concrete specimen at time of testing plays a rather big role when it comes to mechanical properties and behaviour. According to **NS-EN 12390-3** the test should not be performed at an earlier stage than 28 days after casting. At this time the concrete have reached a relative strength of about 90%.

All prism tests for the same type of concrete were performed whit in a couple of days at a relative mature state in terms of age. The difference in the material properties and mechanical behaviour due to varying in age should thus not be of any significance.

Table 4.3 Concrete age at prism testing [days]

Fibre [%]	LWAC				NDC			
	B1	B2	B3	B4	B1	B2	B3	B4
0,0	56	56	58	58	- ¹	-	73	-
0,5	55	56	57	57	71	-	72	74
1,0	56	57	57	57	-	-	73	73

¹ The line “-“ indicates that the test have not yet been performed

4.3.2 Introduction to diagrams

The shown diagrams in this chapter are only those of greatest importance to the purpose of this thesis. That is those which best express the ductility, hence the stress-strain relations for centric compression and load-strain relations for eccentric compression. The rest of the diagrams developed from the test data are presented in Annex C.

The axial stresses from the centric tests have been calculated based on the applied load divided by the total cross sectional area, $\sigma = \frac{P}{A}$. Due to the heterogeneity of concrete, the stress dispersion over the cross section will not be uniform; hence it will not be correct to express the only calculated stress value per prism in correlation to each of the four individual longitudinal strain “recordings” per prism, as they reported quite different strains.

However, since all longitudinal strain curves from the centric tests presented in the diagrams below have been averaged based on all four vertical LVDTs per prism, this way of presenting the stress-strain curve will be valid anyhow, as it expresses the entire prism as a whole.

The cross sectional strains from the centric tests have also been averaged based on recordings from both two horizontal LVDTs per prism.

Poor recordings were excluded from the averaging and are hence not represented in the report. Curves for all recorded data, both good and bad are plotted in the Annex C.

The curves for the longitudinal strains from the eccentrically tested prisms presented in this chapter have been averaged based on the recordings from the 20- and 30cm LVDT per face, resulting in two axial strain curves per prism, one for the compressed north side and one for the tensioned south side.

The lateral strains have only been expressed for the north side¹ for the eccentric tests, due to negligibly low values or poor quality of the recordings on the south face. The complete results from each LVDT have been plotted for both longitudinal and lateral direction in Annex C.

The strains from the eccentric compression tests have however been presented in correlation the applied load. This way of presenting the strains give the best expression of the strain development through an eccentric test, as the actual stresses are hard to estimate, and would most certainly give a false picture of the strain development.

(Not only would it be hard to give a true description of the stresses as they would have been calculated based on the assumption of elastic material behaviour and exactly zero strains at the least stressed side, as Markeset proposed, or based on the recorded

¹ The south-side-horizontal-strain for the “B4 NDC 1,0% eccentric” prism are presented in *Figure 4.10*, as the only strain from the vertically tensioned side which gave actual results.

strains, the applied load and the assumption of a linear stress dispersion over the cross section. The latter suggestion of estimating the stresses were performed in this thesis, but have only been presented in Annex C, due to the probably poor grade of true stress reflection. A thorough description of the calculation, the applied equation and results are presented in Appendix C)

The curves shown in the diagrams reflect the mechanical behaviour during the entire load life of the prism up to failure. For some tests however, it was hard to state the exact time of failure based on the recordings. The “definitions” of failure were therefore several: 1: When one or more of the LVDTs reported error. 2: When the recordings stopped at peak load or immediately after. 3: When the load dropped drastically from one load interval to the next, or 4: When the LVDTs simultaneously reported a big jump in terms of displacement between two recordings.

The original plan was to test 24 prisms, of which 12 were of LWAC and the rest of NDC, ref. Table 3.1. However, based on the experience from the first centric test on a NDC prism and the first eccentric test on a NDC prism without any reinforcement, neither more centric test for the NDC prisms, nor eccentric test on the NDC prism without reinforcement were carried out.

The reason to why the number of tested NDC prisms was reduced to only six was the violent behaviour of failure, which could have lead to human harm or breaking of the test machine.

The reason to why the prisms eccentrically loaded were expressed by a load-strain curve is due to the uneven stress dispersion. For the centrically compressed prisms the stresses are simply calculated by dividing the load on the entire load surface. This procedure of estimating the stresses is valid for the entire load life, both the elastic- and inelastic stage. For the eccentrically loaded prisms the case is quite different. Due to the eccentric load the stress will be all but even across a section of the prism. Regarding to Markest’s research, the stresses should be equal to zero on the “least” stress side, making it easy to calculate the stresses on the opposite side. This theory however, has shown not to be valid. Another way to calculate the stresses when eccentrically loaded is to multiply the strains by Young’s modulus. This however, will only be valid for the

elastic part of the stress-strain curve, and will therefore not be valid as well. However, there have been performed some calculations in this thesis to try to find the stresses in the least and most stressed fibre when exposed to eccentric loading. In this approach, a linear stress dispersion over the cross section was assumed and the total load was divided with the total load area, which gave a point of zero stress close to the least stressed end. The strains were then used to locate this point of zero longitudinal stresses and one demanded that the sum of stresses of the eccentric loaded prisms had to be equal to the stresses if centrally loaded. This approach seemed like a good way to calculate the stresses of the least- and most stressed fibre, but when the strains on the tensioned side got big, the stresses seemed unlikely to be correct. However, the plot of the calculated stresses in relation to the strains can be seen in annex [XX]. The load-strain curves for the eccentric loaded prisms shown in this chapter represent the most “correct” curve, however.)

The curves on the right side of zero presented in the following diagrams do actually represent compressive strains, while the negative strain values do express the tensioned strains.

4.3.3 Stress - Strain and Load - Strain diagrams for LWAC prisms in compression

4.3.3.1 LWAC, 0,0% steel fibre

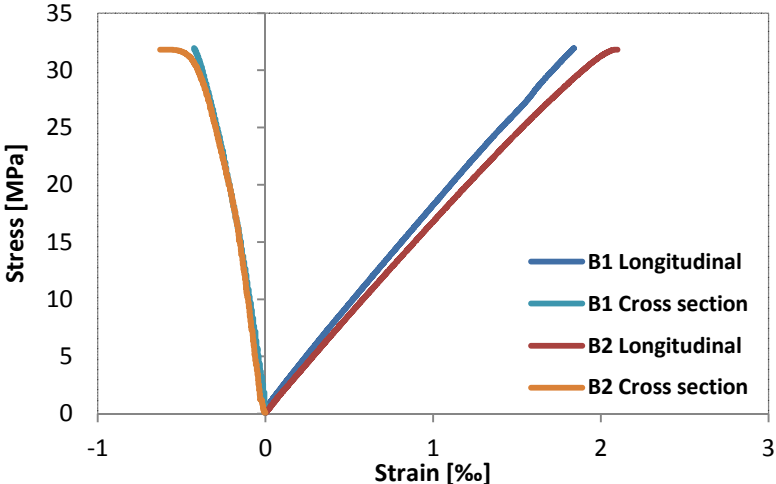


Figure 4.1 Stress-strain relationships for centrally compressed LWAC prisms without any steel fibres per volume fraction

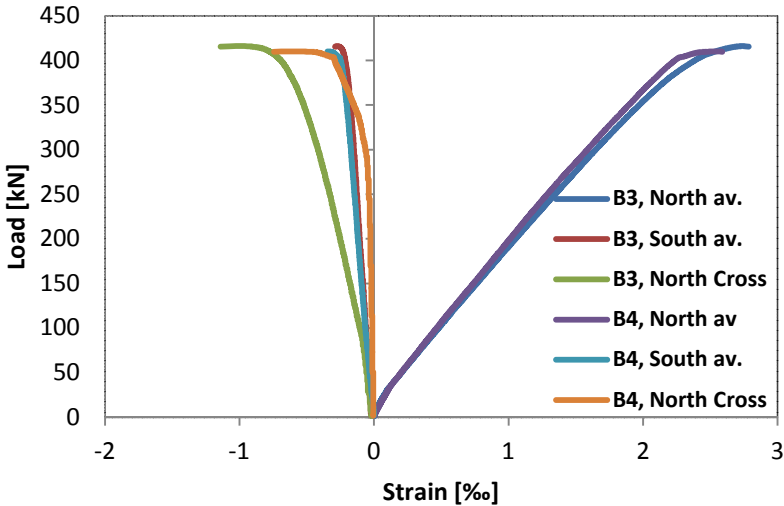


Figure 4.2 Load-strain relationships for eccentrically compressed LWAC prisms containing 0,0% steel fibres per volume fraction

4.3.3.2 LWAC, 0,5% steel fibre

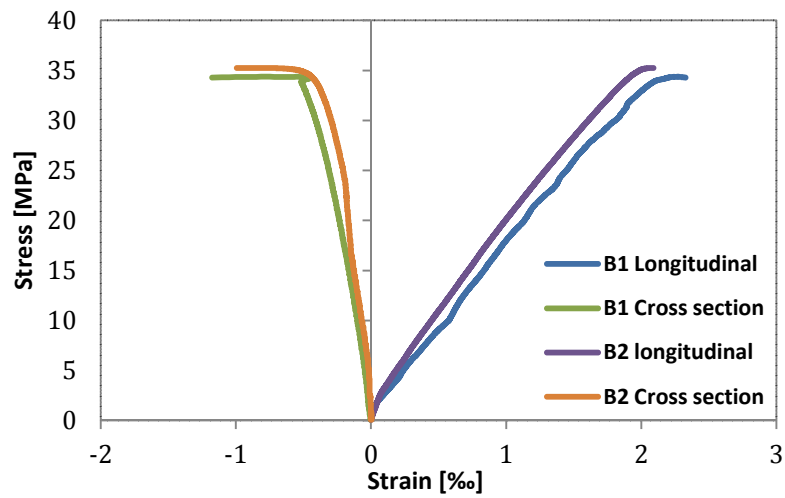


Figure 4.3 Stress-strain relationships for centrally compressed LWAC prisms containing 0,5% steel fibres per volume fraction

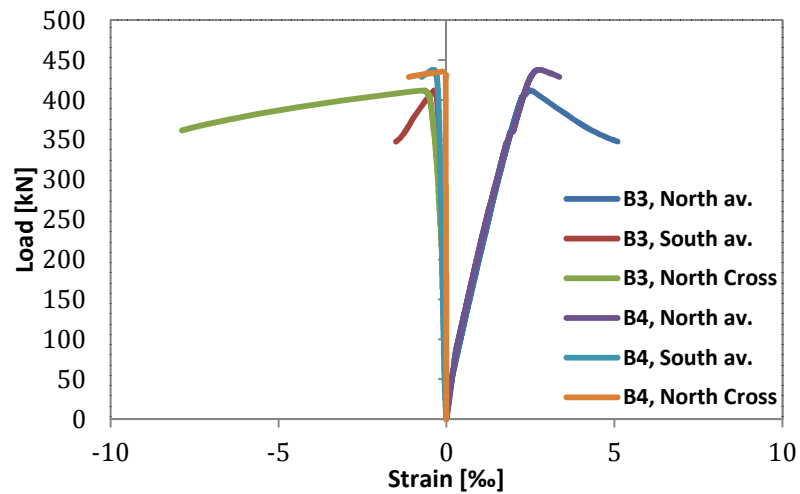


Figure 4.4 Load-strain relationships for eccentrically compressed LWAC prisms containing 0,5% steel fibres per volume fraction

4.3.3.3 LWAC 1,0% steel fibres

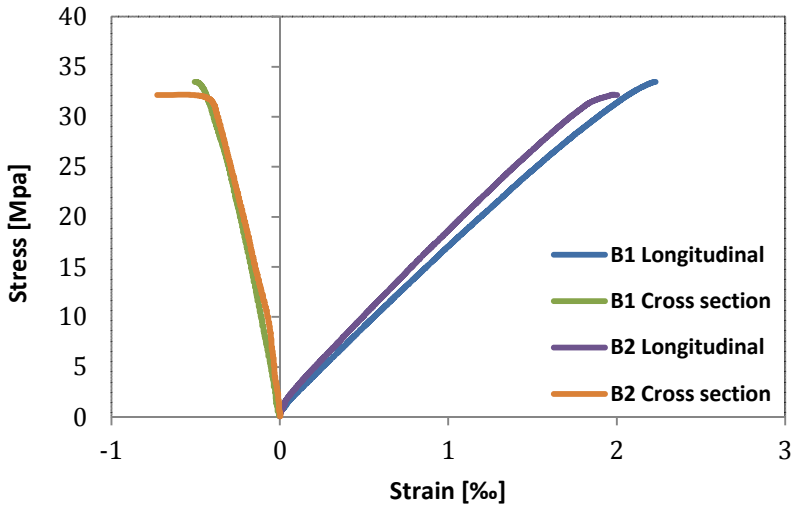


Figure 4.5 Stress-strain relationships for centrically compressed LWAC prism containing 1,0% steel fibres per volume fraction

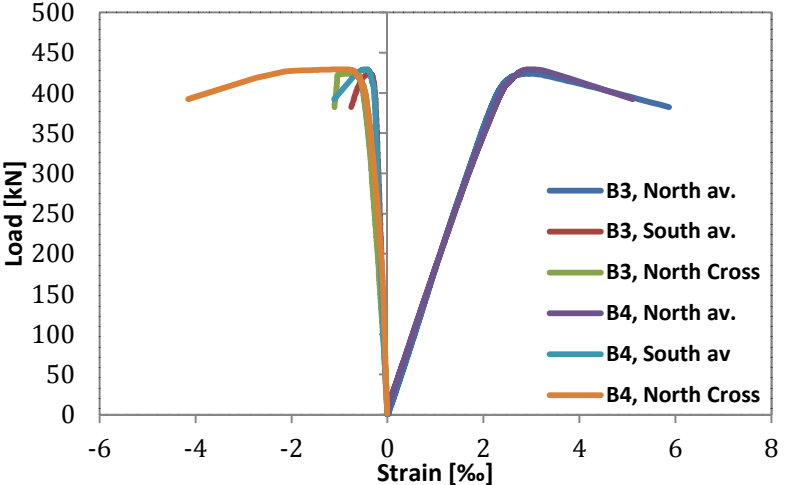


Figure 4.6 Load-strain relationships for eccentrically compressed LWAC prisms containing 1,0% steel fibres per volume fraction

4.3.4 Diagrams for NDC prisms in compression

4.3.4.1 NDC, 0,0% steel fibre

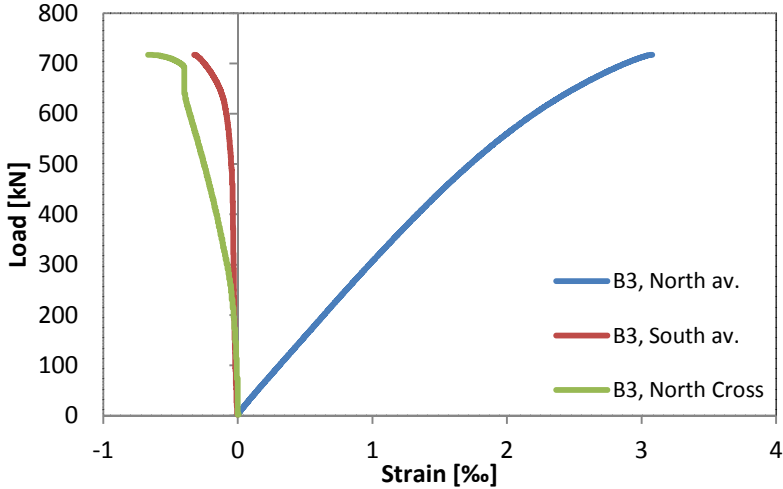


Figure 4.7 Load-strain relationships for one eccentrically compressed NDC prism containing 0,0% steel fibres per volume fraction

The explosive failure experienced from the first tested NDC prism without any steel fibre reinforcement, prevented the remaining three tests from being performed on the NDC prisms with 0,0% steel fibres, partly due to the risk of human injuries and partly due to risk of damage on the test machine when centrally loaded.

The curves in Figure 4.7 therefore only express the results from that one test performed on a NDC prism with no fibre reinforcement. As the figure text explains, the test was performed in eccentric compression.

4.3.4.2 NDC 0,5% steel fibre

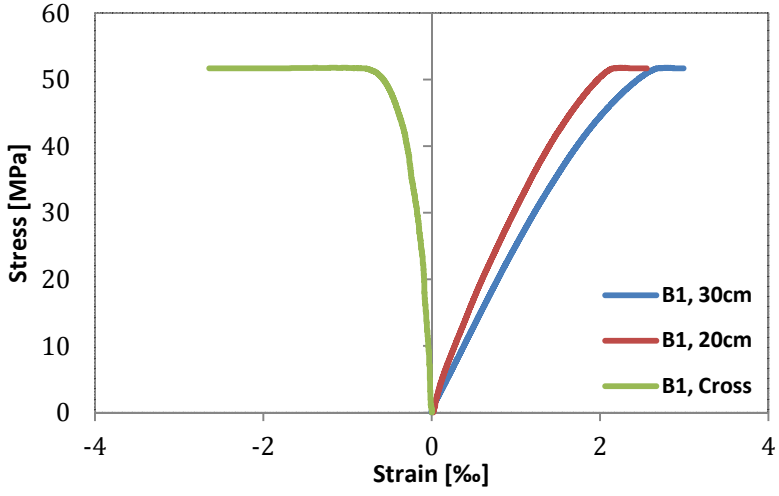


Figure 4.8 Stress-strain relationships for one centrally compressed NDC prism containing 0,5% steel fibres per volume fraction

Figure 4.8 represents the only centric test performed on NDC prisms. The seemingly high compressive strength of the actual prism led to an “overload” of the test machine by about 16%. For a long time it looked like the prism would not fail at all, but immediately before the test was about to be stopped, the prism exploded violently. The flat part at the end of the curves above reflects the rather great increase in strains just prior to the failure, without any rise in stresses. Complete plots are presented in Annexs C.

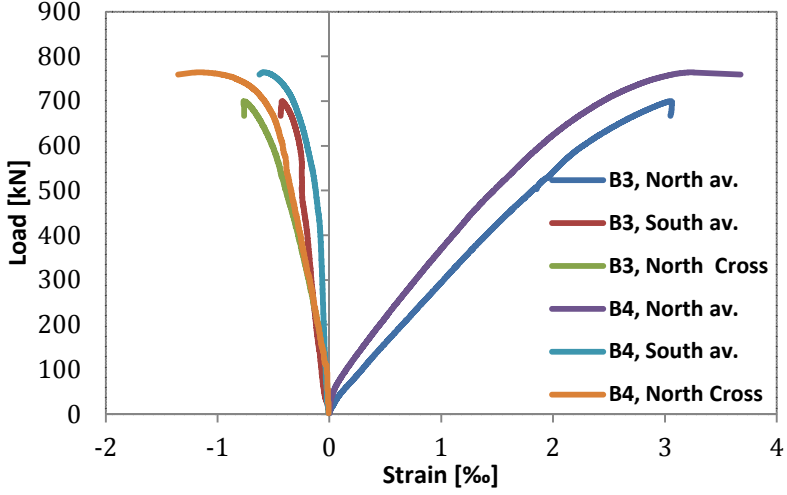


Figure 4.9 Load-strain relationships for eccentrically compressed NDC prisms containing 0,5% steel fibres per volume fraction

4.3.4.3 NDC 1,0% steel fibres

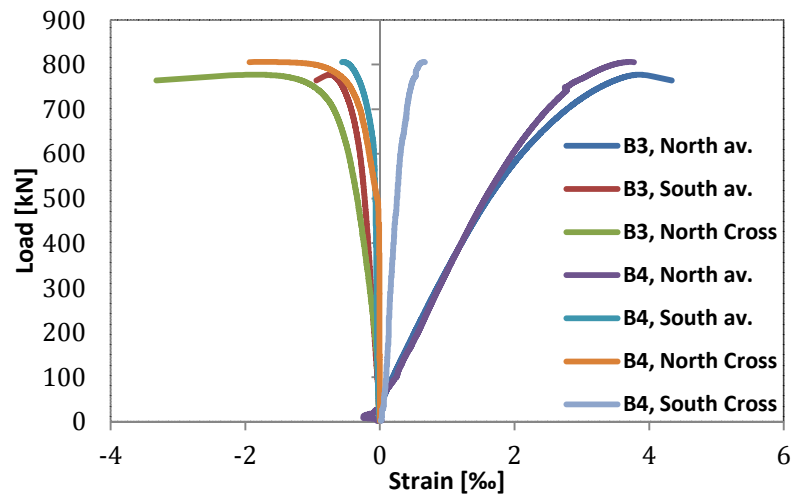


Figure 4.10 Load-strain relationships for eccentrically compressed NDC prisms containing 1,0% steel fibres per volume fraction

Prism B4 with 1,0% of steel fibres per volume fraction was actually the only eccentrically loaded NDC prism that reported some actual strains in the cross sectional direction on the least stressed side. The curve is named “B4, South Cross” in the diagram above.

4.3.5 Comments on the prism test results

The entire purpose of this thesis has been to investigate the effect that steel fibre inclusion into LWAC have on the mechanical behaviour in compressive loading. The diagrams earlier in the chapter gave only a visual expression for the averaged stress-strain and load-strain behaviour for centric and eccentric compression, respectively, for NDC- and LWAC prisms with no- or different grades of steel fibres. In some of the cases there may be difficult to read exact values and to spot explicit changes from test to test. Both averaged and individual results have therefore been explained more thoroughly in the following section.

As seen in the diagrams, the curves that represent the stress-strain relation vary quite a bit from the same prisms respectively. The fact that only two and two prisms are equal in the term of concrete type, steel dosages and the way of loading, makes it hard to tell which of the test results that deviates from the normal. The evaluation of the results from the tests has therefore been based on the average of the recordings that seemed to be most likely to be “correct”. The averaging of the different values presented in this chapter did therefore not take into account the recordings that in some way clearly deviated from the other recordings. All results, good or bad, have been plotted and can be found in its original form in the annex, however.

4.3.5.1 LWAC prisms in centric compression

The development of material behaviour cannot be seen explicit from test to test. However by averaging the most reliable test results from the centric LWAC tests there is possible to state the exact results and changes.

Table 4.4 Maximum load P_{max} , prism compression strength f_{cp} and load at failure P_{fail} for LWAC prisms in centric compression

LWAC – centric				
Fibre [%]	Prism identity	P_{max} [kN]	f_{cp} [MPa]	P_{fail} [kN]
0,0	B1	718,59	31,94	716,27
	B2	715,67	31,81	715,67
0,5	B1	773,22	34,37	768,13
	B2	793,24	35,26	790,08
1,0	B1	753,39	33,48	753,39
	B2	724,32	32,29	723,56

Table 4.5 Longitudinal ϵ_l - and cross sectional ϵ_c strains at peak stress and at failure, plus change of strains from peak state to failure for LWAC prisms in centric compression

LWAC – Centric							
Fibre vol. [%]	Prism identity	ϵ_{lpeak} [‰]	ϵ_{cpeak} [‰]	ϵ_{lfail} [‰]	ϵ_{cfail} [‰]	$\epsilon_{lchange}$ [%]	$\epsilon_{cchange}$ [%]
0,0	B1	1,841	-0,425	1.841	-0,425	0,00	0,00
	B2	2,095	-0,603	2,100	-0,629	0,24	4,31
0,5	B1	2,243	-0,548	2,327	-1,176	3,74	114,60
	B2	2,071	-0,838	2,090	-0,994	0,92	18,62
1,0	B1	2,230 ³	-0,505	2,230 ³	-0,505	0,0	0,0
	B2	1,978 ⁴	-0,557	2,003 ⁴	-0,727	1,26	30,52

¹ The presented values for the longitudinal strains in the table are averaged based on the recordings from all four vertical LVDTs per prism. (Poor recordings were left out of the averaging)

² The presented cross sectional strains have been averaged based on the recordings from both horizontal LVDTs per prism.

³ The recordings from “North 30cm” were left out of the averaging due to very poor recordings. Another interesting result is that the strains calculated from “South 20cm” are larger than for “North 20cm”. This result deviates from all other tests.

⁴ The strains calculated based on the recordings from “South 30cm” is in fact smaller than the strains for “South 20cm”. These results deviates from all other tests and make the recordings from the 30cm LVDT seem to be false. However, the strains of “north 30” have not been excluded.

Table 4.5 shows the averaged strains for each prism individually at the time of maximum load, at failure and also change in strains in percent from the two stages. Some of the recordings from both prisms with 1,0% steel fibres gave results which deviated from all other centric tests. The reason to this will be commented on in the “Discussions of test results”.

Table 4.6 Final averaged values of maximum load P_{max} , load at failure P_{fail} , prism compression strength f_{cp} , longitudinal strain at peak load ϵ_{lpeak} and longitudinal strain at failure ϵ_{lfail} for LWAC prisms in centric compression

LWAC – Centric							
Fibre vol.	P_{max}	P_{fail}	f_{cp}	ϵ_{lpeak}	ϵ_{lfail}	ϵ_{cpeak}	ϵ_{cfail}
[%]	[kN]	[kN]	[MPa]	[‰]	[‰]	[‰]	[‰]
0,0	717,13	715,97	31,88	1,968	1,971	0,514	0,527
0,5	783,23	779,11	34,82	2,157	2,209	0,711	1,085
1,0	738,86	738,48	32,89	2,104	2,117	0,531	0,606

¹These values in this table have been averaged based on the values from

Table 4.4 and Table 4.5.

The values in Table 4.6 express averaged values for each type of LWAC prism in centric compression. It should be mentioned that the averaging have been done based on all recordings that seemed to be relatively good. It is however not possible to state which values that possibly deviates from the normal, due to only two similar tested prisms. The results of Table 4.6 may hence give a false impression of the real values.

There are no difference in loads from the state of maximum load to the state of failure of any importance for the eccentric tested LWAC prisms.

Based on the values of Table 4.6 and compared to the results for the unreinforced LWAC prisms, the compressive strength f_{cp} increased by 9,2% and 3.2% by inclusion of 0,5% and 1,0% steel fibres respectively. The longitudinal strains at failure increased by 12,1% and 7,4%, while the cross sectional strains, also at failure, increased by 106,9% and 15,0% by inclusion of 0,5% and 1,0% steel fibres per volume fraction respectively.

It can also be seen from both Table 4.5 and Table 4.6 that the change of strains from the state of peak load until failure increased with the addition of steel fibres. Based on Table 4.6 it can be found that the change in strains from the state of maximum load up till

failure were 0,2% and 2,5% for longitudinal and transversal strains respectively for the unreinforced LWAC prism. For the LWAC prisms reinforced by 0,5% steel fibres, the increase of strains was as much as 2,4% and 52,6% in the longitudinal and transversal direction respectively. While for the prisms reinforced by 1,0% steel fibres, the increase of strains from the state of maximum load until failure was 0,6- and 14,1% for the longitudinal and transversal direction respectively.

It can also be mentioned that based on Table 4.4 and Table 4.5, amongst two and two similar tested prisms, the prisms with the lowest compressive strength are the one wich have the best strain improvement towards failure.

To get an impression of the stiffness of each prism, Young's modulus was calculate by dividing the stress on the averaged longitudinal strains per prisms and was expressed in correlation to the relative stress level. From analyses on the plots of the Young's modulus it turned out to be hard to state one specific value, since the modulus decreased with increasing load. At a relative load level of 50%, Young's modulus seemed to be between 15- and 20GPa and the shape of the plotted curves were more or less equal.

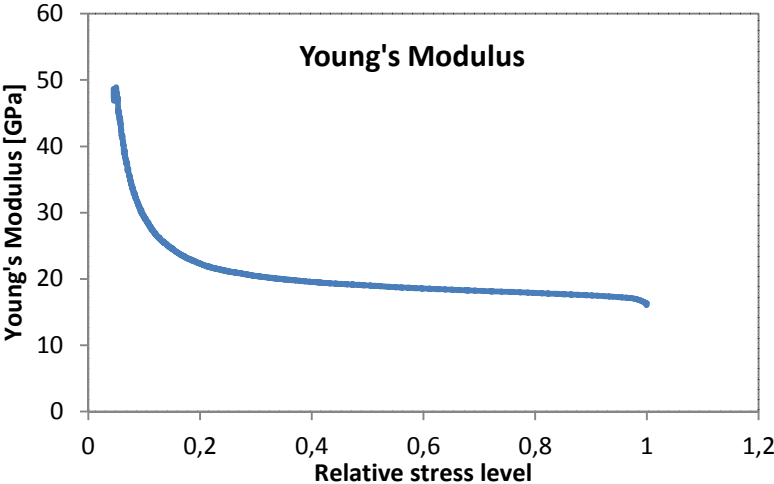


Figure 4.11 Young's Modulus for the centrally compressed LWAC prism B2 with 1,0% steel fibres per volume fraction

Young's modulus have been plotted and are presented in Annex C. From comparing the Young's curves in Annex C one can see that the mean value of the curves of the prisms with 0,5% of steel fibre is slightly higher than for the other prisms. In addition to that,

the curves for the 0,5%-prisms seem to be steeper than especially the 1,0%-curves which seem even flatter than the 0,0%-prisms. The higher mean value and steeper curve for the 0,5%-prisms reflects the higher loads at the same relative stress level at the first part of the curve and the higher strains towards the end of the curve at the same relative load level as compared to the curves for the other prisms. The relative flat Young-curve and at high Young-value for the B2 1,0%-prism reflects a very linear stress-strain behaviour and low strains at the very end of the curve, especially compared to the other 1,0% prism. In short words, the plainer the curve, the more linear the stress-strain curve, and the lower Young-value, the higher the strains at a relative stress level. The plotted curves of the Young modules reflect upon the stresses and strains shown in Table 4.5.)

Calculations of Poisson's Ratio, which were based on the averaged longitudinal and transversal strains, resulted in values of about 0,2 with pretty much similar shape for all of the plotted curves. The curves were more or less plain at the beginning, while they drastically rose towards the end of the curves, showing the development of longitudinal cracks and large lateral deformations. From comparing the plotted curves, one can see that especially one of the prisms containing steel fibres of 0,5% volume fraction, the Poisson Ratio is slightly larger, at just above 0,2, than for the two other type of prism. The reason for this may be a coincidence, or simply just due to better or worse recording of the displacements.

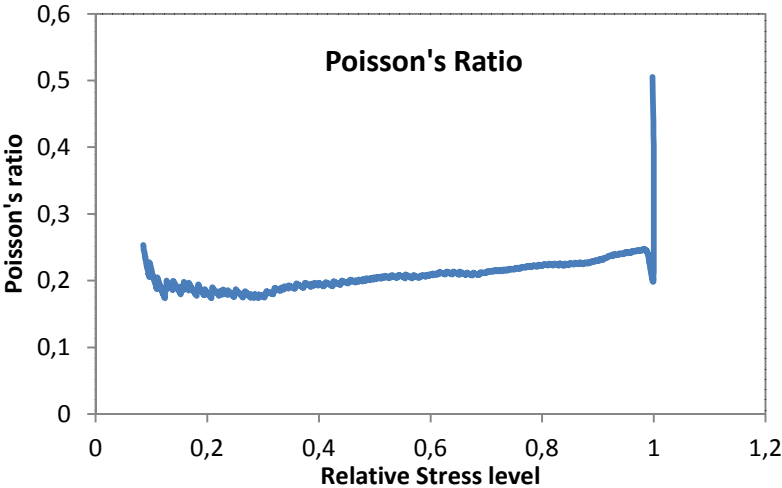


Figure 4.12 Poisson's Ratio for the centrally compressed LWAC B1 prism with 0,5% steel fibres per volume fraction

As for Young's modulus, it is hard to state one specific value for the Poisson Ratio. As an alternative, one could state one value for the elastic part of the load life, (the plain section of the plotted Poisson-curves), while not giving any value for the inelastic part. For a best impression of the Poisson Ratios for the different prisms, have a look in Appendix C.

From witnessing the tests, one could see that the failure mechanism changed quite a bit from the prisms without any steel fibres to those that had 0,5%- and 1,0% steel fibres per volume fraction. For the cases where no steel fibres were added, the prism more or less exploded at the time of failure, throwing concrete pieces around, leaving nothing but dust in the machine. For the case of 0,5% of steel fibres, the fracture were still quite explosive, while the biggest difference from the unreinforced prisms were that the prism remained more or less in on piece, even if cracks had perforated the prisms. The prisms that were reinforced with 1,0% steel fibres per volume fraction held even better together than the prisms reinforced y steel fibres of 0,5%. The fraction of the concrete got less with increasing grade of steel fibres.

It was way much easier to state a time of failure, from observing the tests, due to the explicit failure in terms of explosion or loud bangs, Compared to estimate a time of failure from the recorded data.



Figure 4.14 LWAC 0,0% B1 centric



Figure 4.13 LWAC 0,0% B2 centric



*Figure 4.16 LWAC 0,5% B1 centric,
Close up of shear band on North face*



*Figure 4.15 LWAC 0,5% B2 centric,
South and East face*

4.3.5.2 LWAC prisms in *eccentric compression*

Due to the fact that there is no good way to calculate the specific stresses in the most- and least stressed fibre of a prism in an eccentric compression test, the strains have been expressed in relation to the applied load. The load-strain curve will express the test results better and more clearly than a stress-strain diagram would have done for the eccentric tests. This means that there will also be a problem to state a compressive strength f_{cp} for the prisms. However, some calculations on determining the stresses of the least and most stressed fibre have been done, and have been presented in Annex C.

Table 4.7 Maximum load P_{max} and load at failure P_{fail} for each LWAC prism in eccentric compression

LWAC - Eccentric			
Fibre vol. [%]	Prism identity	P_{max} [kN]	P_{fail} [kN]
0,0	B3	416,08	408,03
	B4	410,16	409,92
0,5	B3	411,76	347,60
	B4	437,75	428,70
1,0	B3	424,01	287,49
	B4	429,38	418,53

Table 4.7 shows the maximum loads and loads at failure for all eccentrically loaded LWAC prisms, while Table 4.8 shows the averaged results of maximum loads, loads at failure and change of loads between the two states, for each of the three types of LWAC prisms.

Table 4.8 Final averaged values for maximum load P_{max} , load at failure P_{fail} and change of load from peak state to failure P_{change} , for LWAC prisms in eccentric compression

LWAC - Eccentric			
Fibre vol. [%]	P_{max} [kN]	P_{fail} [kN]	P_{change} [%]
0,0	413,12	408,78	-1,05
0,5	424,76	388,15	-8,62
1,0	426,70	353,01	-17,66

¹The values have been averaged based on values from Table 4.7

The maximum averaged loads for each type of prisms increased by 2,8- and 3,3% by inclusion of 0,5- and 1,0% steel fibres per volume fraction respectively. The drop in load bearing capacity between the state of maximum load and failure increases by increasing amount of induced fibres.

Table 4.9 Final averaged strains for LWAC Prisms in Eccentric Compression

LWAC - Eccentric					
Fibre vol. [%]	Direction of LVDT	Face	ϵ_{peak} [‰]	ϵ_{fail} [‰]	ϵ_{change} [%]
0	Longitudinal	North	2,640	2,687	1,8
		South	-0,303	-0,318	5,0
	Horizontal	North	-0,794	-0,942	18,6
		South	0,026	0,026	-
0,5	Longitudinal	North	2,612	4,228	61,9
		South	-0,345	-1,118	224,1
	Horizontal	North	-0,650 ¹	-5,128 ²	688,9
		South	0,040 ¹	0,060	50,0
1,0 ³	Longitudinal	North	2,952	4,586	55,4
		South	-0,408	-0,669	64,0
	Horizontal	North	-0,817	-1,611	97,2
		South	0,073 ¹	0,093 ¹	27,4

¹ The value is only based on the results from one test only

² The value is this high due to the "extreme" value of horizontal strain on the north face for prism B3

³ The strains in the column of "failure" for both B3 and B4 with 1,0% steel fibre reinforcement have most likely been taken from an earlier load state than at the actual time of failure. Hence, the strains at failure are actually quite a bit larger than those presented in the table. Have a look at the diagrams for complete load-strain relations in annex C. The reason for doing this is to show the values of the plotted curves, which is mostly interested in what going on around peak load

The results presented in Table 4.9 express the exact same results as plotted in *Figure 4.2*, *Figure 4.4* and *Figure 4.6*. From Table 4.9 it can be seen that the strains at the state of maximum load have not change noticeably by the addition of 0,5% of steel fibres per volume fraction, while by addition of 1,0% of steel fibres the strains have improved a lot. The increase of strains from the state of maximum load till failure is however very large. The strains given in the table for the 1,0% prisms at failure should have been larger, due to the fact that strains have been taken from a load stage which is probably prior to the actual failure, Hence should the load at failure for the 1,0% prisms in Table 4.7 and Table 4.8 have been smaller. The change of strains between the state of maximum load and failure should thus have quite a bit larger.

The complete load-strain curves for the 0,5% prisms presented in the annex, also show a failure at a much later stage , than the values presented in *Figure 4.4* and in the table above, the failure is however assumed to be at the loads and strains given in this table!

Youngs' Modulus and Poisson's Ratio have been calculated based on the strains for each side individually, and have also been plotted this way. The calculations of the Young's Modulus have also been based on the stresses calculated for the most and the least side. The results do actually seem to be good, and were quite similar to the results from the calculations for the eccentric compressed prisms. and will hence probably not be any good for the plastic range. However, the curves seem to have a good fit even for the plastic range, so it might be that the estimation of stresses for the eccentric loaded prisms wasn't too bad anyways. [LWAC]

The results for the Poisson' Ratio was not as good, but are presented in Annex C together with the Young's Modulus.

The results from the calculations on the plastic rotation capacity, based on the difference in strains from the least stressed side to the most stressed side show a large growth by the addition of steel fibres and are presented as a curve in Annex C.



*Figure 4.17 LWAC 0,0% B3 eccentric,
North face*



*Figure 4.18 LWAC 0,0% B4 eccentric,
North and West face*



*Figure 4.20 LWAC 0,5% B4 eccentric,
West face*



*Figure 4.19 LWAC 0,5% B4 eccentric,
East and North face*



*Figure 4.22 LWAC 1,0% B3 eccentric,
North and West face*



*Figure 4.21 LWAC 1,0% B4 eccentric,
West face*

4.3.5.3 NDC centric compression test

There was only performed one centric compression test on the NDC prisms. The reasons for the reduced amount of tests were partly due to the high compressive strength of the first test which nearly broke the test machine and secondly because of the risk of human injuries.

Table 4.10 Maximum load P_{\max} , prism compression strength f_{cp} and load at failure P_{fail} for NDC prisms in centric compression

NDC - centric				
Fibre [%]	Prism identity	P_{\max} [kN]	f_{cp} [MPa]	P_{fail} [kN]
0,0	B1	-	-	-
	B2	-	-	-
0,5	B1	1164,70	51,76	1162,30
	B2	-	-	-
1,0	B1	-	-	-
	B2	-	-	-

¹The sign “ - ” indicates that no tests were performed

From Table 4.10 one can see that the prism compression strength was drastically larger than for the LWAC prism in centric compression. The maximum measured load for the actual prism was actually 16,5% larger than the theoretical compressive capacity of the testing machine. Even if there was quite a long time between the recorded maximum load and the failure, ref. Annex C, the load did not change more than 0,2%. The same behaviour can be seen from *Figure 4.8*.

Table 4.11 Longitudinal ϵ_l and cross sectional ϵ_c strains at peak stress and at failure, plus change of strains ϵ_{change} from state of maximum load to failure, for NDC prisms in centric compression

NDC - Centric							
Fibre [%]	Prism identity	ϵ_{lpeak} [‰]	ϵ_{cpeak} [‰]	ϵ_{lfail} [‰]	ϵ_{cfail} [‰]	$\epsilon_{lchange}$ [%]	$\epsilon_{cchange}$ [%]
0,0	B1	-	-	-	-	-	-
	B2	-	-	-	-	-	-
0,5	B1	2,525	-1,139	2,755	-2,640	9,1	131,8
	B2	-	-	-	-	-	-
1,0	B1	-	-	-	-	-	-
	B2	-	-	-	-	-	-

¹ The longitudinal strains have been based on the recordings from all four LVDTs per prism.

² The cross sectional strains have been averaged based on both two horizontal LVDTs per prism

³ The sign “ - ” indicates that no tests were performed

Comparing the results from Table 4.11 to the results for the 0,5% reinforced prisms of Table 4.6 one can see that the strains at the state of peak load is quite a bit bigger for the NDC prism, especially in the transversal direction. The increase in strains in percent from the state at peak load until failure are about four and two times as large in the longitudinal and transversal direction respectively for the NDC prism reinforced by 0,5% steel fibres. This is however not a good comparison, since the results of the NDC are based on one test only!

Calculations on Young's Modulus on the NDC prisms gave higher values than compared to the LWAC prisms. The plotted curves are of similar shape as for the LWAC, while now the values taken at a relative stress- or load level of 50% showed values of Young's modulus between 25-30GPa

4.3.5.4 NDC in eccentric compression

Only five NDC prisms were eccentrically tested. The reason to why one test was not carried out was due to the explosive failure of the only tested unreinforced NDC prism in eccentric compression

Table 4.12 Maximum load P_{max} and load at failure P_{fail} for each NDC prism in eccentric compression

NDC - Eccentric			
Fibre [%]	Prism identity	P_{max} [kN]	P_{fail} [kN]
0,0	B3	717,03	717,03
	B4 ¹	-	-
0,5	B3	699,85	667,09
	B4	764,13	759,20
1,0	B3	777,34	764,45
	B4	805,81	798,17

¹ No test have been performed

The values presented in Table 4.12 represent the maximum load and load at failure for each eccentrically compressed NDC prism individually, while Table 4.13 presents the averaged values for maximum load, load at failure and the change in load between the two stages, for the three different types of NDC prisms in eccentric compression.

Table 4.13 Final averaged values for maximum load P_{max} , load at failure P_{fail} and change in load from peak state to failure P_{change} , for NDC prisms in eccentric compression

NDC - Eccentric			
Fibre vol. [%]	P_{max} [kN]	P_{fail} [kN]	P_{change} [%]
0,0	717,03	717,03	-
0,5	731,99	713,15	-2,57
1,0	791,58	781,58	-1,26

¹ The values in this table have been averaged based on values from Table 4.7

As can be calculated from Table 4.13, the maximum load have increased by 2,1- and 10,4% by addition of 0,5 – and 1,0% steel fibres respectively. Unlike the results from the eccentric tests on LWAC prisms, the loads have not change especially much from the state of maximum load until failure.

Table 4.14 Averaged strains for NDC Prisms in Eccentric loading

NDC – Eccentric loading					
Fibre vol. [%]	Direction of LVDT	Face	ϵ_{peak} [‰]	ϵ_{fail} [‰]	ϵ_{change} [%]
0 ¹	Longitudinal	North	3,079	3,079	-
		South	-0,323	-0,323	-
	Horizontal	North	-0,661	-0,661	-
		South	0,020	0,020	-
0,5	Longitudinal	North	3,138	3,362	7,1
		South	-0,501	-0,531	6,0
	Horizontal	North	-0,955	-1,057	10,7
		South	0,046	0,053	15,2
1,0	Longitudinal	North	3,773	4,290	13,7
		South	-0,635	-0,731	15,1
	Horizontal	North	-1,756	-3,094	76,2
		South	0,651 ²	0,711 ²	9,2

¹The value is only based on the results from one test only, which failed at peak load.

²The value is not averaged.

From Table 4.14 it can be seen that the inclusion of 0,5% of steel fibres into the NDC prisms which is eccentrically compressed have led to 1,9-, 55,1- and 44,5% increase of strains for the longitudinal north side, longitudinal south side and transversal north side, respectively. The south side transversal strains are of negligibly value.

The inclusion of 1,0% steel fibres however, led to an increase of 22,5-, 96,6- and 165,7% for the North side longitudinal strains, south side longitudinal strains and north side

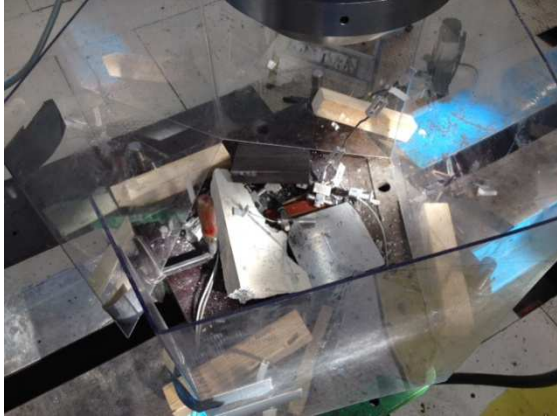
transversal strains respectively. The south side transversal strains for the 1,0% reinforced prisms that gave actual results.

This growth of strains at the state of maximum load by inclusion of different dosages of steel fibres is larger than for the LWAC prism. However, the increase in strains up to the point of failure is less than for the eccentrically compressed LWAC prisms. Especially when taking into account that the values given for the 1,0% reinforced prisms probably are taken from a stage prior to the actual failure.

The Young's Modulus calculated for the eccentric loaded prisms have been based on the stresses calculated for the maximum - and minimum stressed fibres, and will hence probably not be any good for the plastic range. However, the curves seem to have a good fit even for the plastic range, so it might be that the estimation of stresses for the eccentric loaded prisms wasn't too bad anyways.

The Poisson Ratios for the NDC prisms seems to be more or less identical to the Poisson Ratio for the LWAC prisms. The only slight difference from the LWAC to the NDC prisms is the earlier up-swing of the plotted curve, towards the end. This is due to the occurrence of cracks and acceleration of lateral displacements at an earlier relative load level. The results from the Young's Modulus and Poisson's ratio are expressed in curve form in Appendix C.

Calculations of the rotation capacity for the eccentrically loaded NDC prisms have been performed in a similar way as for the LWAC prisms, The results were also quite similar and have been expressed in Appendix C



*Figure 4.23 NDC 0,0% B3 eccentric,
Fraction of the prisms*



*Figur 4.26 NDC 0,0% B3 eccentric,
Fraction of prism*



*Figure 4.24 NDC 1,0% B4
eccentric, West face*



*Figure 4.25 NDC 1,0% B4
eccentric, North and West face*

5 Discussion of results

From evaluating the results from the tests some interesting observations were made. Due to the fact that there were not carried out more than two and two similar tests for each type of prism, it was hard to tell which of the two tests that made most sense. Nonetheless, suggestions and theories to explain the different behaviours were made based on the results and trends from the tests that seemed to be more or less valid.

No exact calculation of ductility have been carried out, due to the fact that it was hard to establish the transition from the elastic to plastic regime only based on two and two similar tests.

The increase of post peak strains have therefore been used as a indication of ductility.

Some of the hypothesis presented in the following chapter have been based on assumptions may be very thin. Nevertheless, the assumptions are to a certain degree based on either studied theory or observations made during the process.

5.1 LWAC prisms in centric compression

Based on Table 4.6 the inclusion of 0,5% steel fibres have given the best effect on the mechanical behaviour of the centric compressed LWAC prisms. Most important is the increase of post peak strains, which can be set in close relation to enhanced ductility.

The improved mechanical behaviour because of the inclusion of steel fibres seem to be due to steel fibres enhancing the confining effect which are ensuring a more controlled crack development, resulting in several more but still slimmer cracks.

The inclusion of steel fibres by the amount of 1,0% did not yield as good results on the mechanical behaviour as for the 0,5% reinforced prism. Possible explanations to this less enhanced mechanical behaviour could be due to uneven fibre dispersion, especially

towards the prisms faces, or because of incomplete filling of formwork due to a too large fibre dosage.

From the measurements of the fresh concretes, the LWAC with 1,0% steel fibres per volume fraction showed signs of slightly worse workability in terms of slump and sink values, than the LWAC with 0,5% steel fibres per volume fraction, ref.

Table 3.8.

The apparently worse workability for the 1,0%-LWAC consolidates the suggestion of uneven fibre and concrete dispersion as an explanation to the less enhanced mechanical behaviour by inclusion of steel fibres in the grade of 1,0%.

Another plausible explanation to the less good results for the 1,0% reinforced LWAC in centric compression is; the fibres in dosage of 1,0% confines the prisms in a such good manner that the confining effect will prevent the longitudinal cracks from growing in the lateral direction. The relative prevention of lateral growth of cracks will lead to less stress release around the cracks, resulting in larger shear stresses in these areas. The larger shear stresses will hence raise above the shear capacity of the prisms at a lower load than for the less reinforced concrete, which is to a larger grade allowed to laterally strain, resulting in a pure shear failure at a lower load, accompanied by smaller strains, both in axial and lateral direction. Ref. *Figure 4.5* and *Figure 4.3*.

This hypothesis are based on rather thin assumptions. (The work of Markeseth on the field of cracking at a meso level, seem however to validate the hypothesis to a certain grade.)

It can be seen that especially the transversal strains have improved a lot during the post peak regime for the LWAC prisms reinforced by 0,5% steel fibres. The greater growth of lateral strains are due to the forming and growth of longitudinal cracks, which when confined by the steel fibres can develop in a controlled manner.

Another interesting observation from comparing the results from Table 4.4 and Table 4.5 is that the prisms that reported largest compressive strength, respectively, failed in a more brittle manner. There can be several reasons to this more brittle behaviour, but a legitimate explanation to the results may be; when the cracks at maximum load are growing in width, the cracks of a prisms compressed by a higher load will accelerate faster and more uncontrolled than the cracks at a lower peak load. The faster crack growth will lead to a more sudden and more brittle failure, with less growth in lateral strains in the post peak regime. (The higher shear stresses for the higher load will fail more suddenly because of the combination of the shear cracks and tensile splitting cracks will form a shear band at lower strains, than the lower loads. Due to a more ductile combination of Shear stresses and lateral tensile stresses.

It is evident that the ductility for the centrally loaded LWAC prisms have been enhanced due to inclusion of fibres, especially in magnitude of 0,5%. The improved ductility is most likely a result of the improved tensile and the flexural strength, allowing the prism to laterally strain. These improvements are again due to the increased confinement altered by the steel fibres.

Common for all centrally compressed prisms were that they seemed to fail due to too high shear stresses, shear band going from high up on the east face towards the lower corner of the west face. Ref. *Figure 4.16*. The east face is always the casting surface.

For both unreinforced LWAC prisms in centric compression, several shear bands seemed to have formed. The main shear band going from top of the east face towards the lower edge of the west face. The secondary shear band seemed to be going from the top of the north face towards the lower edge of the face side. Ref fig(XX) For prism B2 it seemed like also a splitting crack going vertically through the prism from north face to south face, had formed. This tensile spitting crack may be explained by the quite large expansion of the lateral strains just prior to the maximum load.

For the reinforced LWAC prisms in centric compression, a shear band formed without any exception from top east towards bottom-west, only with slightly different inclination of shear band. The shear band seemed to consequently end at the bottom edge of the west side.

Shear stresses towards the top and bottom of the LWAC prisms in centric compression may have been amplified towards the edges of the respective face. This amplification was due to horizontal shear forces caused by the boundary constraints because of no “gliding” between the respective materials in the interface between concrete and steel plate. This increase of shear stresses may have had an impact on the shear band more often than not starting and ending at the very bottom or top of the prisms.

A plausible explanation of the failure mode of the unreinforced LWAC prisms in centric compression may be due to a relatively lower shear friction between the two wedges of a shear band, resulting in the shear failure preceding the tensile splitting failure.

An explanation to the failure modes of the reinforced LWAC prisms have already been given. Nonetheless, it seems like the steel fibres have a more pronounced effect on the tensile type of failure than shear failure.

A LWAC reinforced by an ideal amount of steel fibres are confined in such a way that the development of lateral strains is allowed to a certain point, ensuring stress release around the cracks. However at a certain load level, the shear stress capacity will be passed by the shear stress, forming a shear band, or a shear band in combination with tensile crack.

A LWAC which is too confined will not be allowed to laterally strain, leading to less stress release, resulting in the shear capacity being passed at an earlier load level, ending in a pure shear failure.

From studying the failed prisms, it seemed like the cracks had gone through the aggregates. It is hard to tell whether the microcracks initiated due to high lateral tension stress concentrations at top and bottom of aggregates leading to tension splitting of the aggregate, high shear stresses breaking the aggregates or due to failure of the mortar. A combination of the mentioned aspects seem however to be most likely.

It is obvious from the results that the fibres in appropriate dosages seem to improve tensile strength. It is however uncertain if the confinement directly enhances the shear stress capacity, or if the higher shear stress capacity is due to the more stress relaxation.

5.2 LWAC prisms in eccentric compression

The results of the LWAC in eccentric compression show a very good improvement of post peak strains with the inclusion of steel fibres. Especially do the strains for the inclusion of 0,5% of steel fibres seem to have improved a lot. Due to the fact that the strain values at the time of failure given in the tables for the 1,0% reinforced LWAC prism in eccentric loading, probably and absolutely (two separate tests) are taken from a load level prior to the actual failure, the improvement of the post peak strains are in reality much better than the improvement seen from the values presented in the tables!

If assuming the strains at failure for the 1,0% reinforced LWAC prisms are quite a bit larger than presented in the tables, the enhanced mechanical behaviour would be even better by inclusion of 1,0% steel fibres than for the inclusion of 0,5% steel fibres.

By assuming this, the previously established hypothesis of worse mechanical behaviour for the 1,0% reinforced LWAC prisms due to poor dispersion of concrete and fibres would be invalid.

Nonetheless, the improvement of mechanical behaviour and most of all development of strains through the post peak regime by the inclusion of steel fibres are a result of the combination of the confining effect due to steel fibres and the confining effect from the strain gradient.

By comparing the results for the centrically and eccentrically compressed LWAC prisms it seems to be reasonable to assume that the inclusion of steel fibres has a much more pronounced effect on LWAC prisms which is affected by a strain gradient.

A possible reason to this better effect of the steel fibres when a strain gradient is present may be that the combined confining effect from the steel fibres and the strain gradient allows for the concrete to strain quite a lot in lateral direction, ensuring stress release around the most stressed fibre, leading to the forming of final failure at higher much higher strains.

Based on this it seems to be reasonable to assume that the steel fibres have a more pronounced effect on the tensile cracks than the shear cracks.

The same observation of development of strains through the post peak regime has been observed for the eccentrically compressed LWAC prisms as for the centrally compressed LWAC prisms; the prism with the highest peak load respectively, seems to fail in a more brittle manner.

The biggest change recorded for the eccentric tests by inclusion of fibres are the improved lateral strains at the axially compressed north side and the longitudinal strains at the south side. These observations seem to be in accordance with the assumption of an enhanced tensile capacity for the reinforced LWAC.

From observing the eccentric compression tests being carried out, it seemed to be apparent that the ductility had improved a lot by the inclusion of steel fibres, due to the clearly visible curvature of the prisms just prior to failure.

The unreinforced LWAC prisms in eccentric compression failed due to blow out of most compressed fibres and the forming of a shear band.

The blowout failure seemed to have formed due to very large compressive stresses, forming two shear bands with opposite directions, forming a blow out of concrete.

The shear band of the other unreinforced prism seems to have formed due to the apparent larger stresses towards the east face than the west side. The longitudinal crack on the west side of the prism might be a tensile splitting crack, but this explanation do however not seem to be reasonable. It seems like the longitudinal crack may have formed due to a “blow out” of the upper wedge of the shear band, which did not go all the way through the prism.

The reinforced prisms seemed to have failed due to the combination of tensile splitting and shear stresses. The fibres seemed to have confined the prisms in such way that the prisms will be able to endure much larger strains, both in lateral and axial direction.

The primary shear bands seem to be going from the centre of the north face, to the top of the prism, while a secondary shear band are going from top of east face towards the

west face. This secondary shear band going from the top of the east to low down on the west face may be due to the higher strains and hence higher stresses at the west side

5.3 NDC prisms in centric compression

There were only performed one centric compression test on the NDC prisms. Hence, it is not possible to discuss on the change of mechanical behaviour by different dosages of fibres within. However, one can see a rather large difference in compression strength, strains at peak load, strain at failure and increase of strains trough the post peak regime, compared to the centric tested LWAC prisms with 0,5% of steel fibre reinforcement.

The larger strains can be explained by the less brittle material behaviour for NDC, due to initiation of microcracks at an earlier relative stress level and a more controlled crack propagation which than for the LWAC prism.

The prism failed in a very violent matter, plunging fractions around. Even if the failure seemed to be quite brittle, the inelastic strains prior to failure are witnessing of a ductile behaviour, ref. *Figure 4.8*.

5.4 NDC prisms in eccentric compression

The results for the eccentric compression tests of the NDC prisms showed increasing mechanical behaviour with increasing dosages of steel fibres, ref Table 4.14. The transversal strains were in especial much better for the prisms reinforced by 1,0% steel fibres than for those reinforced by 0,5%

The reason for the improved mechanical behaviour seems to be due to the confining effect from the steel fibres.

Comparing the strain results from the centric NDC test to the eccentric test on the unreinforced NDC prism, the confining effect of the strain gradient seem to be obvious, ref. *Figure 4.17*. The inclusion of steel fibres seems to further magnify the confining effect from the strain gradient with a great deal.

Comparing the increase of strains for the steel fibre reinforced NDC eccentric compression tests to the steel fibre reinforced LWAC compression tests, the increase of strains in the post peak regime seem to have been quite a lot better for the LWAC than for the NDC, indicating that the fibre reinforcement have a more pronounced effect on the LWAC than on the NDC.

For the eccentrically compressed NDC prisms it seemed to be obvious that the larger dosage of steel fibres had the best effect on the mechanical behaviour. This might indicate that there is an even larger potential in the NDC in terms of enhanced mechanical behaviour if more even more reinforced than by 1,0% of steel fibres.

From observing the tests it seemed to be obvious that the ductility had improved a lot by the inclusion of steel fibres, due to a rather curved prism just prior to failure.

The failure of the unreinforced NDC prism in eccentric compression was quite explosive, and it was hence difficult to observe any clear failure band. However from the different fractions it seemed like the final failure bands were inclined, thus the prisms seemed to have failed due to too high shears tresses.

For the reinforced NDC prisms in eccentric compression, the failure seemed to have been caused by either shear cracks going all the way through the prism, or by smaller inclined cracks in combination with tensile splitting cracks.

5.5 General observations

From evaluating the results there were made some quite interesting observations on the recordings from the different LVDTs. As can be seen in Appendix C, the calculated strains varied quite a lot from the four different LVDTs per prism.

By studying the curves plotted for the stress-strain and load-strain curves, several patterns were discovered.

For the centrally compressed LWAC prisms the strains calculated for the 30cm LVDTs were without exceptions larger than for the strains calculated by the 20cm LVDTs.

The strains for the north side were also larger than for the south side.

Eccentrically loaded LWAC prism: The pattern was not as explicit, but nonetheless: the strains for the 30cm LVDT on the north side were more often than not larger than the strains for the 20cm LVDT up to the point of peak load, while the 20cm strains got larger than the 30cm strains during the post peak behaviour.

NDC-Eccentric: the longitudinal strains at the compressed north side seem to be equal up to the point where the microcracking starts, from that point the strains from the 20cm LVDTs increases more than the 30cm LVDTs.

The pattern of larger strains for the 30cm LVDTs than the strains for the 20cm LVDT can of course be due to poor recordings, but this seems very unlikely.

As both 30cm LVDTs from the North and South face are mounted towards the east edge of their face respectively, it seems like the east face have been more compressed than the west side.

An explanation to this pattern could be a slightly inclined load pointing towards east. Another explanation to the larger strains at the east and north side, could be due to poor centring of either prism or/and spherical ball bearing. Just a slight displacement of the load would yield quite large differences in strains.

However, the most likely reason to the more compressed east side is due to the east side always being the casting surface. The concrete was poured into the formwork consequently with the “eastside” facing up. Even if ACI 213R-87 [19] claims that there will be no floating of lighter aggregates for concretes with slump values below 100mm, it seems to be highly possible that some of the lighter aggregates might have floated towards the casting surface, while some of the heavier particles have sunk towards the bottom of the formwork during the first hours of hardening, even if the slump value were well below 100mm for LWACs.

“Floating and sinking” of aggregates would have led to a weaker and less rigid concrete towards the casting surface while at the same time stronger and more rigid concrete towards the bottom of the formwork.

If this explanation is valid, it would also explain the evident pattern of shear bands starting at the east face.

The suggested explanation of the more strained east side does not explain the more compressed north face compared to the south side. Thus it seems likely that the more compressed north face is due to a slightly inclined load, pointing towards north, which would be magnified by the spherical ball bearing, or because of the prism being consequently slightly out of position to the same side every time. These suggestions might seem to be valid due to the fact that there are certain uncertainties regarding the geometry and the accurateness of the test machine, as it has only been manually calibrated in terms of position and alignment.

The suggestion of a less rigid concrete towards the casting surface due to “floating” and “sinking” of different particles do also explain the larger strains found towards the east face of the prism even in the eccentrically compressed tests. The difference in strains was however less pronounced.

The strains from the 20cm LVDTs developing to be larger than the strains from the 30cm LVDTs during the post peak regime were only observed for the reinforced LWAC prisms, probably due to the very modest post peak existence of the unreinforced LWAC prisms. Nonetheless, the development of the strains at the north side can be explained by localization of strains and strain-softening due to the development of the final failure band. Put in other words, if the concrete masses just around the final failure band would be displaced by one millimetre, this one millimetre would give a larger increase of the strains for the 20cm LVDT than for the 30cm LVDT.

The difference in strains from the 20 and 30cm LVDTs for the inelastic regime on the north side of the eccentrically compressed NDC prisms can probably not be explained by the “floating” and “sinking” theory, due to no light aggregates.

However a explanation that may be valid is the forming of a final failure band which have been recorded by both vertical LVDTs. If the concrete masses just around the failure band would be compressed by one millimetre, this one millimetre would give a larger increase of the strains for the 20cm LVDT than for the 30cm LVDT.

An ironic bi-result of this thesis has been observed for the strength-to-weight ratio. The poor strength-to-weight ratio for NDC was one of the reasons for the introduction of LWAC. LWAC was supposed to yield a better strength-to-weight ratio due to lower density at the same strength. However, from the work performed in this thesis, it seems like the strength-to-weight ratio is even worse for the LWAC than for the NDC. At least if one by strength refers to the compressive strength or load bearing capacity for the prisms respectively. If strength rather meant ductility, tensile strength or flexural strength, the strength-to-weight ratio would at least be better for the reinforced LWAC prisms in eccentric compression than for the reinforced NDC prisms in eccentric compression.

It seems to be obvious that the ductility have improved a lot for the LWAC with induced steel fibres, especially for those in eccentric compression. The improvement of toughness has however not been by far as good. This is due to the large drop of load bearing capacity as the concrete is straining in the post peak behaviour.

6 Conclusion and suggestion to further work

6.1 Conclusion

The work performed in this thesis has to a certain degree confirmed some of the theory on the field of improved ductility by fibre induction into LWAC.

The inclusion of steel fibres of 60mm length, with cramped ends in dosages of 0,5% and 1,0% per volume fraction, into LWAC have proved to have a positive effect on the mechanical behaviour of LWAC prisms in compression.

The results from the centric tests were however not as good as anticipated based on studies of previous performed work. Especially was the inclusion of fibres by the amount of 1,0% not particularly good and showed only a very slight improvement of ductility, compared to the unreinforced LWAC prisms in centric compression.

For the eccentrically compressed LWAC prisms however, the improvement of mechanical behaviour was of great magnitude and the improvement got increasingly better with increasing amount of steel fibres.

The tests on the LWAC prisms reviled that the inclusion of steel fibres have a much more pronounced effect on eccentrically compressed prisms than prisms in centric compression. These result indicate that the application of steel fibres to LWAC have a larger effect on specimens where a strain gradient is present or in general when exposed to large tension stresses.

From the relatively slim amount of tests performed on NDC prisms it is obvious that the mechanical behaviour is better for NDC without steel fibres than for LWAC without steel fibres.

However, by comparing the results from the eccentric tests of LWAC and NDC it is obvious that the steel fibres have a more pronounced effect on the ductility of LWAC than NDC when a strain gradient is present.

6.2 Suggestion to further work

For the purpose of further work I have some suggestions to actions that probably will improve the quality of the work:

1: Perform several more tests per type of prism! This is due to the fact that a larger database of recorded results would give a better foundation for the calculation of the results, give a better establishment of a normal value and will hence help to validate the discussed result.

2: Place the LVDTs further towards the edges of the respective faces to get a better recording of the assumed most strained fibres.

3: Try to measure the displacements in a three dimensional manner, by the use of a DIC. If the DIC (Digital Image C...) would have recorded the results in an adequately detailed manner, this would have given a much better impression of displacements and strains for all directions, for the entire prism. Hence it would have been easier to capture the point of failure, both in terms of time and location.

4: Digital adjustment and calibration of the test machine and positioning of prisms would have reduced the risk of poor and uneven recordings caused by a slight inclination or displacement.

5: Make sure that the test machine is able to load all prisms until failure.

6: Use a more solid cover around the prism to avoid injuries caused by flying concrete particles.

7: Compress the prism at a slower pace to get a more explicit impression of the behaviour in terms of strain developing and load loss for the post peak regime. If possible, a more sensitive testing machine which could adjust the pace and magnitude of load and displacement would also have given a more detailed impression of the mechanical behaviour and development around failure.

8: Make the geometry of the prism more slender to be sure to avoid any effects from the boundary restraints on the forming end developing of the final failure. A slenderness of 3,0 could yield "better" results.

9: Cut some of the prisms in two, to check the fibre dispersion and if possible register an effect of floating and sinking of lighter and heavier particles respectively.

10: Try to make the compression strength capacity for the LWAC and NDC more similar, so that the actual mechanical behaviour can be tested at relatively equal strength. From the results above it would be interesting to compare the mechanical behaviour for NDC and LWAC at the same loads.

7 Siterte verk

- [1] Judy Brewer c/o MMAST Modules, History of Concrete, Urbana, Illinois.
- [2] Cement Trust, "What is the development impact of concrete?," [Online]. Available: <http://cementtrust.wordpress.com/a-concrete-plan/>.
- [3] Håvard Nedrelid, Towards a better understanding of the ultimate behaviour of lightweight aggregate concrete in compression and bending., Trondheim: Ntnu, 2012, p. 7.
- [4] Richard C. Dorf, "Material Properties," in *The engineering handbook, second edition*, New York: CRC Press, 1996.
- [5] F.P. Zhou, A. NAdeem, A.Y.T Leung, RV Balendran, "Influence of steel fibres on strength and ductility of normal and lightweight high strengthconcrete," *Building and Environment*, no. 37, pp. 1361-1367, Desember 2002.
- [6] Payam Shafiq, Hilmi Bin Mahmud, Mahmoud Hassanpour, "Lightweight aggregate concrete fiber reinforcement – A review," *Construction and Building Materials*, pp. 452-461, 5 September 2012.
- [7] Weber-Norge, "Weber-Norge.no," 01 Januar 2014. [Online]. Available: <http://www.weber-norge.no/lecar-lettklinker/produkter-loesninger/leca-lettklinker/leca-lettklinker-loes-leca/lecar-lettklinker-2-4-mm.html>. [Accessed 24 April 2014].
- [8] Gro Markeset, Erik Thorenfeldt, Einar AAssved HANSEN, "Brite EuRam Project 5480, Economic Design and Construction with High Strength Concrete, Task 2: Mechanical Properties, CONCRETE BRITTLENESS," SINTEF, 1994.
- [9] Wikipedia, "Brittleness," [Online]. Available: <http://en.wikipedia.org/wiki/Brittleness>. [Accessed 28 April 2014].
- [10] BIG Barr, FD Lydon, FP Zhou, "Fracture mechanical propertties of high strength concrete

- with varying silica fume contents and AGGREGATES," in *Fracture mechanical properties of high strength concrete with varying silica fume contents and AGGREGATES*, Cem Concr Res, 1994, pp. 543-552.
- [11] A Dvorkin, L Dvorkin, "Basics of Concrete Science," 2006. [Online]. Available: <http://www.scribd.com/doc/6004561/Basics-of-Concrete-Science>. [Accessed 1 Mai 2014].
- [12] PJ Monterio, PK Metha, *Concrete; microstructure, properties and materials*, 3. ed., 3 ed., New York: McGraw-Hill, 2006.
- [13] L Domagala, "Modification of properties of structural lightweight concrete with steel fibres," in *LENGVOJO BETONO SAVYBIŲ MODIFIKAVIMAS PLIENINĖMIS FIBROMIS*, Taylor&Fracins, 2011, pp. 36-44.
- [14] L Bertsson, S Chandra, "Lightweight aggregate concrete, science, technology and applications," Noyes/William, 2002.
- [15] M Chanbaz, IB Topcu, "Effect of different fibres on the mechanical properties of concrete containing fly ash," in *Constructinon and Building Materials*, Elsevier Lt., 2007, pp. 1486-1491.
- [16] F Altun, I Yigit, Y Sahin, F Koksai, "Combined effect of silica fume and steel fibre on the mechanical properties of high strength concretes," in *Constructions and Building Materials*, vol. 22, 2008, pp. 1874-1880.
- [17] LS Li, CC Chang. CL Hwang, CT Tsai, "Durability design consideration and application of steel fibre reinforced concrete in Taiwan," in *Arabian Journal for Science and Engineering*, vol. 34, 2009, pp. 57-79.
- [18] N Mariaglia, M Papia, G Campione, "Mechanical properties of steel fibre reinforced lightweight concrete with pumice stone or expanded clay aggregate," in *Materials and structures*, vol. 34, 2001, pp. 201-210.
- [19] American Concrete Institute, *ACI 213R-87 - Guide for Structural Lightweight Concrete*, American Concrete Institute, 1987, p. 27.
- [20] N Dhang, AP Gupta, MC Nataraja, "Stress-strain curves for steel-fibre reinforced concrete under compression," Kharagpur, India, 1999.
- [21] DJ Hannant, RIT Williams, J Eddington, "Steel fibre reinforced concrete.," in *Materials and structures*, Kluwer Academic Publishers, 1974, pp. 154-170.
- [22] Tore Myrland Jensen, Jan Arve Øverli, "Experimental study on flexural duc- tility in over-

- reinforced lightweight aggregate concrete beams," SINTEF, Oslo, 2013.
- [23] SP Shah, N Balaguru, "Fiber reinforced cement composites," New York, MacGraw-Hill, 1992, pp. 179-214.
- [24] M Shekarchi, M Mhoutian, P Sorousian, NA Libre, "Mechanical properties of hybrid fiber reinforced lightweight aggregate concrete made with natural pumice," in *Construction and Building Materials*, vol. 25, 2011, pp. 2458-2464.
- [25] G. MArkeset, "Failure of concrete under compressive strain gradients Phd," NTH (Ntnu), Trondheim, 1993.
- [26] G. Markeset, "Failure of concrete under compressive strain gradients," Nth, Trondheim, 1993.
- [27] P. Schumaker, "Rotation Capacity of Self-Compacting Steel Fibre Reinforced Concrete," Darmstadt University, 2006.
- [28] P. Langer, "Verdrehfähigkeit plastizierter Tragwerksbereiche im Stahlbetonbau," University of Stuttgart, Stuttgart, 1987.
- [29] C. Graubner, "Schnittgrößenverteilung in statisch unbestimmten Stahlbetonbalken unter Berücksichtigung wirklichkeitsnaher Stoffgesetze -- Baustoffbedingte Abweichungen von elastizitätstheoretischen und plastizitätstheoretischen Lösungen," TU Munic, Munic, 1989.
- [30] A. Bigaj, "Structural Dependence of Rotation Capacity of Plastic Hinges in RC Beams and Slabs," Delft University of Technology, Delft, 1999.
- [31] P. Schumacher, "Rotation Capacity on self-compacting steel fibre reinforced concrete," Darmstadt, Darmstadt, 2006.
- [32] P. Schumacher, "Rotation Capacity of Steel Fibre Reinforced Self-Compacting Concrete," Darmstadt, 2006.
- [33] H Weigler, S Karl, P Grübl, *Beton*, Berlin: Ernst & Sohn Verlag, 2001.
- [34] AJ Bigaj-van Vliet, U. Mayer, "Round Robin analysis of available rotation capacity of plastic hinges- Evaluation," 1998.
- [35] D Abrishami, HH Mindess. S. Mitchell, "The effect of steel fibers and epoxy-coated reinforcement on tension stiffening and cracking of reinforced concrete," 1996.
- [36] C. D. R. Sangha, *Strength and complete Stress-Strain relationships for Concrete Tested in Uniaxial Compression Under Different Testing Conditions*, 5 ed., RILEM, Materieux et

Constructions, Vol 5, 1972, pp. 361-370.

- [37] M. Kotsovos, "Effect of Testing Techniques on the Post-Ultimate Behaviour of Concrete in Compression," vol. Vol 16, no. 91, pp. 3-12, 1983.
- [38] N. AS, "HeidelbergCement," [Online]. Available:
http://www.heidelbergcement.com/no/no/norcem/sementtyper/standard_fa.htm.
[Accessed 9 Mail 2014].
- [39] P.-. A. C. Manufactures, "PCA- America's Cement Manufactures," PCA, [Online]. Available:
<http://www.cement.org/for-concrete-books-learning/concrete-technology/durability/alkali-aggregate-reaction>. [Accessed 9 Mai 2014].
- [40] Betongelement.no, "Betongbok Bind D, Del 2, D10, Bestandighet av Betong og Stål," [Online]. Available:
http://www.betongelement.no/betongbok/BindD/Del_2/D10/10_2_4_Alkalireaksjoner.pdf.
[Accessed 9 Mai 2014].
- [41] Wikipedia, "Pozzolan," [Online]. Available: <http://en.wikipedia.org/wiki/Pozzolan>.
[Accessed 9 Mai 2014].
- [42] Bekaert, "Bekaert," 2008. [Online]. Available: www.bekaert.com/dosingdramix.
- [43] N. Betongforening, "Lettbetong, Prosjektveiledning," Oslo, 1999.
- [44] P. M. PK Mehta, "Concrete; microstructure, properties and material, 3. ed," New York, New York: McGraw-Hill, 2006.
- [45] G. Markeset, "Failure of Concrte under Compressive Strain Gradinets," NTH, Trondheim, 1993.
- [46] Wikipedia, "en.wikipedia.org/wiki/Expanded_clay_aggregate," [Online].
- [47] University of Michigan, "<http://ace.mrl.engin.umich.edv>," [Online].


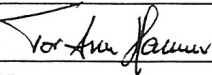
Appendix

A. Appendix Water absorption of aggregate

The approach and results of determination of the one-hour water absorption amount, the water content and the particle density of the different aggregates.

There were performed tests on both Lightweight aggregates and “ordinary” aggregates. The results presented in Appendix A is however only for the Lightweight aggregates.

A.a Appendix Description of testing procedure

 SINTEF SINTEF Konstruksjoner og betong Postadresse: 7034 Trondheim Foretaksnr.: 948007029		KVALITETSSIKRING		
		GJELDER: PRØVING AV LETT-TILSLAG - partikkeldensitet og 1-times vannabsorpsjon		
DATO: 1993-11-02		GRADERING: Intern	GODKJENT AV: Tor Arne Hammer 	GYLDIG FRA: 1993-11-08
IB NR: KS 70 119	UTGAVE NR: 2	ELEKTRONISK ARKIVKODE: I:\KA\PRO\709110\XOSKE085.W51		ANTALL SIDER: 1

1 Begrensning

Metoden kan benyttes for lett-tilslag med partikkelstørrelser fra 1-16 mm

2 Utstyr

- Tørkeskap
- Pyknometerkolbe med trang, gradert hals, 1000 ml
- Vekt 0-6 kg

3 Gjennomføring

- To tilslagsprøver, begge på ca 0,5 kg, vaskes på en sikteduk ett nivå finere enn nedre fraksjonsgrense, og tørkes deretter ved 105°C i 1 døgn. Tilslaget avkjøles.
- Pyknometerkolben fylles med tilslag, ca 2/3 full. Netto tørr tilslagsmengde i kolben (m_t) bestemmes. Kolben fylles opp med vann.
- 1 time etter vannutsetting etterfylles kolben til 1000 ml (V_k), netto vekt av vann og tilslag i kolben (m_k) bestemmes.
- Vannet siles av kolben, tilslaget helles ut og overflatetørkes ved hjelp av en fuktig, ikke loende bomullsklut eller lignende. Det skal ikke forekomme fritt vann på tilslagsoverflatene etter denne behandlingen, men heller ikke fargeomslag pga uttørking. Vekten av det fuktige tilslaget (m_f) bestemmes.
- Tilslaget tørkes i tørkeskap ved 105 °C i 1 døgn. Tørr vekt etter endt forsøk (m_d) bestemmes.

4 Beregning

Dersom m_d avviker fra m_t med mer enn 0,2 % for noen av prøvene skal forsøket forkastes og gjentas.

1 times vannabsorpsjon, w_{1t} , bestemmes som: $w_{1t} = 100(m_f - m_t) / m_t$

Dersom forskjellen i 1 times vannabsorpsjon mellom prøvene er større enn 0,4 % absorpsjon skal resultatene forkastes og forsøket gjentas.

Tørr partikkeldensitet, Q_p , bestemmes som: $Q_p = m_t / (V_k - (m_k - m_f)/Q_w)$
der Q_w er vannets densitet.

Dersom forskjellen i partikkeldensitet mellom prøvene er større enn 50 kg/m³ skal resultatene forkastes og forsøket gjentas.

5 Rapportering

1 times vannabsorpsjon rapporteres med en desimal, tørr partikkeldensitet rapporteres uten desimaler.

A.1.

B.1.

C.1.

D.1.

E.1.

F.1. Appendix Dry LECA aggregate

A.b Appendix 1-times vannabsorpsjon, dry LECAaggregate

KS70 119 1-times vannabsorpsjon og partikkeldensitet, for tørt LECA tilsag

Bunn

Målt /resultat	2-4		4-8	
	Prøve 1	Prøve 2	Prøve 1	Prøve 2
Volum av kolbe (cm ³)	1000,00		1000,00	
Vekt av kolbe (g)	296,24		299,50	
Vekt av tørt tilslag og kolbe (g)	530,20		933,90	
Vekt av vann, tilslag og kolbe (g)	1123,80		1495,30	
Vekt av fuktig tilslag (g)	270,10		679,20	
Vekt av fuktig tilslag etter trykktank (g)				
Tørr sluttvekt (g)	233,00		633,30	
Tørr Partikkeldensitet (kg/m ³)	528,68		1312,37	
1-times vannabsorpsjon (%)	15,45		7,06	
Trykkmetning (%)	-		-	

Midt

Målt /resultat	2-4		4-8	
	Prøve 1	Prøve 2	Prøve 1	Prøve 2
Volum av kolbe (cm ³)	1000,00		1000,00	
Vekt av kolbe (g)	294,70		291,92	
Vekt av tørt tilslag og kolbe (g)	528,90		870,90	
Vekt av vann, tilslag og kolbe (g)	1128,70		1475,50	
Vekt av fuktig tilslag (g)	280,50		618,90	
Vekt av fuktig tilslag etter trykktank (g)				
Tørr sluttvekt (g)	233,20		578,20	
Tørr Partikkeldensitet (kg/m ³)	524,52		1330,01	
1-times vannabsorpsjon (%)	19,77		6,89	

Trykkmetning (%)	-	-
------------------	---	---

Topp

Målt /resultat	2-4		4-8	
	Prøve 1	Prøve 2	Prøve 1	Prøve 2
Volum av kolbe (cm ³)	1000,00		1000,00	
Vekt av kolbe (g)	320,90		298,37	
Vekt av tørt tilslag og kolbe (g)	539,00		897,00	
Vekt av vann, tilslag og kolbe (g)	1163,20		1481,00	
Vekt av fuktig tilslag (g)	257,40		641,10	
Vekt av fuktig tilslag etter trykktank (g)				
Tørr sluttvekt (g)	216,80		597,38	
Tørr Partikkeldensitet (kg/m ³)	525,42		1305,71	
1-times vannabsorpsjon (%)	18,02		7,09	
Trykkmetning (%)	-		-	

A.c. Appendix Dense LECA aggregate

KS70 119 1-times vannabsorpsjon og partikkeldensitet for fuktig LECA tilslag

Bunn

Målt /resultat	2-4		4-8	
	Prøve 1	Prøve 2	Prøve 1	Prøve 2
Volum av kolbe (cm ³)	1000,00		1000,00	
Vekt av kolbe (g)	296,24		299,50	
Vekt av tørt tilslag og kolbe (g)	549,90		950,00	
Vekt av vann, tilslag og kolbe (g)	1128,90		1563,10	
Vekt av fuktig tilslag (g)	291,10		662,60	
Tørr sluttvekt (g)	252,50		550,20	
Partikkeldensitet (kg/m ³), fuktig	602,52		1681,31	
1-times vannabsorpsjon (%)	14,76		1,86	
Partikkeldensitet ved lagring (kg/m ³)	553,31		1630,33	
Absorbent fuktighet i tilslag ved lagring	0,46 %		18,23 %	

Midt

Målt /resultat	2-4		4-8	
	Prøve 1	Prøve 2	Prøve 1	Prøve 2
Volum av kolbe (cm ³)	1000,00		1000,00	
Vekt av kolbe (g)	294,70		291,92	
Vekt av tørt tilslag og kolbe (g)	515,30		918,19	
Vekt av vann, tilslag og kolbe (g)	1122,50		1535,80	
Vekt av fuktig tilslag (g)	262,50		640,80	
Tørr sluttvekt (g)	219,50		637,00	
Partikkeldensitet (kg/m ³), fuktig.	561,61		1637,78	
1-times vannabsorpsjon (%)	18,99		2,32	

Partikkeldensitet ved lagring	507,48		1577,82	
Absorbent fuktighet i tilslag ved lagring	0,50 %		-1,68 %	(?!)

Topp

Målt /resultat	2-4		4-8	
	Prøve 1	Prøve 2	Prøve 1	Prøve 2
Volum av kolbe (cm ³)	1000,00		1000,00	
Vekt av kolbe (g)	320,90		298,37	
Vekt av tørt tilslag og kolbe (g)	563,20		1024,10	
Vekt av vann, tilslag og kolbe (g)	1152,70		1579,00	
Vekt av fuktig tilslag (g)	285,70		748,40	
Tørr sluttvekt (g)	240,50		637,00	
Partikkeldensitet (kg/m ³), med faktisk fuktigh.	590,26		1630,49	
1-times vannabsorpsjon (%)	17,91		3,12	
Partikkeldensitet ved lagring	533,82		1551,47	
Absorbent fuktighet i tilslag ved lagring	0,75 %		13,93 %	

B. Appendix Matrixes

Appendix B. presents the matrixes for the six different concretes.

The proportioning, material state for fresh concrete, mixing procedure, density, water content are presented in this Appendix.

The LWAC concrete comes first, whit increasing steel fibre content, then the NDC with increasing steel fibre contetnt.

B.a. Appendix Matrix of LWAC without steel fibre reinforcement

**Proporsjonering av betong
LWAC 1800 0% Dramix 65/60 3D**



©2008-11-12 ss

Utført av	Firma	Dato
G. Kjellmark	SINTEF Byggforsk	25.02.2013

Initialparametre	Verdi	K
$v/(c+\Sigma kp)$	0,38	-
s/c (silikastøv) [%]	10,0	2,00
f/c (filler, flyveaske) [%]	1,0	0,00
Luftinnhold [%]	2,0	-
Tilsetningsstoff	% av C	% av S
Dynamon SX-N	1,80	0,00
	0,00	0,00
Fiber	Vol %	
Dramix 65/60 3D	0,0	
	0,0	
Matriks	Verdi	
Ønsket matriksvolum [l/m^3]	400	
Oppnådd matriksvolum** [l/m^3]	400	
Volum sementlim [l/m^3]	375	
v/p	0,36	



**Tilpass matriksvolum; Ctrl M

Sett "Oppnådd" lik "Ønsket"; Ctrl N

Proporsjonert betong

Materialer	kg/m ³
Norcem Standard	454,4
Elkem Microsilica 940U (A-4066)	45,4
Kalksteinsmel	4,5
Fritt vann	207,2
Absorbert vann	30,7
Leca 2-4 mm (A-4048)	119,2
Leca 800 4-8 mm (A-4048)	230,7
0/8mm NSBR (A-3995)	431,3
0/2mm vasket maskin (A-3726)	269,6
	0,0
	0,0
Dynamon SX-N	8,18
	0,00
Dramix 65/60 3D	0,0
0,0	0,0
Prop. betongdens. (kg/m ³)	1795

Ønsket Oppnådd

kg	kg
45,4	45,4
4,5	4,5
0,5	0,5
20,7	20,7
3,1	3,1
11,9	11,9
23,1	23,1
43,1	43,1
27,0	27,0
0,0	0,0
0,0	0,0
0,82	0,82
0,00	0,00
0,0	0,0
0,0	0,0

Materiale	Densitet * [kg/m ³]	Tørrestoff [%]	Alkalier [%]	Klorider [%]
Norcem Standard	3150	-	0,00	0,00
Elkem Microsilica 940U (A-4066)	2200	100	0,00	0,00
Kalksteinsmel	2740	100	0,00	0,00
Dynamon SX-N	1060	18,5	0,50	0,10
	1100	0	0,00	0,00
	1200	0	0,00	0,00
	1000	0	0,00	0,00
Dramix 65/60 3D	7800	-	-	-
0	7800	-	-	-

*For sement, pozzolaner og fillere oppgis densitet av tørrestoff. For TSS oppgis våt densitet.

***Nullstill korreksjon; Ctrl K

Fersk betong

Egenskap	
Ønsket volum	100,0
Innveid volum (l)	100,0
Luftinnhold (%)	2,0
Målt betongdensitet (kg/m ³)	1795
Effektivt v/(c+Σkp)	0,380

Aggressiver	
Kloridinnhold [% av cem.]	0,00
Alkalier [kg/m ³]	0,04
Andel reakt. bergarter [%]	0,0

Volumkorreksjon***

korr.luft	korr.dens	Korrigert
0,0	0,0	454,4
0,0	0,0	45,4
0,0	0,0	4,5
0,0	0,0	207,2
0,0	0,0	30,7
0,0	0,0	119,2
0,0	0,0	230,7
0,0	0,0	431,3
0,0	0,0	269,6
0,0	0,0	0,0
0,0	0,0	0,0
0,0	0,0	0,0
0,0	0,0	0,0
0,0	0,0	0,0
0,0	0,0	0,0
0,0	0,0	8,18
0,0	0,0	0,00
0,0	0,0	0,00
0,0	0,0	0,00
0,0	0,0	0,0
0,0	0,0	0,0
0,0	0,0	1795

Prosj./id.: LWC 1800 0% Dramix 65/60 3D, Blandeskjema

Blandevidde:	100 liter
Dato:	
Tidspunkt for vanntilsetning	
Ansvarlig:	
Utført av:	

Materialer	Resept kg/m ³	Sats kg	Fukt* %	Korr. kg	Oppveid** kg	
Norcem Standard	454,4	45,444			45,444	
Elkem Microsilica 940U (A-4066)	45,4	4,544	0	0,000	4,544	
Kalksteinsmel	4,5	0,454	0	0,000	0,454	
Fritt vann	207,2	20,722		-2,058	18,665	21,730
Absorbent vann	30,7	3,066			3,066	
Leca 2-4 mm (A-4048)	119,2	11,923	0,0	0,000	11,923	
Leca 800 4-8 mm (A-4048)	230,7	23,072	0,0	0,000	23,072	
0/8mm NSBR (A-3995)	431,3	43,129	2,6	1,121	44,250	
0/2mm vasket maskin (A-3726)	269,6	26,955	1,0	0,270	27,225	
0	0,0	0,000	0,0	0,000	0,000	
	0,0	0,000	0,0	0,000	0,000	
	0,0	0,000	0,0	0,000	0,000	
Dynamon SX-N	8,2	0,818	81,5	0,667	0,818	
	0,0	0,000	100	0,000	0,000	
	0,0	0,000	100	0,000	0,000	
	0,0	0,000	100	0,000	0,000	
Dramix 65/60 3D	0,0	0,000			0,000	
0	0,0	0,000			0,000	

** NB! Våte mengder, også for pozzolaner og fillere

*Se fotnote på delark "Proporsjonering"

Fersk betong					
Tid etter vanntilsetning					
Synkmål	T-50	1,88	s		
Utbredelsesmål		590	mm		
Luft		7	%		
Densitet		1696,65	kg/m ³		

Sammensatt tilslag

Fraksjon	Navn	Densitet	Abs. fukt	Alk. reakt.	Klorider	Andel		Bruk
		[kg/m ³]	[%]	[%]	[%]	volum	vekt	
I	Leca 2-4 mm (A-4048)	590	17,9	0,0	0,00	0,334	0,130	ok
II	Leca 800 4-8 mm (A-4048)	1630	3,1	0,0	0,00	0,234	0,220	ok
III	0/8mm NSBR (A-3995)	2680	0,3	0,0	0,00	0,266	0,400	ok
IV	0/2mm vasket maskin(A-3726)	2680	0,3	0,0	0,00	0,166	0,250	ok
V		2680	0,3	0,0	0,00	0,000	0,000	
VI		2700	0,0	0,0	0,00	0,000	0,000	
VII		2700	0,0	0,0	0,00	0,000	0,000	
VIII		2700	0,0	0,0	0,00	0,000	0,000	
IX		2700	0,0	0,0	0,00	0,000	0,000	
X		2700	0,0	0,0	0,00	0,000	0,000	
Sam.		1673		0,0	0,00	1,000	1,000	

Finhetsmoduler	
FM _{vekt} =	3,61
FM _{vol} =	3,99
FM _{ref} =	4,00
FM _g =	5,07

Åpning	Gjennomgang		Ref. grad. [vol. %]	Vekt ved tilpasning
	vol.[%]	vekt [%]		
32	100,0	100,0	100,0	1
22,4	100,0	100,0	100,0	1
16	100,0	100,0	100,0	1
11,2	100,0	100,0	99,4	1
8	99,3	98,9	95,7	1
4	71,0	69,6	64,8	1
2	31,5	47,4	34,6	1
1	23,2	34,9	25,3	2
0,5	15,0	22,6	16,9	2
0,25	8,5	12,8	10,1	2
0,125	4,2	6,3	4,9	2
0,063	1,5	2,2	2,4	2

B.b. Appendix Matrix for LWAC with 0,5% steel fibre reinforcement

**Proporsjonering av betong
LWAC 1800 0,5% Dramix 65/60 3D**



©2008-11-12 ss

Utført av	Firma	Dato
G. Kjellmark	SINTEF Byggforsk	25.02.2013

Initialparametre	Verdi	k
$v/(c+\Sigma kp)$	0,38	-
s/c (silikastøv) [%]	10,0	2,00
f/c (filler, flyveaske) [%]	1,0	0,00
Luftinnhold [%]	2,0	-
Tilsetningsstoff	% av C	% av S
Dynamon SX-N	1,80	0,00
	0,00	0,00
	0,00	0,00
	0,00	0,00
Fiber	Vol %	
Dramix 65/60 3D	0,5	
	0,0	
Matriks	Verdi	
Ønsket matriksvolum [l/m^3]	400	
Oppnådd matriksvolum** [l/m^3]	400	
Volum sementlim [l/m^3]	375	
v/p	0,36	



**Tilpass matriksvolum; Ctrl M

Sett "Oppnådd" lik "Ønsket"; Ctrl N

Proporsjonert betong

Materialer	kg/m^3
Norcem Standard	454,7
Elkem Microsilica 940U (A-4066)	45,5
Kalksteinsmel	4,5
Fritt vann	207,3
Absorbent vann	30,4
Leca 2-4 mm (A-4048)	118,2
Leca 800 4-8 mm (A-4048)	228,7
0/8mm NSBR (A-3995)	427,6
0/2mm vasket maskin (A-3726)	267,2
	0,0
Dynamon SX-N	8,18
	0,00
Dramix 65/60 3D	39,0
0,0	0,0
Prop. betongdens. (kg/m^3)	1825

Ønsket Oppnådd

kg	Kg
45,5	45,4
4,5	4,5
0,5	0,5
20,7	20,7
3,0	3,1
11,8	11,9
22,9	23,1
42,8	43,1
26,7	27,0
0,0	0,0
0,82	0,82
0,00	0,00
3,9	0,0
0,0	0,0

Materiale	Densitet * [kg/m ³]	Tørrestoff [%]	Alkalier [%]	Klorider [%]
Norcem Standard	3150	-	0,00	0,00
Elkem Microsilica 940U (A-4066)	2200	100	0,00	0,00
Kalksteinsmel	2740	100	0,00	0,00
Dynamon SX-N	1060	18,5	0,50	0,10
	1100	0	0,00	0,00
	1200	0	0,00	0,00
	1000	0	0,00	0,00
Dramix 65/60 3D	7800	-	-	-
0	7800	-	-	-

*For sement, pozzolaner og fillere oppgis densitet av tørrestoff. For TSS oppgis våt densitet.

***Nullstill korleksjon; Ctrl K

Fersk betong

Egenskap	
Ønsket volum	100,0
Innveid volum (l)	100,0
Luftinnhold (%)	2,0
Målt betongdensitet (kg/m ³)	1795
Effektivt v/(c+Σkp)	0,380

Aggressiver	
Kloridinnhold [% av cem.]	0,00
Alkalier [kg/m ³]	0,04
Andel reakt. bergarter [%]	0,0

Volumkorleksjon***

korr.luft	korr.dens	Korrigert
0,0	0,0	454,4
0,0	0,0	45,4
0,0	0,0	4,5
0,0	0,0	207,2
0,0	0,0	30,7
0,0	0,0	119,2
0,0	0,0	230,7
0,0	0,0	431,3
0,0	0,0	269,6
0,0	0,0	0,0
0,0	0,0	0,0
0,0	0,0	0,0
0,0	0,0	0,0
0,0	0,0	0,0
0,0	0,0	0,0
0,0	0,0	0,0
0,0	0,0	0,0
0,0	0,0	0,0
0,0	0,0	0,0
0,0	0,0	0,0
0,0	0,0	0,0
0,0	0,0	0,0
0,0	0,0	1795

Prosj./id.: LWC 1800 0,5% Dramix 65/60 3D, Blandeskjema

Blandevolum:	100 liter
Dato:	
Tidspunkt for vanntilsetning	
Ansvarlig:	
Utført av:	

Materialer	Resept kg/m ³	Sats kg	Fukt* %	Korr. kg	Oppveid** kg	
Norcem Standard	454,7	45,470			45,470	
Elkem Microsilica 940U (A-4066)	45,5	4,547	0	0,000	4,547	
Kalksteinsmel	4,5	0,455	0	0,000	0,455	
Fritt vann	207,3	20,734		-2,046	18,688	21,728
Absorbent vann	30,4	3,039			3,039	
Leca 2-4 mm (A-4048)	118,2	11,821	0,0	0,000	11,821	
Leca 800 4-8 mm (A-4048)	228,7	22,873	0,0	0,000	22,873	
0/8mm NSBR (A-3995)	427,6	42,757	2,6	1,112	43,868	
0/2mm vasket maskin (A-3726)	267,2	26,723	1,0	0,267	26,990	
	0,0	0,000	0,0	0,000	0,000	
	0,0	0,000	0,0	0,000	0,000	
Dynamon SX-N	8,2	0,818	81,5	0,667	0,818	
	0,0	0,000	100	0,000	0,000	
	0,0	0,000	100	0,000	0,000	
	0,0	0,000	100	0,000	0,000	
Dramix 65/60 3D	39,0	3,900			3,900	
	0,0	0,000			0,000	

** NB! Våte mengder, også for pozzolaner og fillere

*Se fotnote på delark "Proporsjonering"

Fersk betong					
Tid etter vanntilsetning					
Synkmål	T-50	1,97	s		
Utbredelsesmål		570	mm		
Luft		5,8	%		
Densitet		1774,9	kg/m ³		

Sammensatt tilslag

Fraksjon	Navn	Densitet [kg/m ³]	Abs. fukt [%]	Alk. reakt. [%]	Klorider [%]	Andel		Bruk
						volum	vekt	
I	Leca 2-4 mm (A-4048)	590	17,9	0,0	0,00	0,334	0,130	ok
II	Leca 800 4-8 mm (A-4048)	1630	3,1	0,0	0,00	0,234	0,220	ok
III	0/8mm NSBR (A-3995)	2680	0,3	0,0	0,00	0,266	0,400	ok
IV	0/2mm vasket maskin(A-3726)	2680	0,3	0,0	0,00	0,166	0,250	ok
V	0	2680	0,3	0,0	0,00	0,000	0,000	
VI		2700	0,0	0,0	0,00	0,000	0,000	
VII		2700	0,0	0,0	0,00	0,000	0,000	
VIII		2700	0,0	0,0	0,00	0,000	0,000	
IX		2700	0,0	0,0	0,00	0,000	0,000	
X		2700	0,0	0,0	0,00	0,000	0,000	
Sam.		1673		0,0	0,00	1,000	1,000	

Finhetsmoduler	
FM _{vekt} =	3,61
FM _{vol} =	3,99
FM _{ref} =	4,00
FM _g =	5,07

Åpning	Gjennomgang		Ref. grad. [vol. %]	Vekt ved tilpasning
	vol.[%]	vekt [%]		
32	100,0	100,0	100,0	1
22,4	100,0	100,0	100,0	1
16	100,0	100,0	100,0	1
11,2	100,0	100,0	99,4	1
8	99,3	98,9	95,7	1
4	71,0	69,6	64,8	1
2	31,5	47,4	34,6	1
1	23,2	34,9	25,3	2
0,5	15,0	22,6	16,9	2
0,25	8,5	12,8	10,1	2
0,125	4,2	6,3	4,9	2
0,063	1,5	2,2	2,4	2

B.c. Appendix Matrix for LWAC with 1,0% steel fibre reinforcement

**Proporsjonering av betong
LWAC 1800 1,0% Dramix 65/60 3D**



©2008-11-12 ss

Utført av	Firma	Dato
G. Kjellmark	SINTEF Byggforsk	25.02.2013

Initialparametre	Verdi	k
$v/(c+\Sigma kp)$	0,38	-
s/c (silikastøv) [%]	10,0	2,00
f/c (filler, flyveaske) [%]	1,0	0,00
Luftinnhold [%]	2,0	-
Tilsetningsstoff	% av C	% av S
Dynamon SX-N	1,80	0,00
	0,00	0,00
	0,00	0,00
	0,00	0,00
Fiber	Vol %	
Dramix 65/60 3D	1,0	
	0,0	
Matriks	Verdi	
Ønsket matriksvolum [l/m^3]	400	
Oppnådd matriksvolum** [l/m^3]	400	
Volum sementlim [l/m^3]	375	
v/p	0,36	



**Tilpass matriksvolum; Ctrl M

Sett "Oppnådd" lik "Ønsket"; Ctrl N

Proporsjonert betong

Materialer	kg/m ³
Norcem Standard	455,0
Elkem Microsilica 940U (A-4066)	45,5
Kalksteinsmel	4,5
Fritt vann	207,5
Absorbert vann	30,1
Leca 2-4 mm (A-4048)	117,2
Leca 800 4-8 mm (A-4048)	226,7
0/8mm NSBR (A-3995)	423,9
0/2mm vasket maskin (A-3726)	264,9
	0,0
Dynamon SX-N	8,19
	0,00
Dramix 65/60 3D	78,0
0,0	0,0
Prop. betongdens. (kg/m ³)	1855

Ønsket Oppnådd

kg	kg
45,5	45,4
4,5	4,5
0,5	0,5
20,7	20,7
3,0	3,1
11,7	11,9
22,7	23,1
42,4	43,1
26,5	27,0
0,0	0,0
0,82	0,82
0,00	0,00
7,8	0,0
0,0	0,0

Materiale	Densitet * [kg/m ³]	Tørrestoff [%]	Alkalier [%]	Klorider [%]
Norcem Standard	3150	-	0,00	0,00
Elkem Microsilica 940U (A-4066)	2200	100	0,00	0,00
Kalksteinsmel	2740	100	0,00	0,00
Dynamon SX-N	1060	18,5	0,50	0,10
	1100	0	0,00	0,00
	1200	0	0,00	0,00
	1000	0	0,00	0,00
Dramix 65/60 3D	7800	-	-	-
0	7800	-	-	-

*For sement, pozzolaner og fillere oppgis densitet av tørrestoff. For TSS oppgis våt densitet.

***Nullstill korreksjon; Ctrl K

Fersk betong

Egenskap	
Ønsket volum	100,0
Innveid volum (l)	100,0
Luftinnhold (%)	2,0
Målt betongdensitet (kg/m ³)	1795
Effektivt v/(c+Σkp)	0,380

Aggressiver	
Kloridinnhold [% av cem.]	0,00
Alkalier [kg/m ³]	0,04
Andel reakt. bergarter [%]	0,0

Volumkorreksjon***

korr.luft	korr.dens	Korrigert
0,0	0,0	454,4
0,0	0,0	45,4
0,0	0,0	4,5
0,0	0,0	207,2
0,0	0,0	30,7
0,0	0,0	119,2
0,0	0,0	230,7
0,0	0,0	431,3
0,0	0,0	269,6
0,0	0,0	0,0
0,0	0,0	0,0
0,0	0,0	0,0
0,0	0,0	0,0
0,0	0,0	0,0
0,0	0,0	0,0
0,0	0,0	0,0
0,0	0,0	0,0
0,0	0,0	0,0
0,0	0,0	0,0
0,0	0,0	0,0
0,0	0,0	0,0
0,0	0,0	0,0
0,0	0,0	0,0
0,0	0,0	0,0
0,0	0,0	1795

Prosj./id.:

LWC 1800 1,0% Dramix 65/60 3D, Blandeskjema

Blande volum:	100 liter
Dato:	
Tidspunkt for vanntilsetning	
Ansvarlig:	
Utført av:	

Materialer	Resept kg/m ³	Sats kg	Fukt* %	Korr. kg	Oppveid** kg
Norcem Standard	455,0	45,496			45,496
Elkem Microsilica 940U (A-4066)	45,5	4,550	0	0,000	4,550
Kalksteinsmel	4,5	0,455	0	0,000	0,455
Fritt vann	207,5	20,746		-2,034	18,712
Absorbent vann	30,1	3,013			3,013
Leca 2-4 mm (A-4048)	117,2	11,718	0,0	0,000	11,718
Leca 800 4-8 mm (A-4048)	226,7	22,674	0,0	0,000	22,674
0/8mm NSBR (A-3995)	423,9	42,385	2,6	1,102	43,487
0/2mm vasket maskin(A-3726)	264,9	26,491	1,0	0,265	26,756
0	0,0	0,000	0,0	0,000	0,000
	0,0	0,000	0,0	0,000	0,000
	0,0	0,000	0,0	0,000	0,000
	0,0	0,000	0,0	0,000	0,000
	0,0	0,000	0,0	0,000	0,000
	0,0	0,000	0,0	0,000	0,000
	0,0	0,000	0,0	0,000	0,000
Dynamon SX-N	8,2	0,819	81,5	0,667	0,819
	0,0	0,000	100	0,000	0,000
	0,0	0,000	100	0,000	0,000
	0,0	0,000	100	0,000	0,000
Dramix 65/60 3D	78,0	7,800			7,800
0	0,0	0,000			0,000

21,725

** NB! Våte mengder, også for pozzolaner og fillere

*Se fotnote på delark "Proporsjonering"

Fersk betong					
Tid etter vanntilsetning					
Synkmål	T-50	2,88	s		
Utbredelsesmål		560	mm		
Luft		5,6	%		
Densitet		1726	kg/m ³		

Sammensatt tilslag

Fraksjon	Navn	Densitet [kg/m ³]	Abs. fukt [%]	Alk. reakt. [%]	Klorider [%]	Andel		Bruk
						volum	vekt	
I	Leca 2-4 mm (A-4048)	590	17,9	0,0	0,00	0,334	0,130	ok
II	Leca 800 4-8 mm (A-4048)	1630	3,1	0,0	0,00	0,234	0,220	ok
III	0/8mm NSBR (A-3995)	2680	0,3	0,0	0,00	0,266	0,400	ok
IV	0/2mm vasket maskin (A-3726)	2680	0,3	0,0	0,00	0,166	0,250	ok
V		2680	0,3	0,0	0,00	0,000	0,000	
VI		2700	0,0	0,0	0,00	0,000	0,000	
VII		2700	0,0	0,0	0,00	0,000	0,000	
VIII		2700	0,0	0,0	0,00	0,000	0,000	
IX		2700	0,0	0,0	0,00	0,000	0,000	
X		2700	0,0	0,0	0,00	0,000	0,000	
Sam.		1673		0,0	0,00	1,000	1,000	

Finhetsmoduler	
FM _{vekt} =	3,61
FM _{vol} =	3,99
FM _{ref} =	4,00
FM _g =	5,07

Åpning	Gjennomgang		Ref. grad. [vol. %]	Vekt ved tilpasning
	vol.[%]	vekt [%]		
32	100,0	100,0	100,0	1
22,4	100,0	100,0	100,0	1
16	100,0	100,0	100,0	1
11,2	100,0	100,0	99,4	1
8	99,3	98,9	95,7	1
4	71,0	69,6	64,8	1
2	31,5	47,4	34,6	1
1	23,2	34,9	25,3	2
0,5	15,0	22,6	16,9	2
0,25	8,5	12,8	10,1	2
0,125	4,2	6,3	4,9	2
0,063	1,5	2,2	2,4	2

B.d. Appendix NDC without steel fibre reinforcement

**Proporsjonering av betong
NDC 0% Dramix 65/60 3D**



©2008-11-12 ss

Utført av	Firma	Dato
TAMH/GK	SINTEF Byggforsk	19.03.2013

Initialparametre	Verdi	k
$v/(c+\Sigma kp)$	0,57	-
s/c (silikastøv) [%]	10,0	2,00
f/c (filler, flyveaske) [%]	15,0	0,00
Luftinnhold [%]	2,0	-
Tilsetningsstoff	% av C	% av S
Dynamon SX-N	1,50	0,00
	0,00	0,00
Sika demper	0,10	0,00
	0,00	0,00
Fiber	Vol %	
Dramix 65/60 3D	0,0	
	0,0	
Matriks	Verdi	
Ønsket matriksvolum [l/m^3]	400	
Oppnådd matriksvolum** [l/m^3]	400	
Volum sementlim [l/m^3]	341	
v/p	0,39	



**Tilpass matriksvolum; Ctrl M

Sett "Oppnådd" lik "Ønsket"; Ctrl N

Proporsjonert betong

Materialer	kg/m ³
Norcem Standard FA (STD FA 10)	301,1
Elkem Microsilica 940 U (A-4066)	30,1
Fly ash (A-4076)	45,2
Fritt vann	206,0
Absorbert vann	6,7
Årdal 0-2 mm (A-3726)_vasket maskin	594,2
Årdal 0-8 mm (A-3995)	1100,3
	0,0
Dynamon SX-N	4,52
0,0	0,00
Sika demper	0,30
	0,00
Dramix 65/60 3D	0,0
0,0	0,0
Prop. betongdens. (kg/m ³)	2284

Ønsket Oppnådd

kg	kg
30,1	30,1
3,0	3,0
4,5	4,5
20,6	20,6
0,7	0,7
59,4	59,4
110,0	110,0
0,0	0,0
0,45	0,45
0,00	0,00
0,03	0,03
0,00	0,00
0,0	0,0
0,0	0,0

Materiale	Densitet * [kg/m ³]	Tørrestoff [%]	Alkalier [%]	Klorider [%]
Norcem Standard FA (STD FA 10)	2990	-	0,00	0,00
Elkem Microsilica 940 U (A-4066)	2200	100	0,00	0,00
Fly ash (A-4076)	2300	100	0,00	0,00
Dynamon SX-N	1060	18,5	0,00	0,00
0	2500	100	0,00	0,00
Sika demper	1000	0	0,00	0,00
	1000	0	0,00	0,00
Dramix 65/60 3D	7800	-	-	-
0	7800	-	-	-

*For sement, pozzolaner og fillere oppgis densitet av tørrestoff. For TSS oppgis våt densitet.

***Nullstill korreksjon; Ctrl K

Fersk betong

Egenskap	
Ønsket volum	100,0
Innveid volum (l)	100,0
Luftinnhold (%)	2,0
Målt betongdensitet (kg/m ³)	2284
Effektivt v/(c+Σkp)	0,570

Aggressiver	
Kloridinnhold [% av cem.]	0,00
Alkalier [kg/m ³]	0,00
Andel reakt. bergarter [%]	0,0

Volumkorreksjon***

korr.luft	korr.dens	Korrigert
0,0	0,0	301,1
0,0	0,0	30,1
0,0	0,0	45,2
0,0	0,0	206,0
0,0	0,0	6,7
0,0	0,0	594,2
0,0	0,0	1100,3
0,0	0,0	0,0
0,0	0,0	0,0
0,0	0,0	0,0
0,0	0,0	0,0
0,0	0,0	0,0
0,0	0,0	0,0
0,0	0,0	0,0
0,0	0,0	4,52
0,0	0,0	0,00
0,0	0,0	0,30
0,0	0,0	0,00
0,0	0,0	0,0
0,0	0,0	0,0
0,0	0,0	2284

Prosj./id.:

NDC 0% Dramix 65/60 3D, Blandeskjema

Blandevidde:	100 liter
Dato:	
Tidspunkt for vanntilsetning	
Ansvarlig:	
Utført av:	

Materialer	Resept kg/m ³	Sats kg	Fukt* %	Korr. kg	Oppveid** kg
Norcem Standard FA (STD FA 10)	301,1	30,110			30,110
Elkem Microsilica 940 U (A-4066)	30,1	3,011	0	0,000	3,011
Fly ash (A-4076)	45,2	4,516	0	0,000	4,516
Fritt vann	206,0	20,595		-3,853	16,742
Absorbent vann	6,7	0,669			0,669
Årdal 0-2 mm (A-3726)_vasket maskin	594,2	59,424	1,0	0,594	60,018
Årdal 0-8 mm (A-3995)	1100,3	110,029	2,6	2,861	112,890
	0,0	0,000	0,0	0,000	0,000
	0,0	0,000	0,0	0,000	0,000
	0,0	0,000	0,0	0,000	0,000
	0,0	0,000	0,0	0,000	0,000
	0,0	0,000	0,0	0,000	0,000
	0,0	0,000	0,0	0,000	0,000
	0,0	0,000	0,0	0,000	0,000
	0,0	0,000	0,0	0,000	0,000
Dynamon SX-N	4,5	0,452	81,5	0,368	0,452
0	0,0	0,000	0	0,000	0,000
Sika demper	0,3	0,030	100	0,030	0,030
	0,0	0,000	100	0,000	0,000
Dramix 65/60 3D	0,0	0,000			0,000
0	0,0	0,000			0,000

17,411

** NB! Våte mengder, også for pozzolaner og fillere

*Se fotnote på delark "Proporsjonering"

Fersk betong					
Tid etter vanntilsetning					
Synkmål	T-50	4,88	s		
Utbredelsesmål		660	mm		
Luft		3,5	%		
Densitet		2267,3	kg/m ³		

Sammensatt tilslag

Fraksjon	Navn	Densitet [kg/m ³]	Abs. fukt [%]	Alk. reakt. [%]	Klorider [%]	Andel		Br uk
						volum	vekt	
I	Årdal 0-2 mm(A-3726)vasket maskin	2650	0,2	0,0	0,00	0,351	0,350	ok
II	Årdal 0-8 mm (A-3995)	2650	0,5	0,0	0,00	0,649	0,650	ok
III		2700	0,0	0,0	0,00	0,000	0,000	
IV		2700	0,0	0,0	0,00	0,000	0,000	
V		2700	0,0	0,0	0,00	0,000	0,000	
VI		2700	0,0	0,0	0,00	0,000	0,000	
VII		2700	0,0	0,0	0,00	0,000	0,000	
VIII		2700	0,0	0,0	0,00	0,000	0,000	
IX		2700	0,0	0,0	0,00	0,000	0,000	
X		2700	0,0	0,0	0,00	0,000	0,000	
Sam.		2650		0,0	0,00	1,000	1,000	

Finhetsmoduler	
FM _{vekt} =	2,83
FM _{vol} =	2,83
FM _{ref} =	2,83
FM _g =	5,07

Åpning	Gjennomgang		Ref. grad. [vol. %]	Vekt ved tilpasning
	vol.[%]	vekt [%]		
32	100,0	100,0	100,0	1
22,4	100,0	100,0	100,0	1
16	100,0	100,0	100,0	1
11,2	100,0	100,0	100,0	1
8	98,2	98,2	97,9	1
4	86,4	86,4	83,5	1
2	71,8	71,8	68,4	1
1	52,7	52,7	53,4	2
0,5	33,9	33,9	37,6	2
0,25	19,1	19,1	22,1	2
0,125	9,3	9,3	9,0	2
0,063	3,3	3,3	2,7	2

B.e Appendix NDC with 0,5% Steel fibre reinforcement

**Proporsjonering av betong
NDC 0,5% Dramix 65/60 3D**



©2008-11-12 ss

Utført av	Firma	Dato
TAMH/GK	SINTEF Byggforsk	19.03.2013

Initialparametre	Verdi	k
$v/(c+\Sigma kp)$	0,57	-
s/c (silikastøv) [%]	10,0	2,00
f/c (filler, flyveaske) [%]	15,0	0,00
Luftinnhold [%]	2,0	-
Tilsetningsstoff	% av C	% av S
Dynamon SX-N	1,50	0,00
	0,00	0,00
Sika demper	0,10	0,00
	0,00	0,00
Fiber	Vol %	
Dramix 65/60 3D	0,5	
	0,0	
Matriks	Verdi	
Ønsket matriksvolum [l/m^3]	400	
Oppnådd matriksvolum** [l/m^3]	400	
Volum sementlim [l/m^3]	341	
v/p	0,39	



**Tilpass matriksvolum; Ctrl M

Sett "Oppnådd" lik "Ønsket"; Ctrl N

Proporsjonert betong

Materialer	kg/m ³
Norcem Standard FA (STD FA 10)	301,6
Elkem Microsilica 940 U (A-4066)	30,2
Fly ash (A-4076)	45,2
Fritt vann	206,3
Absorbert vann	6,6
Årdal 0-2 mm (A-3726)_vasket maskin	589,1
Årdal 0-8 mm (A-3995)	1090,8
	0,0
Dynamon SX-N	4,52
0,0	0,00
Sika demper	0,30
	0,00
Dramix 65/60 3D	39,0
0,0	0,0
Prop. betongdens. (kg/m ³)	2310

Ønsket Oppnådd

kg	kg
30,2	30,1
3,0	3,0
4,5	4,5
20,6	20,6
0,7	0,7
58,9	59,4
109,1	110,0
0,0	0,0
0,45	0,45
0,00	0,00
0,03	0,03
0,00	0,00
3,9	0,0
0,0	0,0

Materiale	Densitet * [kg/m ³]	Tørrstoff [%]	Alkalier [%]	Klorider [%]
Norcem Standard FA (STD FA 10)	2990	-	0,00	0,00
Elkem Microsilica 940 U (A-4066)	2200	100	0,00	0,00
Fly ash (A-4076)	2300	100	0,00	0,00
Dynamon SX-N	1060	18,5	0,00	0,00
0	2500	100	0,00	0,00
Sika demper	1000	0	0,00	0,00
	1000	0	0,00	0,00
Dramix 65/60 3D	7800	-	-	-
0	7800	-	-	-

*For sement, pozzolaner og fillere oppgis densitet av tørrstoff. For TSS oppgis våt densitet.

***Nullstill korreksjon; Ctrl K

Fersk betong

Egenskap	
Ønsket volum	100,0
Innveid volum (l)	100,0
Luftinnhold (%)	2,0
Målt betongdensitet (kg/m ³)	2284
Effektivt v/(c+Σkp)	0,570

Aggressiver	
Kloridinnhold [% av cem.]	0,00
Alkalier [kg/m ³]	0,00
Andel reakt. bergarter [%]	0,0

Volumkorreksjon***

korr.luft	korr.dens	Korrigert
0,0	0,0	301,1
0,0	0,0	30,1
0,0	0,0	45,2
0,0	0,0	206,0
0,0	0,0	6,7
0,0	0,0	594,2
0,0	0,0	1100,3
0,0	0,0	0,0
0,0	0,0	0,0
0,0	0,0	0,0
0,0	0,0	0,0
0,0	0,0	0,0
0,0	0,0	0,0
0,0	0,0	0,0
0,0	0,0	0,0
0,0	0,0	0,0
0,0	0,0	4,52
0,0	0,0	0,00
0,0	0,0	0,30
0,0	0,0	0,00
0,0	0,0	0,0
0,0	0,0	0,0
0,0	0,0	2284

Prosj./id.:

NDC 0,5% Dramix 65/60 3D, Blandeskjema

Blande volum:	100 liter
Dato:	
Tidspunkt for vanntilsetning	
Ansvarlig:	
Utført av:	

Materialer	Resept kg/m ³	Sats kg	Fukt* %	Korr. kg	Oppveid** kg
Norcem Standard FA (STD FA 10)	301,6	30,155			30,155
Elkem Microsilica 940 U (A-4066)	30,2	3,016	0	0,000	3,016
Fly ash (A-4076)	45,2	4,523	0	0,000	4,523
Fritt vann	206,3	20,626		-3,824	16,802
Absorbent vann	6,6	0,663			0,663
Årdal 0-2 mm (A-3726)_vasket maskin	589,1	58,912	1,0	0,589	59,501
Årdal 0-8 mm (A-3995)	1090,8	109,08	2,6	2,836	111,917
	0,0	0,000	0,0	0,000	0,000
	0,0	0,000	0,0	0,000	0,000
	0,0	0,000	0,0	0,000	0,000
	0,0	0,000	0,0	0,000	0,000
	0,0	0,000	0,0	0,000	0,000
	0,0	0,000	0,0	0,000	0,000
	0,0	0,000	0,0	0,000	0,000
	0,0	0,000	0,0	0,000	0,000
	0,0	0,000	0,0	0,000	0,000
Dynamon SX-N	4,5	0,452	81,5	0,369	0,452
0	0,0	0,000	0	0,000	0,000
Sika demper	0,3	0,030	100	0,030	0,030
	0,0	0,000	100	0,000	0,000
Dramix 65/60 3D	39,0	3,900			3,900
0	0,0	0,000			0,000

17,465

** NB! Våte mengder, også for pozzolaner og fillere

*Se fotnote på delark "Proporsjonering"

Fersk betong					
Tid etter vanntilsetning					
Synkmål	T-50	5	s		
Utbredelsesmål		640	mm		
Luft		2,7	%		
Densitet		2298,1	kg/m ³		

Sammensatt tilslag

Fraksjon	Navn	Densitet [kg/m ³]	Abs fukt [%]	Alk. reakt. [%]	Klorider [%]	Andel		Bruk
						volum	vekt	
I	Årdal 0-2 mm (A-3726)vasket maskin	2650	0,2	0,0	0,00	0,351	0,350	ok
II	Årdal 0-8 mm (A-3995)	2650	0,5	0,0	0,00	0,649	0,650	ok
III		2700	0,0	0,0	0,00	0,000	0,000	
IV		2700	0,0	0,0	0,00	0,000	0,000	
V		2700	0,0	0,0	0,00	0,000	0,000	
VI		2700	0,0	0,0	0,00	0,000	0,000	
VII		2700	0,0	0,0	0,00	0,000	0,000	
VIII		2700	0,0	0,0	0,00	0,000	0,000	
IX		2700	0,0	0,0	0,00	0,000	0,000	
X		2700	0,0	0,0	0,00	0,000	0,000	
Sam.		2650		0,0	0,00	1,000	1,000	

Finhetsmoduler	
FM _{vekt} =	2,83
FM _{vol} =	2,83
FM _{ref} =	2,83
FM _g =	5,07

Åpning	Gjennomgang		Ref. grad. [vol. %]	Vekt ved tilpasning
	vol. [%]	vekt [%]		
32	100,0	100,0	100,0	1
22,4	100,0	100,0	100,0	1
16	100,0	100,0	100,0	1
11,2	100,0	100,0	100,0	1
8	98,2	98,2	97,9	1
4	86,4	86,4	83,5	1
2	71,8	71,8	68,4	1
1	52,7	52,7	53,4	2
0,5	33,9	33,9	37,6	2
0,25	19,1	19,1	22,1	2
0,125	9,3	9,3	9,0	2
0,063	3,3	3,3	2,7	2

B.f. Appendix NDC with 1,0% steel fibre reinforcement

**Proporsjonering av betong
NDC 1,0% Dramix 65/60 3D**



©2008-11-12 ss

Utført av	Firma	Dato
TAMH/GK	SINTEF Byggforsk	19.03.2013

Initialparametre	Verdi	k
$v/(c+\Sigma kp)$	0,57	-
s/c (silikastøv) [%]	10,0	2,00
f/c (filler, flyveaske) [%]	15,0	0,00
Luftinnhold [%]	2,0	-
Tilsetningsstoff	% av C	% av S
Dynamon SX-N	1,50	0,00
	0,00	0,00
Sika demper	0,10	0,00
	0,00	0,00
Fiber	Vol %	
Dramix 65/60 3D	1,0	
	0,0	
Matriks	Verdi	
Ønsket matriksvolum [l/m^3]	400	
Oppnådd matriksvolum** [l/m^3]	400	
Volum sementlim [l/m^3]	342	
v/p	0,39	



**Tilpass matriksvolum; Ctrl M

Sett "Oppnådd" lik "Ønsket"; Ctrl N

Proporsjonert betong

Materialer	kg/m ³
Norcem Standard FA (STD FA 10)	302,0
Elkem Microsilica 940 U (A-4066)	30,2
Fly ash (A-4076)	45,3
Fritt vann	206,6
Absorbent vann	6,6
Årdal 0-2 mm (A-3726)_vasket maskin	584,0
Årdal 0-8 mm (A-3995)	1081,3
	0,0
Dynamon SX-N	4,53
0,0	0,00
Sika demper	0,30
	0,00
Dramix 65/60 3D	78,0
0,0	0,0
Prop. betongdens. (kg/m ³)	2335

Ønsket Oppnådd

kg	kg
30,2	30,1
3,0	3,0
4,5	4,5
20,7	20,6
0,7	0,7
58,4	59,4
108,1	110,0
0,0	0,0
0,45	0,45
0,00	0,00
0,03	0,03
0,00	0,00
7,8	0,0
0,0	0,0

Materiale	Densitet * [kg/m ³]	Tørrestoff [%]	Alkalier [%]	Klorider [%]
Norcem Standard FA (STD FA 10)	2990	-	0,00	0,00
Elkem Microsilica 940 U (A-4066)	2200	100	0,00	0,00
Fly ash (A-4076)	2300	100	0,00	0,00
Dynamon SX-N	1060	18,5	0,00	0,00
0	2500	100	0,00	0,00
Sika demper	1000	0	0,00	0,00
	1000	0	0,00	0,00
Dramix 65/60 3D	7800	-	-	-
0	7800	-	-	-

*For sement, pozzolaner og fillere oppgis densitet av tørrestoff. For TSS oppgis våt densitet.

***Nullstill korreksjon; Ctrl K

Fersk betong

Egenskap	
Ønsket volum	100,0
Innveid volum (l)	100,0
Luftinnhold (%)	2,0
Målt betongdensitet (kg/m ³)	2284
Effektivt v/(c+Σkp)	0,570

Aggressiver	
Kloridinnhold [% av cem.]	0,00
Alkalier [kg/m ³]	0,00
Andel reakt. bergarter [%]	0,0

Volumkorreksjon***

korr.luft	korr.dens	Korrigert
0,0	0,0	301,1
0,0	0,0	30,1
0,0	0,0	45,2
0,0	0,0	206,0
0,0	0,0	6,7
0,0	0,0	594,2
0,0	0,0	1100,3
0,0	0,0	0,0
0,0	0,0	0,0
0,0	0,0	0,0
0,0	0,0	0,0
0,0	0,0	0,0
0,0	0,0	0,0
0,0	0,0	0,0
0,0	0,0	4,52
0,0	0,0	0,00
0,0	0,0	0,30
0,0	0,0	0,00
0,0	0,0	0,0
0,0	0,0	0,0
0,0	0,0	2284

Prosj./id.:

NDC 1% Dramix 65/60 3D, Blandeskjema

Blande volum:	100 liter
Dato:	
Tidspunkt for vanntilsetning	
Ansvarlig:	
Utført av:	

Materialer	Resept kg/m ³	Sats kg	Fukt* %	Korr. kg	Oppveid** kg
Norcem Standard FA (STD FA 10)	302,0	30,200			30,200
Elkem Microsilica 940 U (A-4066)	30,2	3,020	0	0,000	3,020
Fly ash (A-4076)	45,3	4,530	0	0,000	4,530
Fritt vann	206,6	20,657		-3,795	16,862
Absorbent vann	6,6	0,657			0,657
Årdal 0-2 mm (A-3726)_vasket maskin	584,0	58,399	1,0	0,584	58,983
Årdal 0-8 mm (A-3995)	1081,3	108,13	2,6	2,811	110,944
	0,0	0,000	0,0	0,000	0,000
	0,0	0,000	0,0	0,000	0,000
	0,0	0,000	0,0	0,000	0,000
	0,0	0,000	0,0	0,000	0,000
	0,0	0,000	0,0	0,000	0,000
	0,0	0,000	0,0	0,000	0,000
	0,0	0,000	0,0	0,000	0,000
	0,0	0,000	0,0	0,000	0,000
Dynamon SX-N	4,5	0,453	81,5	0,369	0,453
	0	0,0	0,000	0	0,000
Sika demper	0,3	0,030	100	0,030	0,030
	0,0	0,000	100	0,000	0,000
Dramix 65/60 3D	78,0	7,800			7,800
	0	0,0			0,000

17,520

** NB! Våte mengder, også for pozzolaner og fillere

*Se fotnote på delark "Proporsjonering"

Fersk betong					
Tid etter vanntilsetning					
Synkmål	T-50	7	s		
Utbredelsesmål		600	mm		
Luft		2,5	%		
Densitet		2326,5	kg/m ³		

Sammensatt tilslag

Fraksjon	Navn	Densitet [kg/m ³]	Abs. fukt [%]	Alk. reakt. [%]	Klorider [%]	Andel		Bruk
						volum	vekt	
I	Årdal 0-2 mm (A-3726)vasket maskin	2650	0,2	0,0	0,00	0,351	0,350	ok
II	Årdal 0-8 mm (A-3995)	2650	0,5	0,0	0,00	0,649	0,650	ok
III		2700	0,0	0,0	0,00	0,000	0,000	
IV		2700	0,0	0,0	0,00	0,000	0,000	
V		2700	0,0	0,0	0,00	0,000	0,000	
VI		2700	0,0	0,0	0,00	0,000	0,000	
VII		2700	0,0	0,0	0,00	0,000	0,000	
VIII		2700	0,0	0,0	0,00	0,000	0,000	
IX		2700	0,0	0,0	0,00	0,000	0,000	
X		2700	0,0	0,0	0,00	0,000	0,000	
Sam.		2650		0,0	0,00	1,000	1,000	

Finhetsmoduler	
FM _{vekt} =	2,83
FM _{vol} =	2,83
FM _{ref} =	2,83
FM _g =	5,07

Åpning	Gjennomgang		Ref. grad. [vol. %]	Vekt ved tilpasning
	vol.[%]	vekt [%]		
32	100,0	100,0	100,0	1
22,4	100,0	100,0	100,0	1
16	100,0	100,0	100,0	1
11,2	100,0	100,0	100,0	1
8	98,2	98,2	97,9	1
4	86,4	86,4	83,5	1
2	71,8	71,8	68,4	1
1	52,7	52,7	53,4	2
0,5	33,9	33,9	37,6	2
0,25	19,1	19,1	22,1	2
0,125	9,3	9,3	9,0	2
0,063	3,3	3,3	2,7	2

C. Appendix Test results

Appendix C. presents the test results obtained from the prism tests.

Appendix C.a presents all equations that have been used to find the results that have been presented in the diagrams and tables.

Appendix C.b and C.c shows the complete and most relevant results for the tests, in form of diagrams and tables.

C.a. Appendix Equations used to obtain test results

Equations used in the thesis		
Stress, centric	$\sigma = \frac{P}{A}$	(C.a.1)
Strains	$\varepsilon = \frac{w}{l_{LVDT}}$	(C.a.2)
Least stressed fibre, ecc.	$\sigma_{tmax} = \frac{\sigma_{total}}{\left(\left(\frac{\left(\frac{\varepsilon_{lnorth}}{\varepsilon_{lsouth}} \right) * \left(\frac{\varepsilon_{lnorth}}{\varepsilon_{ltot}} \right)}{2} \right) - \left(\frac{\left(\frac{\varepsilon_{lsouth}}{\varepsilon_{ltot}} \right)}{2} \right) \right)}$	(C.a.3)
Most stressed fibre, ecc	$\sigma_{cmax} = \sigma_{tmax} * \left(\frac{\varepsilon_{lnorth}}{\varepsilon_{lsouth}} \right)$	(C.a.4)
Young's Modulus	$E = \frac{\sigma}{\varepsilon}$	(C.a.5)
Poisson Ratio	$\nu = \frac{\varepsilon_c}{\varepsilon_l}$	(C.a.6)
Curvature, eccentric	$\kappa = \left(\frac{180}{\pi} \right) * \sin^{-1} \left(\frac{\left(\frac{\left(\frac{w_{north30} - w_{south30}}{l_{prism}} \right)}{\left(\frac{l_{LVDT30}}{h_{prism}} \right)} \right)}{\left(\frac{l_{LVDT30}}{h_{prism}} \right)} \right)$	(C.a.7)

Notations

P = Load

A = Total load area

ε = Strain

w = Displacement

l_{LVDT} = Length of the actual LVDT

σ_{tmax} = Stress at least stressed fibre

σ_{cmax} = Stress at most stressed fibre

$\sigma_{total} = \sigma$

ε_{north} = Strains at north side of prism

ε_{south} = Strains at south side of prism

ε_{total} = Total strains (difference from north to south)

ε_c = Cross sectional strains (Transversal strains)

ε_l = Longitudinal strains

$w_{north30}$ = Displacements on the north 30cm LVDT

$w_{south30}$ = Displacements on the south 30cm LVDT

l_{prism} = Length of prism (375mm)

l_{LVDT} = Length of 30cm LVDT

h_{prism} = Height of prism, 150mm

Description of stress calculation

Calculations of most and least stressed fibre in eccentric compression:

There is no easy nor completely correct way to calculate the stresses in an eccentric compressed prism test. There was however made an attempt on calculating the stresses in the most- and least stressed fibre. The results are however of a such uncertain grade of correctness, especially at the inelastic part of the curve, that results will only be plotted and presented in the annex. The approach however was based on an assumption of completely linear stress behaviour across the prism width; the sum of the total stresses had to be the same as for the centric compressed prisms and a direct unaffected relation between longitudinal stresses and strains. The sum of all this assumptions which really are based on the fundamental behaviour of concrete, in an elastic state, makes the stress results as uncertain as they appear.

Simply explained, the averaged strains, north in compression and south in tension, was used to determine the point of zero stresses across the prisms. Based on the assumption of a total stress resultant, the strains on each side in combination with the total strains were used to determine the stress on the least stressed fibre. Assuming a linear stress dispersion over the width, “knowing” the point of zero stress and assuming that the max and least stressed fibre are located at the outmost fibre of the respective faces, the stresses at the tensioned side was used to determine the stresses of the most stressed side.

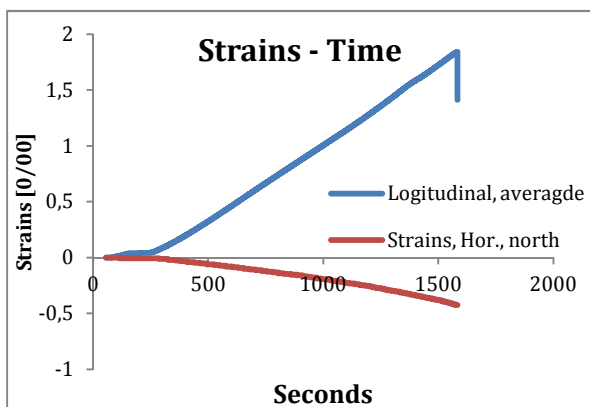
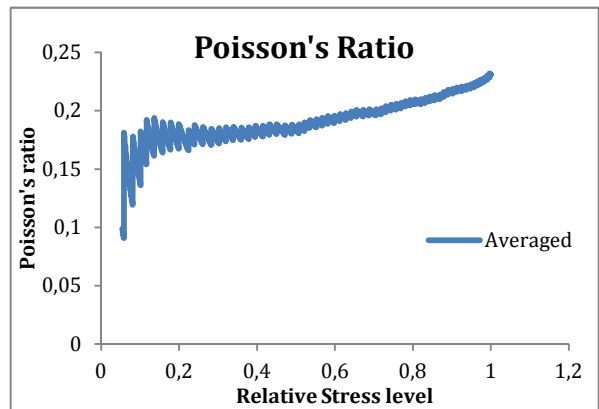
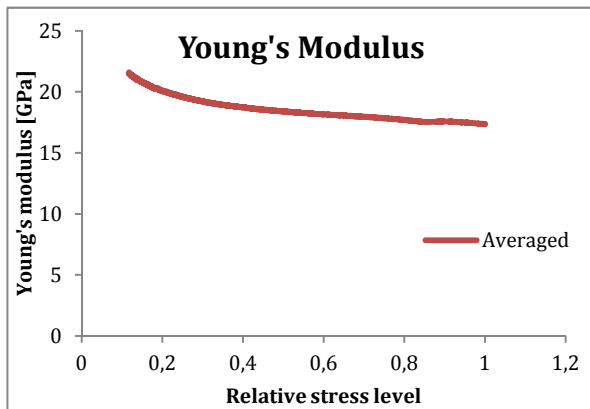
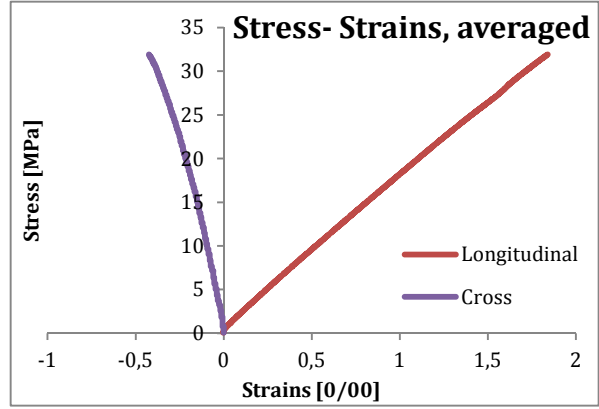
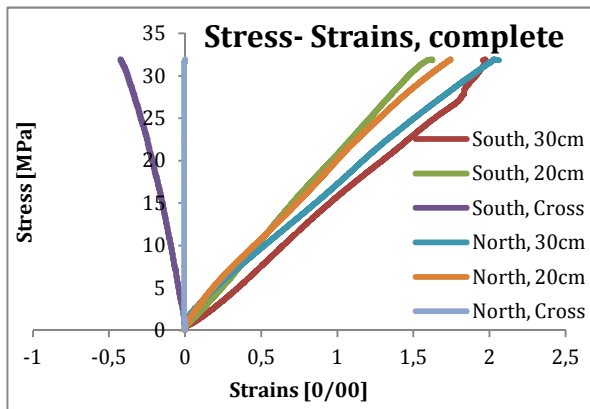
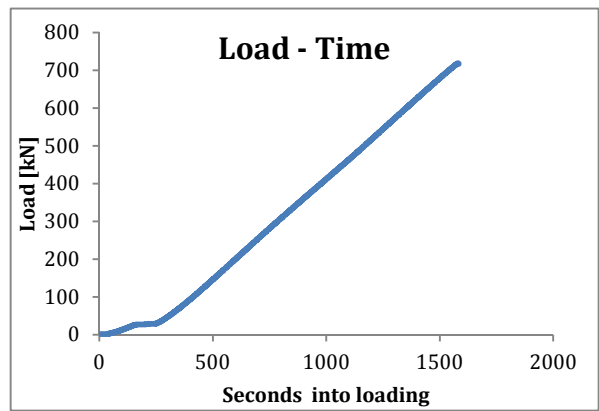
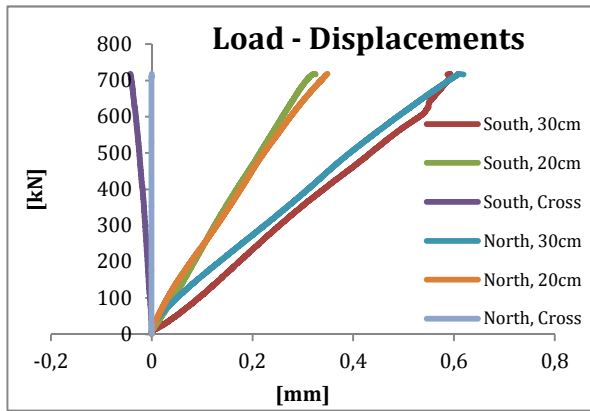
$$f_{tmax} = \frac{f_{total}}{\left(\left(\frac{\epsilon_{lnorth}}{\epsilon_{lsouth}} \right) \left(\frac{\epsilon_{lnorth}}{\epsilon_{ltot}} \right) \right) - \left(\frac{\epsilon_{lsouth}}{\epsilon_{ltot}} \right)} \quad (0.1)$$

Where f_{tmax} is the stress at the least stressed fibre, f_{total} is the stress if the load would have been centric, ϵ_{lnorth} is the longitudinal strain from the north side (compressed), ϵ_{lsouth} is the strain at the tensioned side (south) and ϵ_{ltot} is the difference in strain from north to south side. Having found the stress at the least stressed fibre, which is really the fibre which is most stressed, but only in tension, it is fairly straight forward to find the stress at the maximum stressed fibre at the compressed side.

$$f_{cmax} = f_{tmax} * \left(\frac{\epsilon_{lnorth}}{\epsilon_{lsouth}} \right) \quad (0.2)$$

Where f_{cmax} is the stress at the most stressed fibre in compression. The highest stress calculated was found for prism B3 reinforced by 0,5% steel fibres and was nearly 60MPa! This value is hardly correct due to the assumptions the calculations are based on, and the fact the stress value was found at a highly inelastic state of loading, at a time where the strains were increasing at a high pace. The complete results and plotted curves from the stress calculations are expressed in annex[XX].

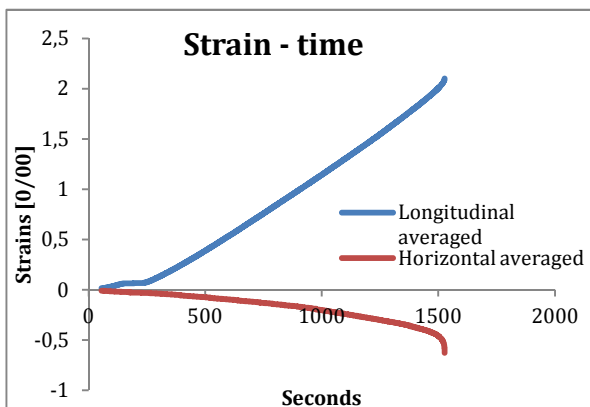
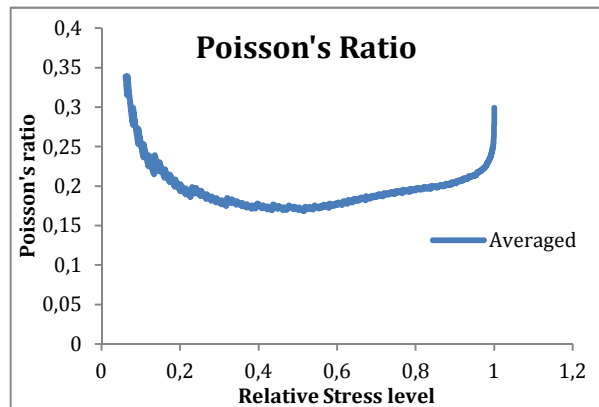
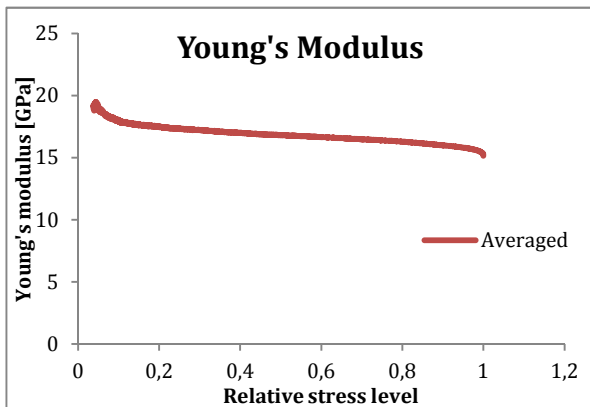
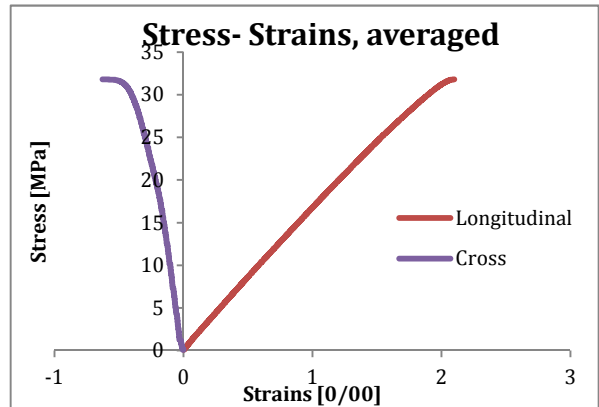
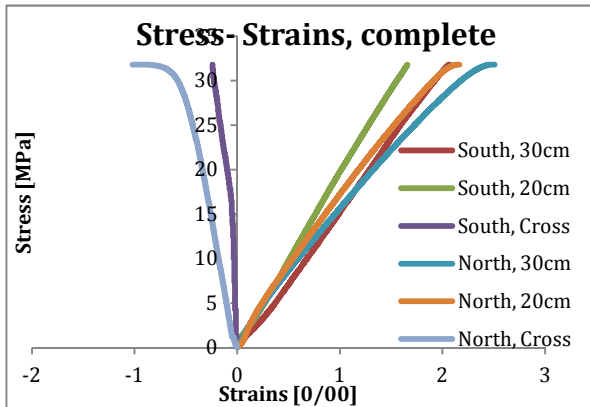
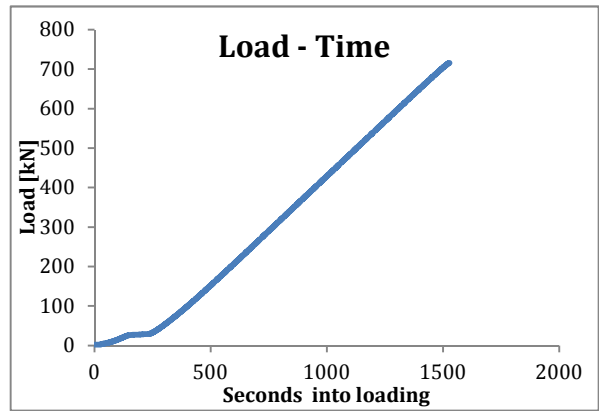
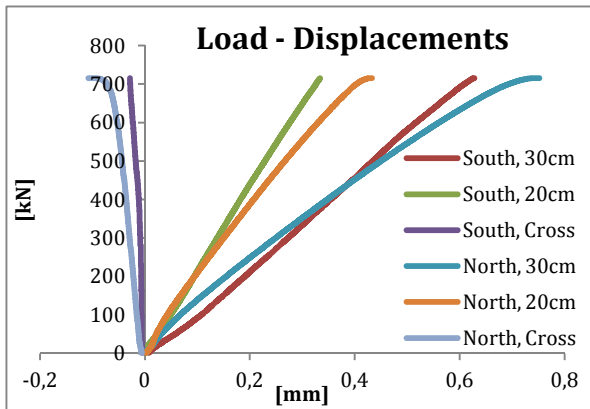
C.b.1. Appendix LWAC 0,0% steel fibre, Centric Loading, Prism B1



LWAC 0,0% Centric B1			
P_{peak} [kN]	f_{cp} [MPa]	P_{fail} [kN]	P_{change} [%]
718,59	31,937	718,55	0

LWAC 0,0% Centric B1			
LVDT id.	ϵ_{peak} [‰]	ϵ_{fail} [‰]	ϵ_{change} [%]
South 30	1,9696	1,9696	0
South 20	1,619	1,6225	0,2
South Cross	-0,4251	-0,4251	0
North 30	2,0276	2,0277	0
North 20	1,7455	1,7455	0
North Cross	0	0	0

C.b.2. Appendix LWDC 0,0% steel fibres, Centric Loading, Prism B2

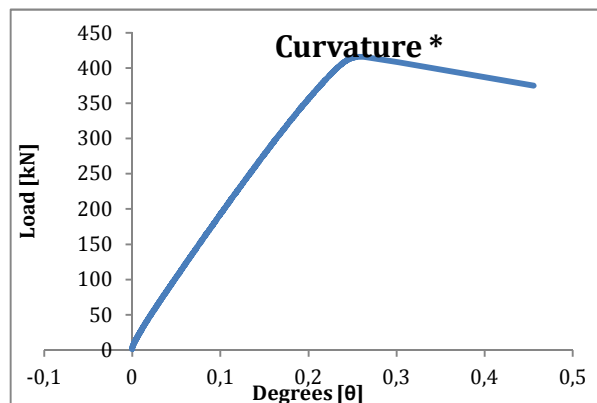
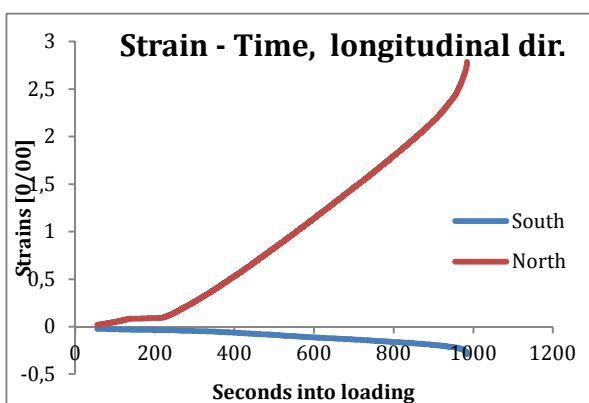
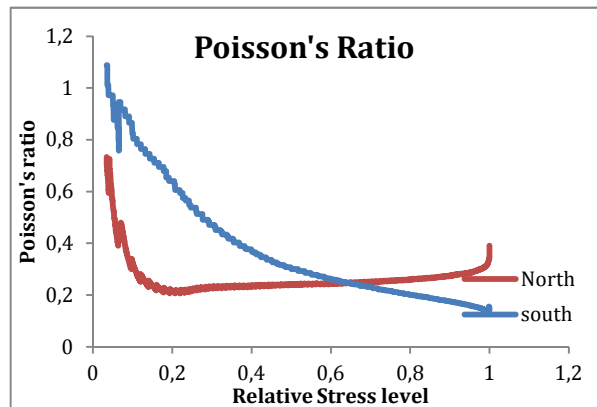
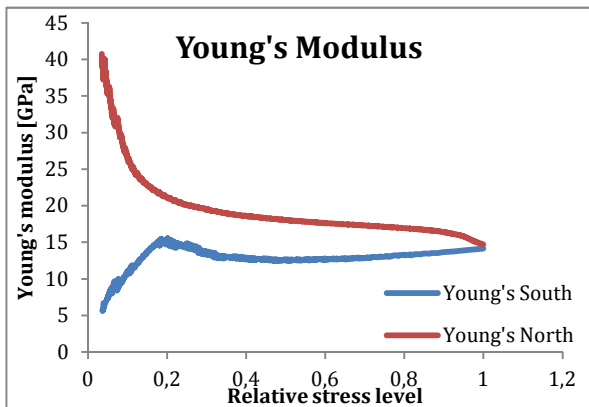
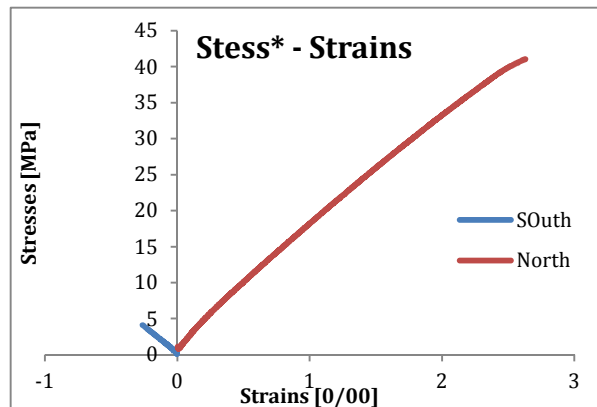
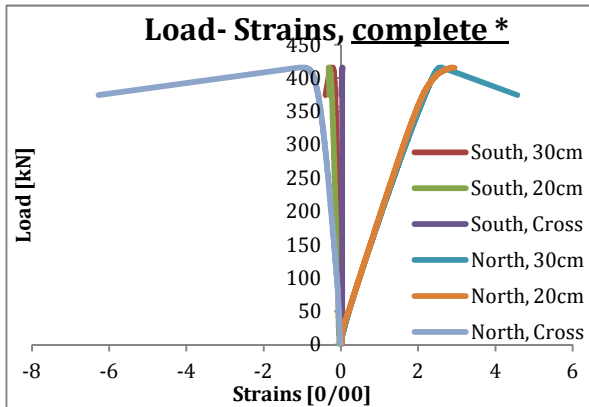
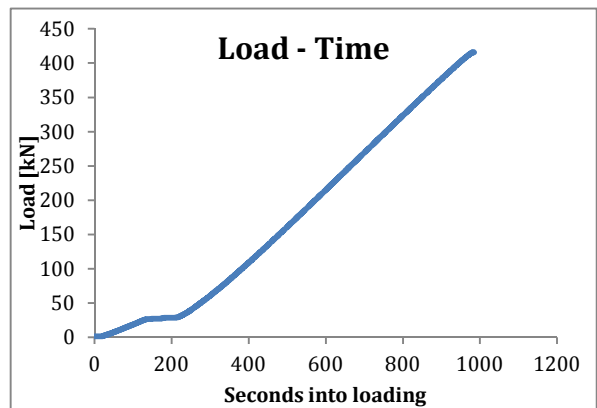
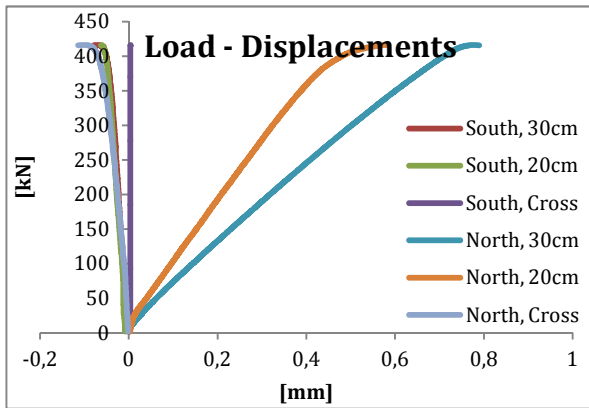


LWAC 0,0% Centric Loading, Prism B2

LWAC 0,0% Centric B2			
P_{peak} [kN]	f_{cp} [MPa]	P_{fail} [kN]	P_{change} [%]
715,67	31,808	715,67	0

LWAC 0,0% Centric B2			
LVDT id.	ϵ_{peak} [‰]	ϵ_{fail} [‰]	ϵ_{change} [%]
South 30	2,0675	2,06947	0,1
South 20	1,6599	1,6599	0
South Cross	-0,2391	-0,2391	0
North 30	2,4947	2,5067	0,5
North 20	2,1575	2,1635	0,3
North Cross	-0,9674	-1,0184	5,23

C.b.3. Appendix LWAC 0,0% steel fibres, Eccentric Loading, Prism B3



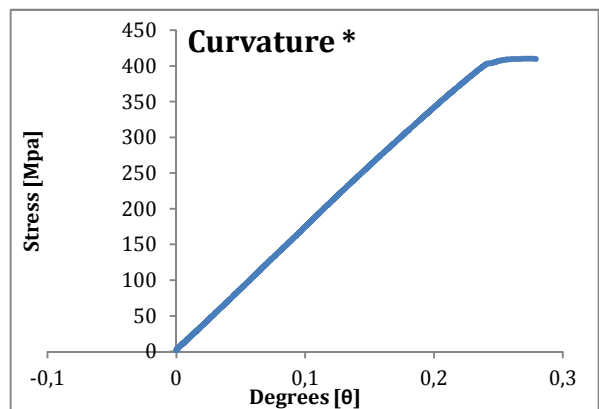
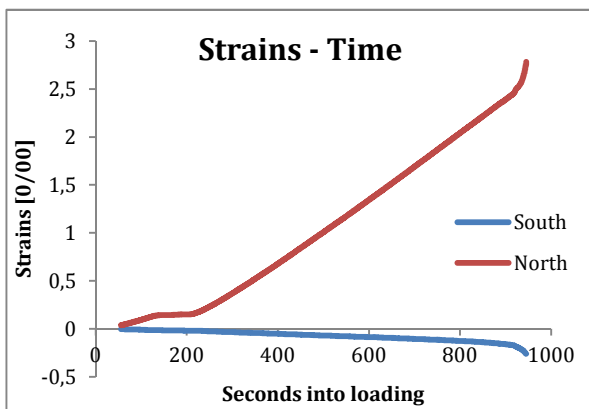
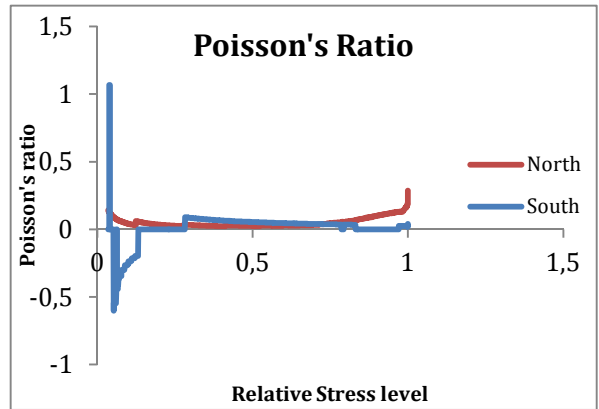
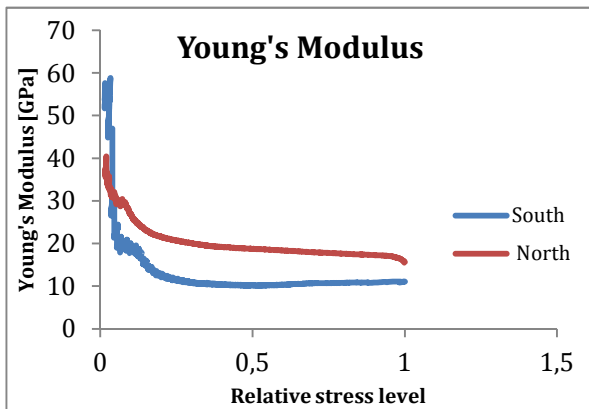
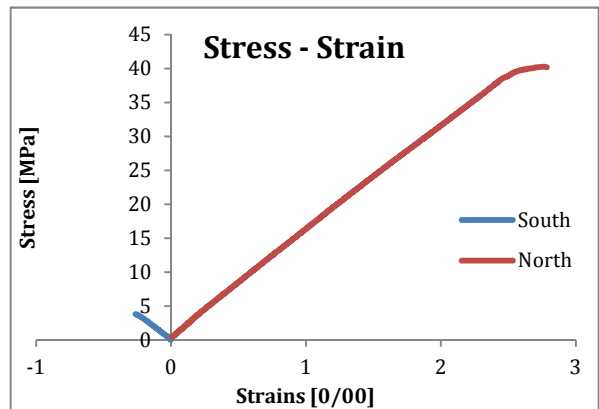
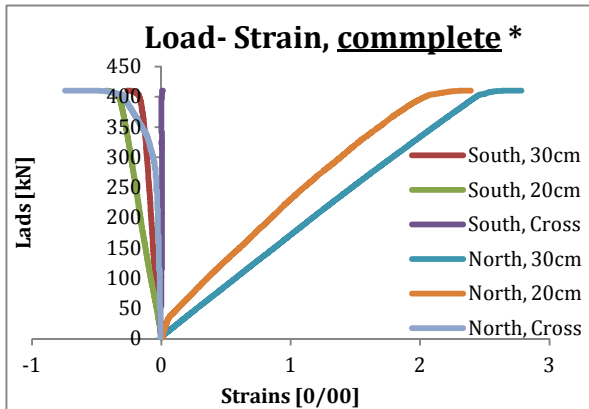
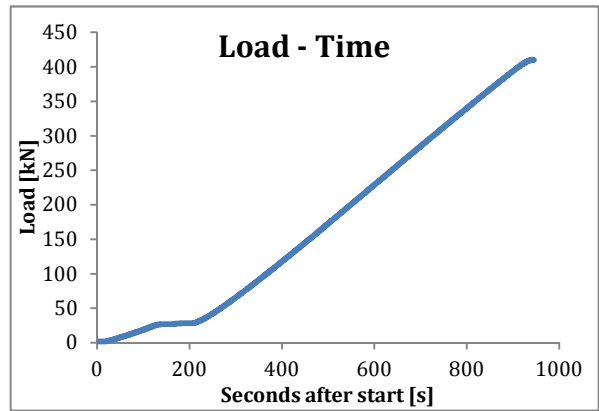
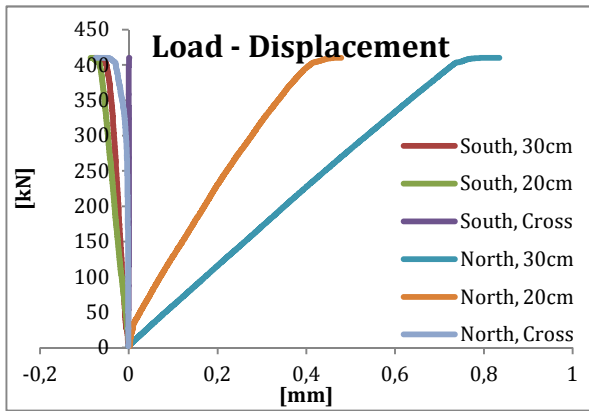
LWAC 0,0% Eccentric Loading, Prism B3

LWAC 0,0% Eccentric B3			
P_{peak} [kN]	f_{cp} [MPa]	P_{fail} [kN]	P_{change} [%]
416,08	-	415,6	-0,1

LWAC 0,0% Eccentric B3			
LVDT id.	ϵ_{peak} [‰]	ϵ_{fail} [‰]	ϵ_{change} [%]
South 30	-0,2343	-0,2625	12,0
South 20	-0,3082	-0,3156	2,4
South Cross	0,0399	0,0399	0
North 30	2,5693	2,6303	2,4
North 20	2,8850	2,9400	1,9
North Cross	-0,9864	-1,1400	15,6

The complete load-strain relation fro Prism B3 with 1,0% steel fibres shown above should have been stopped at on load interval earlier, due to the reason that the large strain development at the end of the curves express a part of the actual failure. The curve plotted in the report is actually the true curve.

C.b.4. Appendix LWAC 0,0% steel fibres, Eccentric loading, Prism B4

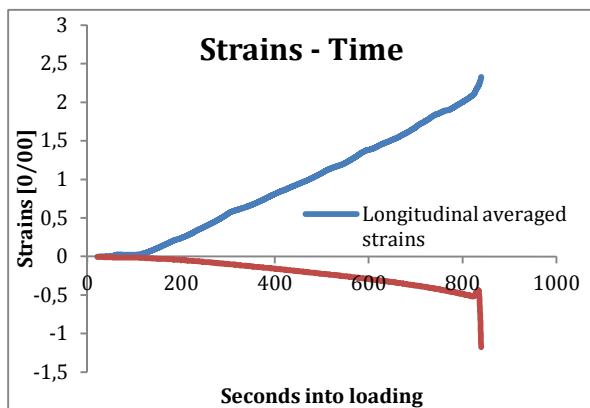
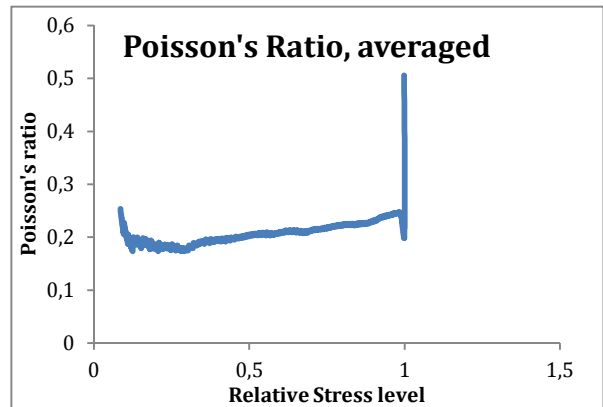
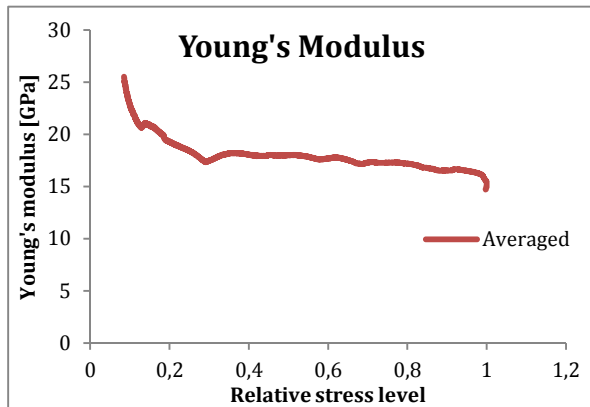
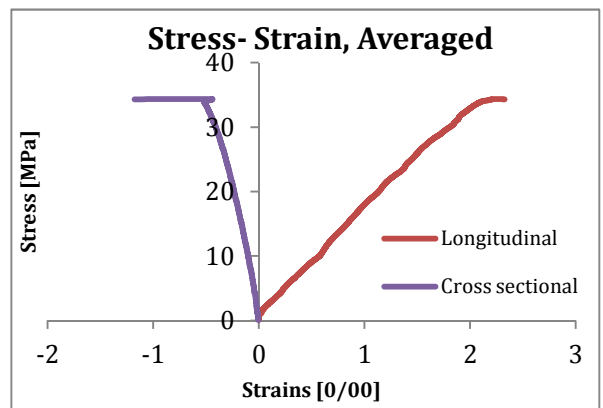
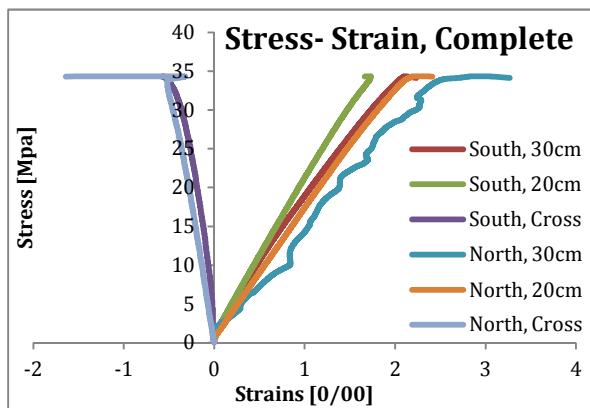
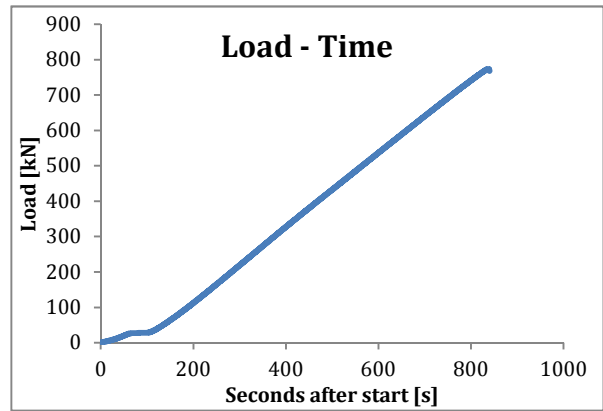
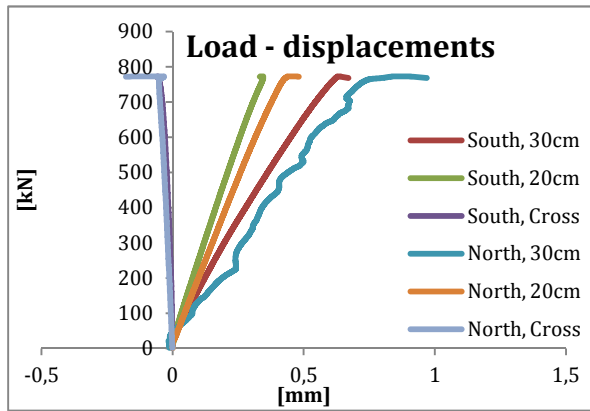


LWAC 0,0% Eccentric Loading, Prism B4

LWAC 0,0% Eccentric B4			
P_{peak} [kN]	f_{cp} [MPa]	P_{fail} [kN]	P_{change} [%]
410,16	-	409,92	-0,1

LWAC 0,0% Eccentric B4			
LVDT id.	ϵ_{peak} [‰]	ϵ_{fail} [‰]	ϵ_{change} [%]
South 30	-0,2516	-0,2603	3,5
South 20	-0,4196	-0,4308	2,7
South Cross	0,0133	0,0133	0
North 30	2,7220	2,7840	2,3
North 20	2,3645	2,3935	1,2
North Cross	-0,6021	-0,7430	23,4

C.b.5. Appendix LWAC 0,5% steel fibre, Centric loading, Prism B1



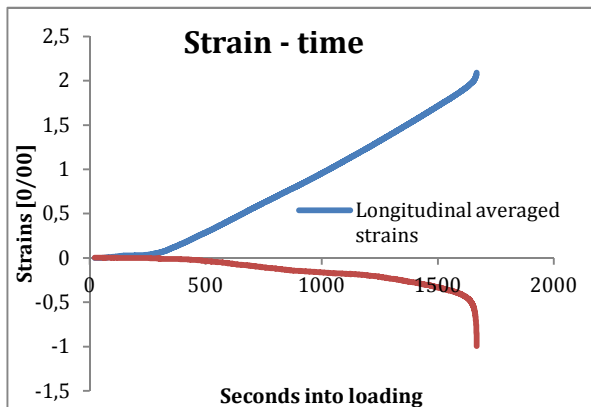
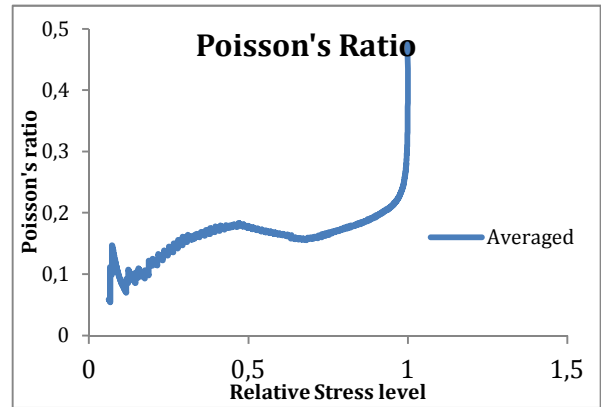
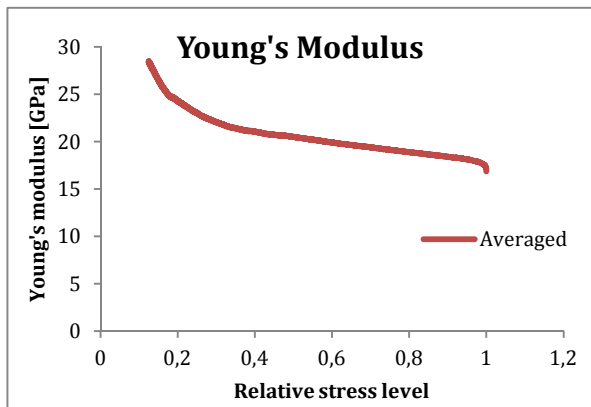
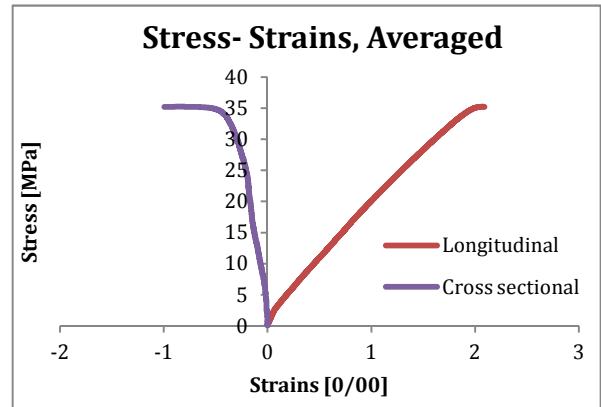
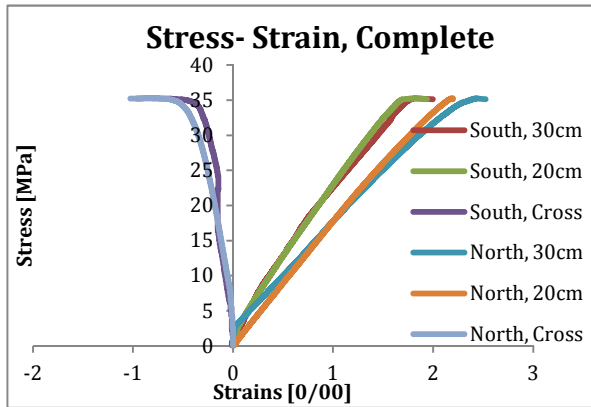
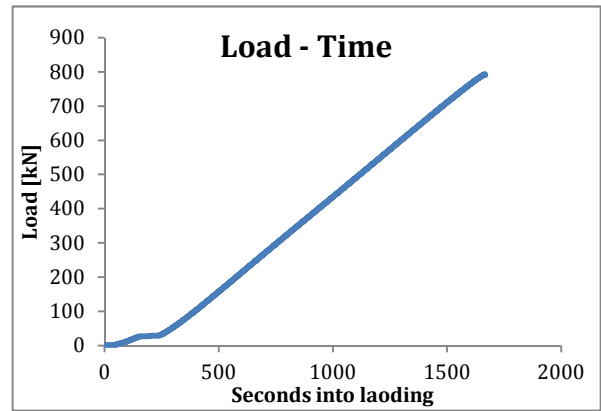
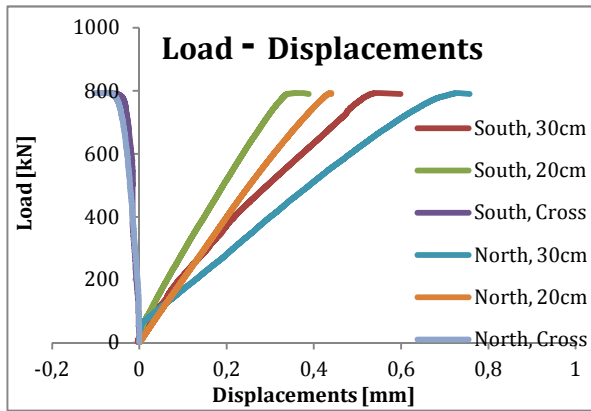
LWAC 0,5% Centric Loading, Prism B1

LWAC 0,5% Centric B1			
P_{peak} [kN]	f_{cp} [MPa]	P_{fail} [kN]	P_{change} [%]
773,22	34,3653	771,53	-0,2

LWAC 0,5% Centric B1			
LVDT id.	ϵ_{peak} [‰]	ϵ_{fail} [‰]	ϵ_{change} [%]
South 30	2,1063	2,1410	1,6
South 20	1,7120	1,6600	-3,6 ¹
South Cross	-0,5579	-0,5778	3,6
North 30	2,9012	3,0976	6,8
North 20	2,2530	2,4095	6,9
North Cross	-0,5380	-1,7740	229,7

¹ Seems like a final failure crack is under development outside the 20cm LVDT.

C.b.6. Appendix LWAC 0,5% steel fibre, Centric Loading, Prism B2

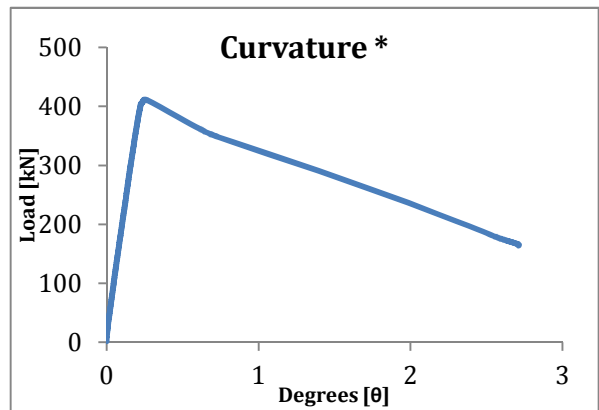
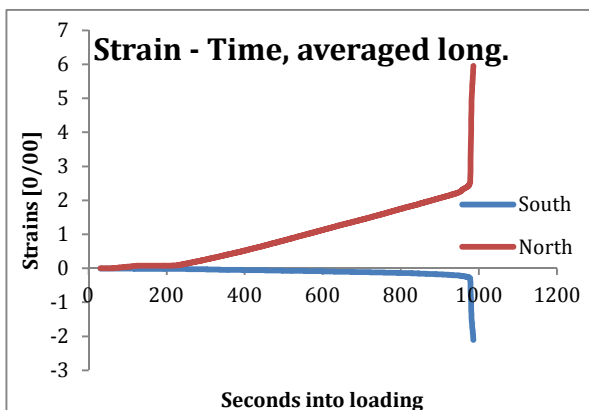
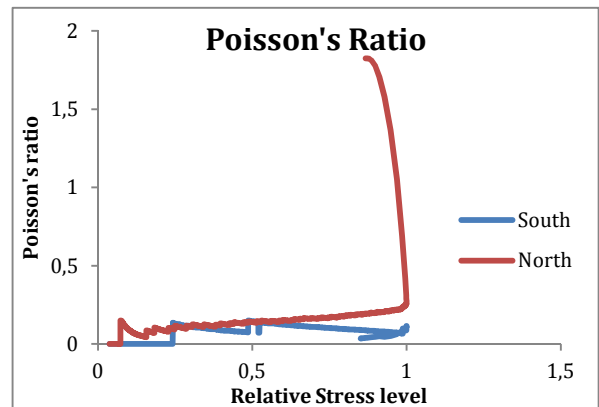
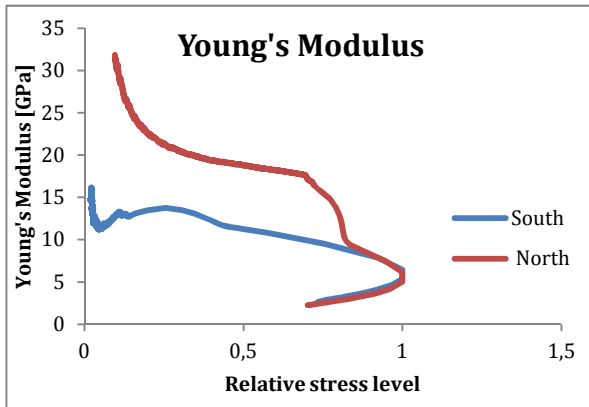
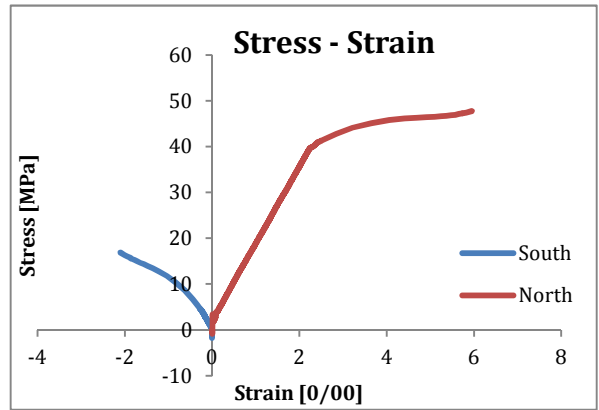
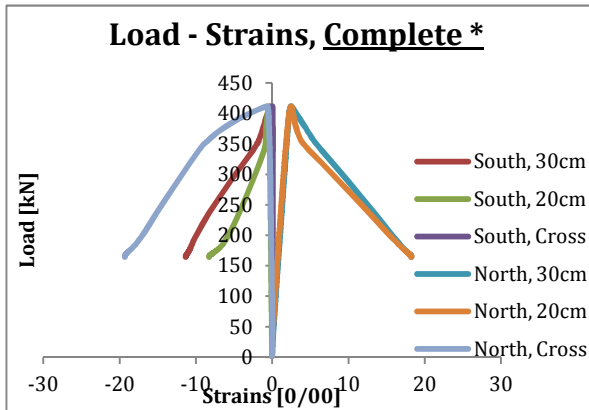
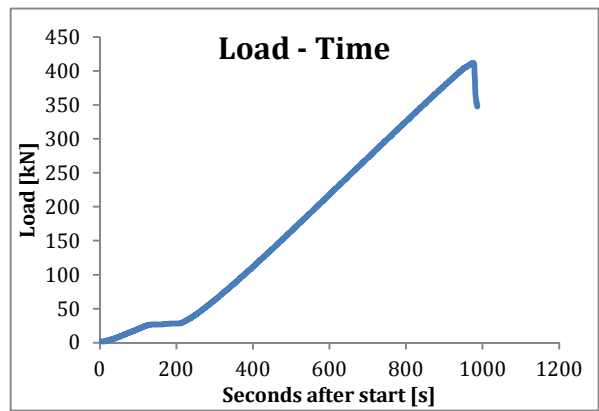
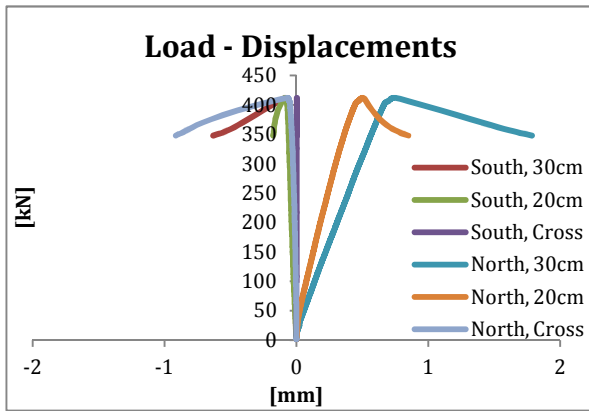


LWAC 0,5% Centric Loading, Prism B2

LWAC 0,5% Centric B2			
P_{peak} [kN]	f_{cp} [MPa]	P_{fail} [kN]	P_{change} [%]
793,24	35,255	792,84	-0,1

LWAC 0,5% Centric B2			
LVDT id.	ϵ_{peak} [‰]	ϵ_{fail} [‰]	ϵ_{change} [%]
South 30	1,8223	1,8397	1,0
South 20	1,8380	1,8825	2,42
South Cross	-0,8103	-0,963	18,8
North 30	2,4347	2,4407	0,2
North 20	2,1890	2,1985	0,4
North Cross	-0,8647	-1,0250	18,5

C.b.7. Appendix LWAC 0,5% steel fibres, Eccentric Loading, Prism B3



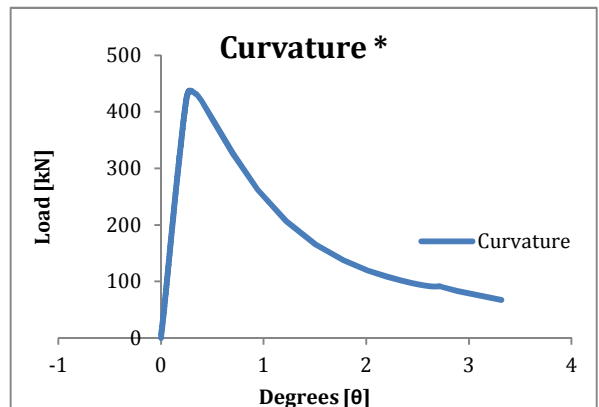
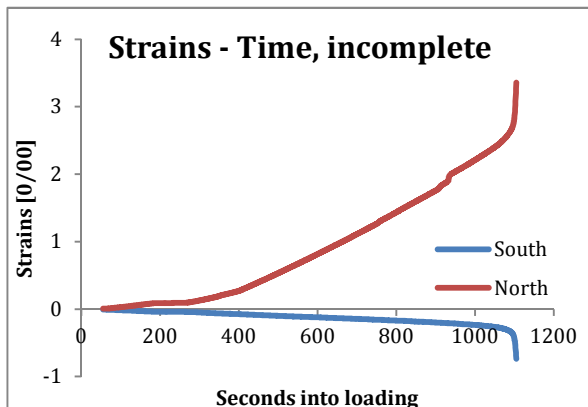
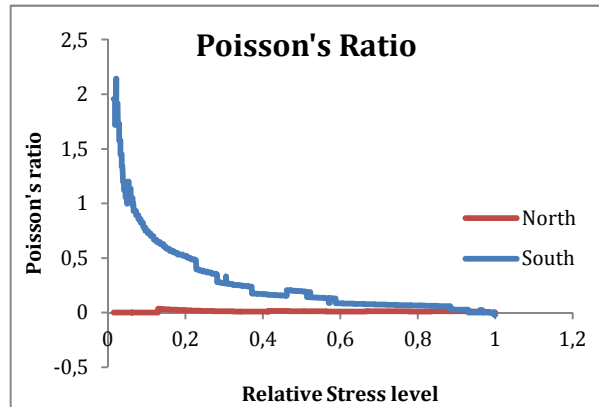
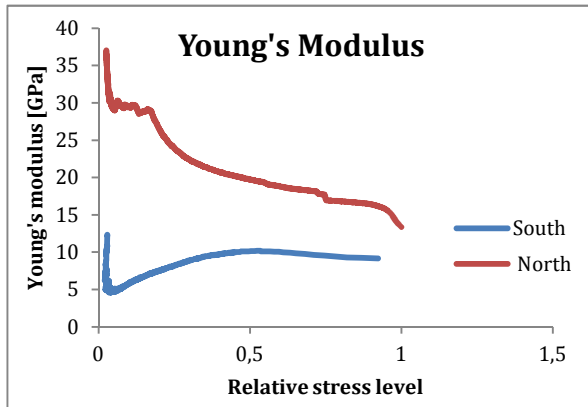
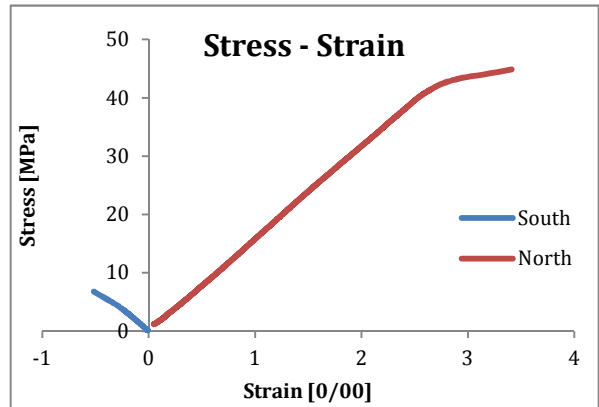
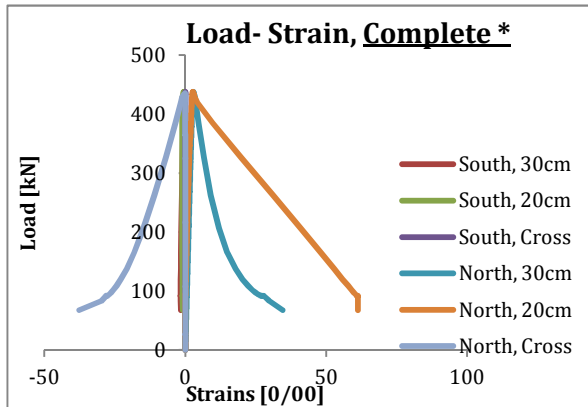
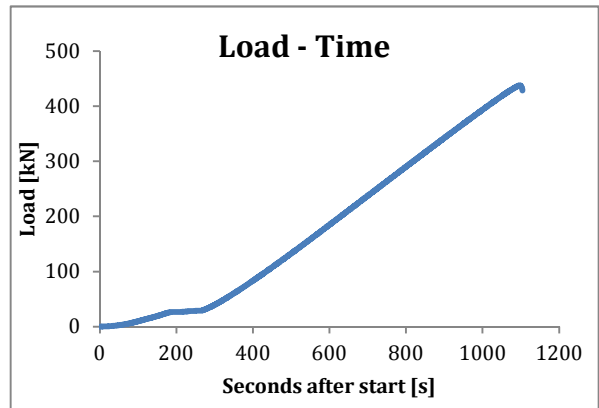
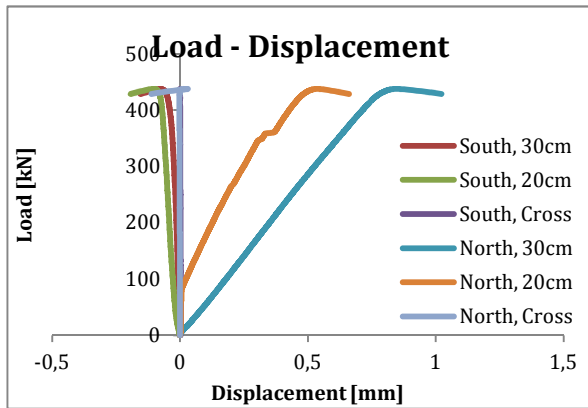
LWAC 0,5% Eccentric Loading, Prism B3

LWAC 0,5% Eccentric B3			
P_{peak} [kN]	f_{cp} [MPa]	P_{fail} [kN]	P_{change} [%]
411,76	-	347,6	-15,6

LWAC 0,5% Eccentric B3			
LVDT id.	ϵ_{peak} [‰]	ϵ_{fail} [‰]	ϵ_{change} [%]
South 30	-0,2700	-2,1033	679,0
South 20	-0,4350	-0,8900	104,6
South Cross	0,0400	0,0500	25
North 30	2,4633	5,9530	141,7
North 20	2,5	4,2400	69,6
North Cross	-0,65	-9,1400	1306,2

¹ It was hard to establish the exact point of failure, due to the more or less constant and even growth of strains

C.b.8. Appendix C.c.ii.4 LWAC 0,5% steel fibres, Eccentric Loading, Prism B4

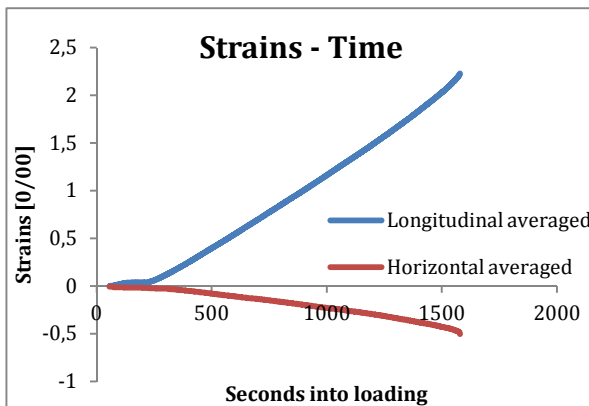
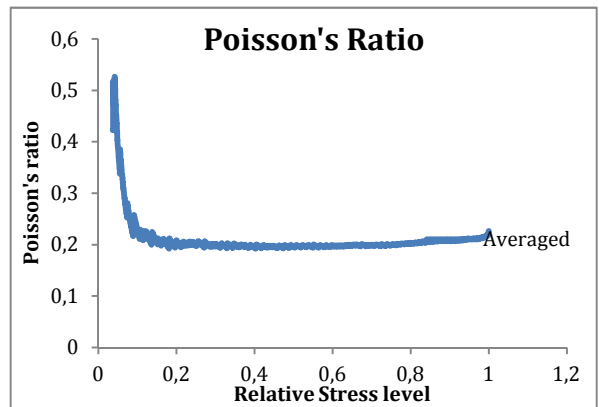
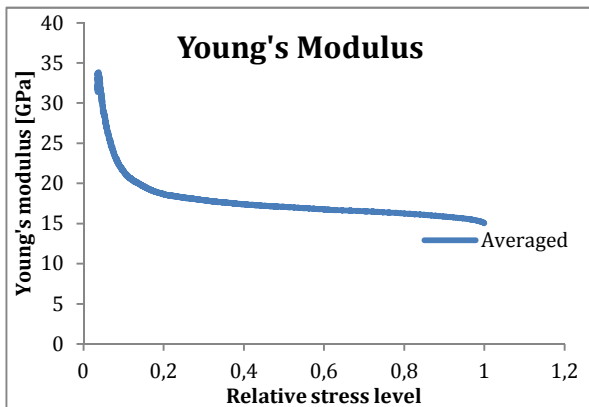
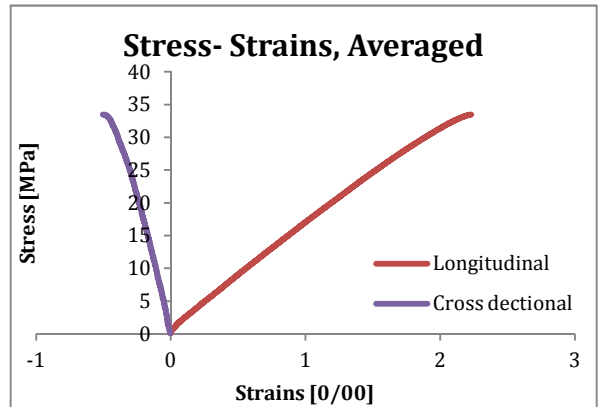
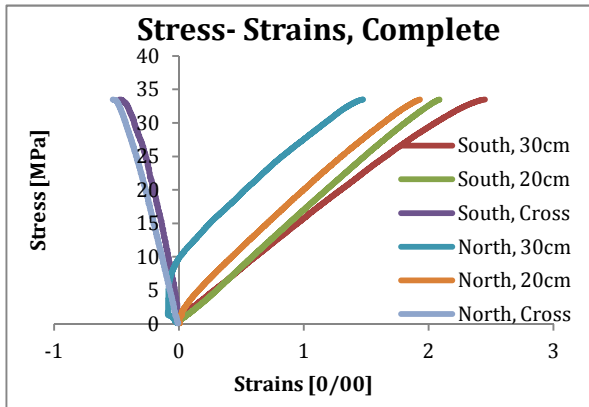
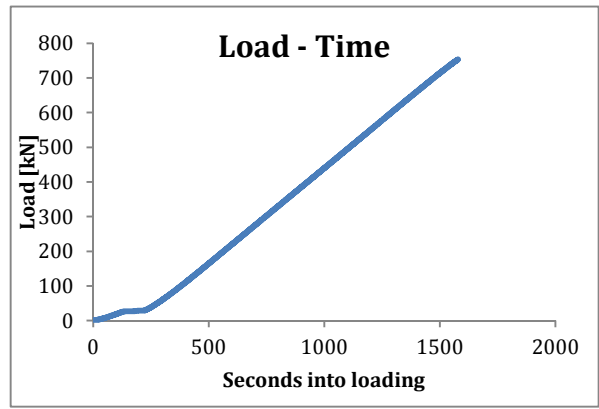
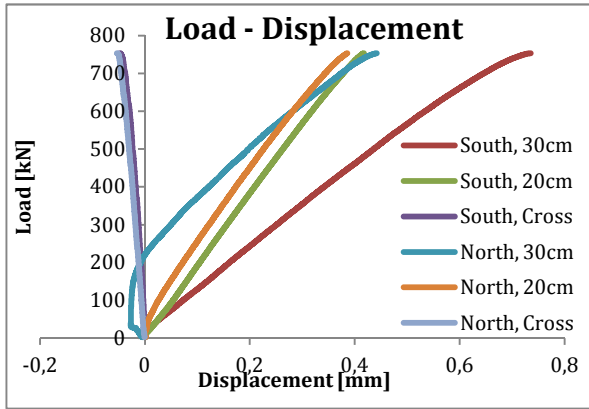


LWAC 0,5% Eccentric Loading, Prism B4

LWAC 0,5% Eccentric B4			
P_{peak} [kN]	f_{cp} [MPa]	P_{fail} [kN]	P_{change} [%]
437,5	-	428,27	-2,1

LWAC 0,5% Eccentric B4			
LVDT id.	ϵ_{peak} [‰]	ϵ_{fail} [‰]	ϵ_{change} [%]
South 30	-0,2560	-0,5140	100,8
South 20	-0,5058	-0,9615	90,9
South Cross	-	-	-
North 30	2,8120	3,4100	21,3
North 20	2,6710	3,3060	23,8
North Cross	-	-1,1150	-

C.b.9. Appendix LWAC 1,0% steel fibre, Centric Loading, Prism B1



LWAC 1,0% Centric Loading, Prism B1

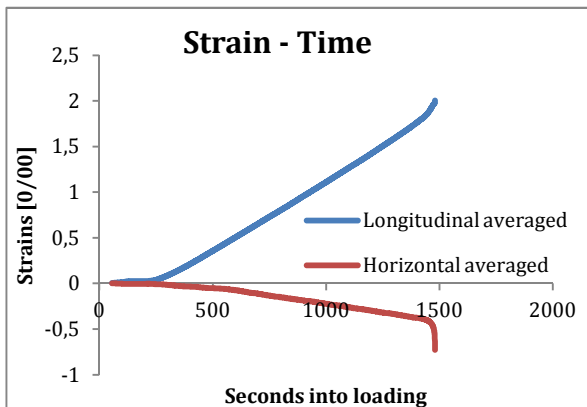
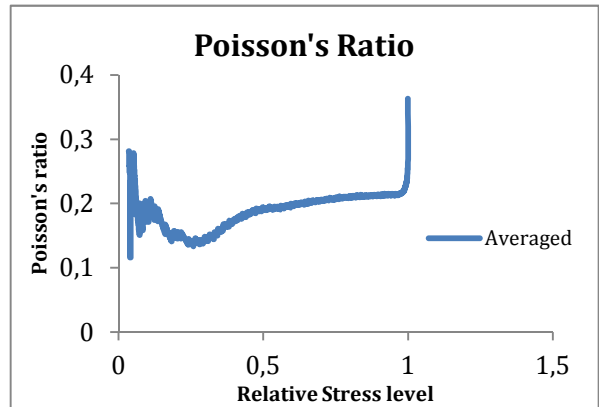
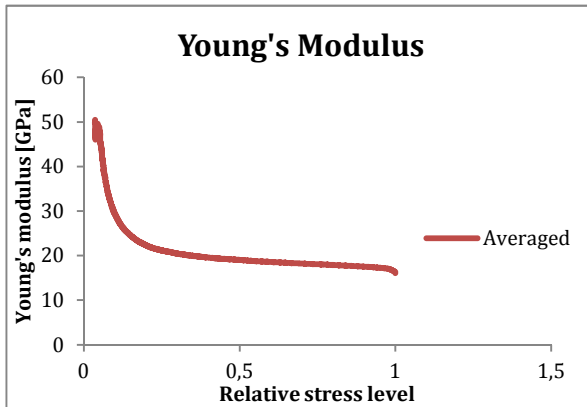
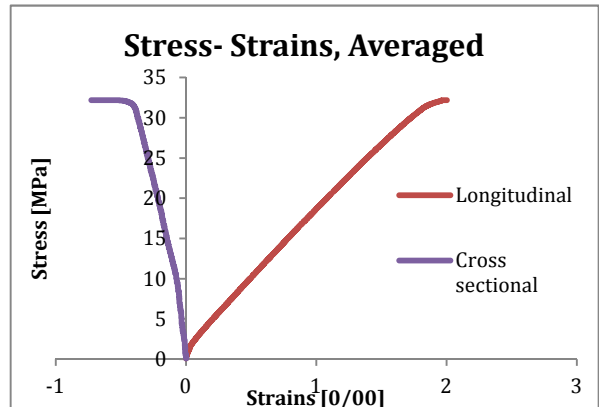
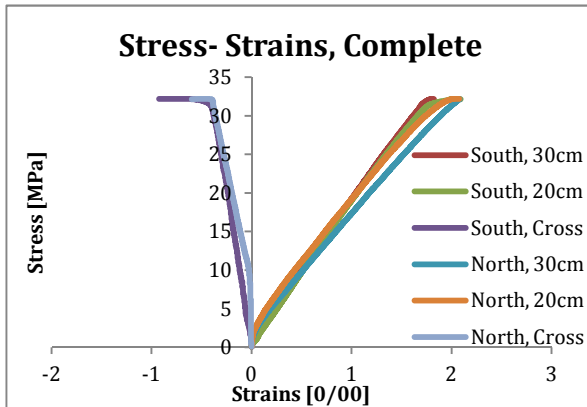
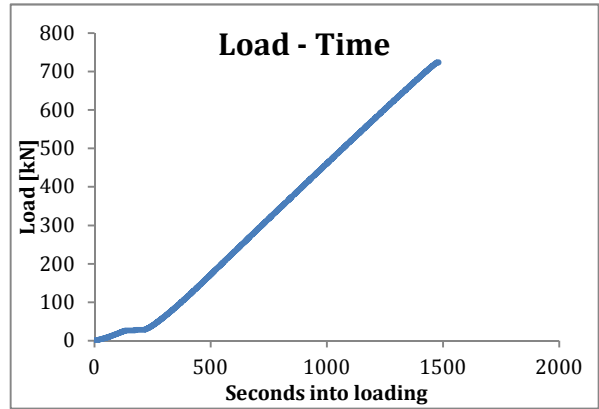
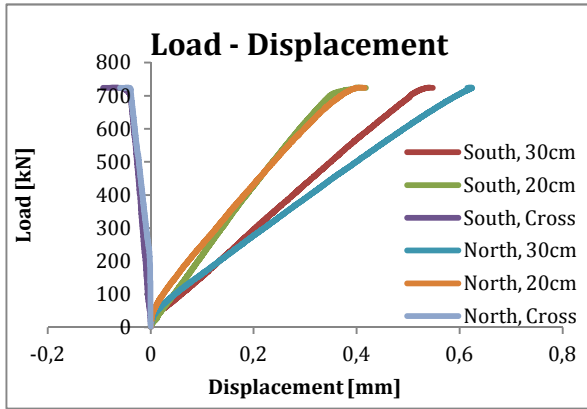
LWAC 1,0% Centric B1			
P_{peak} [kN]	f_{cp} [MPa]	P_{fail} [kN]	P_{change} [%]
753,39	33,484	753,39	0

LWAC 1,0% Centric B1			
LVDT id.	ϵ_{peak} [‰]	ϵ_{fail} [‰]	ϵ_{change} [%]
South 30	2,4513	2,5413	0
South 20	2,0870	2,0870	0
South Cross	-0,4782	-0,4782	0
North 30	1,4729 ¹	1,4729 ¹	0
North 20	1,9305 ²	1,9305 ²	0
North Cross	-0,5316	-0,5316	0

1 The results from LVDT North 30cm was highly doubted to be correct. See diagram. If the test is correct however, it is very strange.

2 This is the only time that the 20cm recordings from the south side is larger than the strains on the north side.

C.b.10. Appendix LWAC with 1,0% steel fibre, Centric Loading, Prism B2



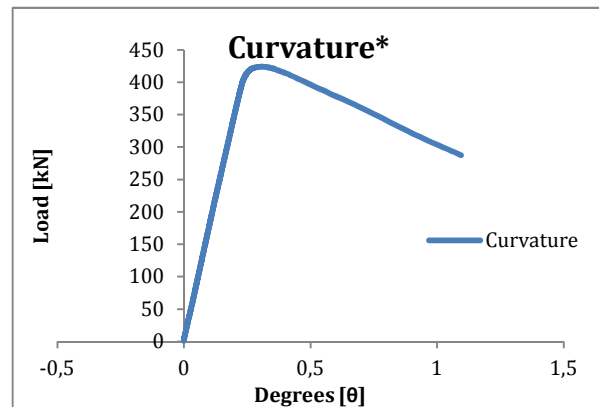
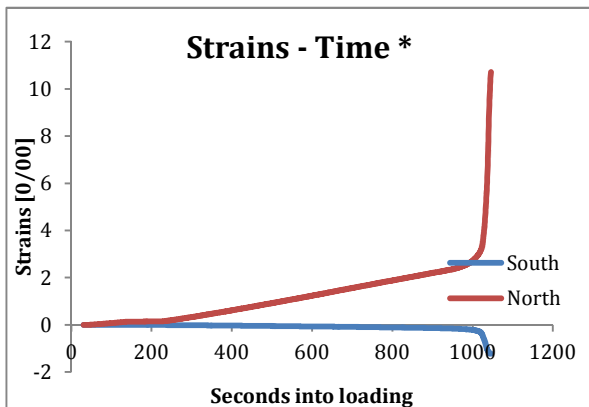
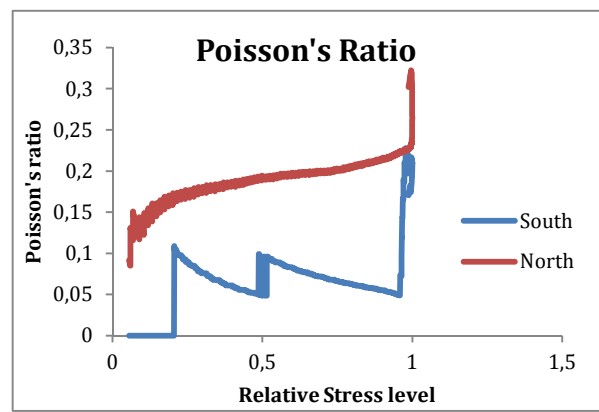
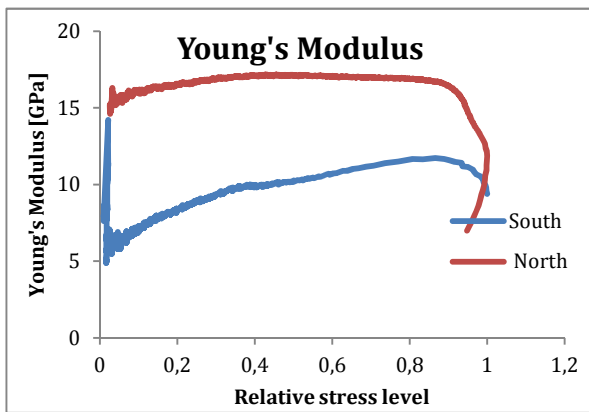
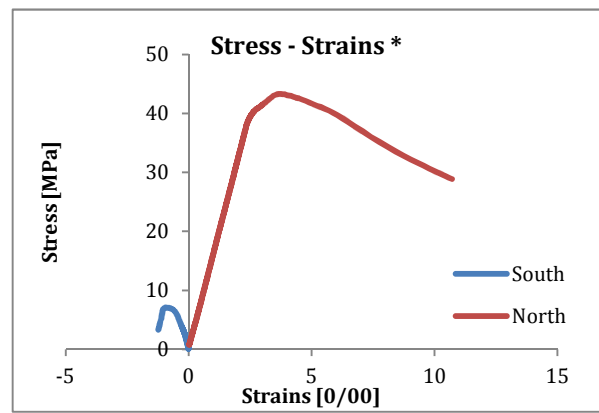
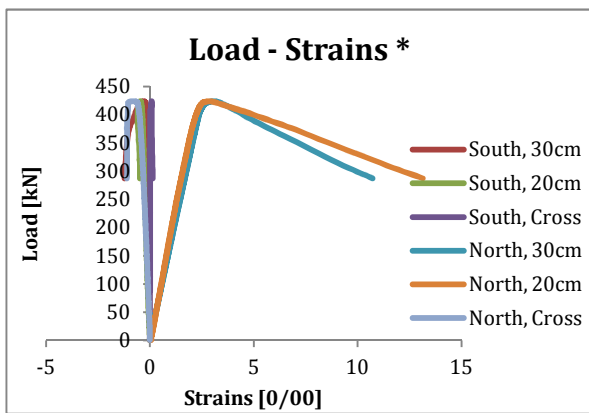
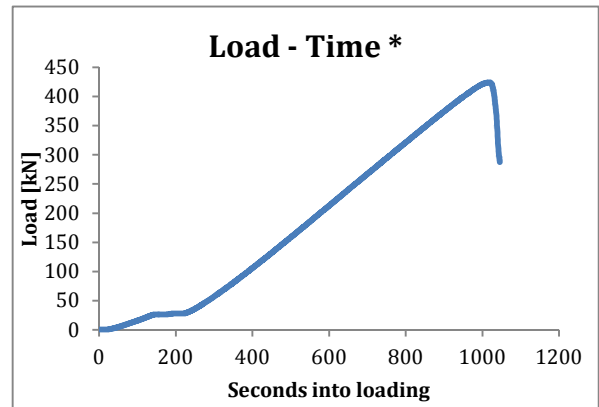
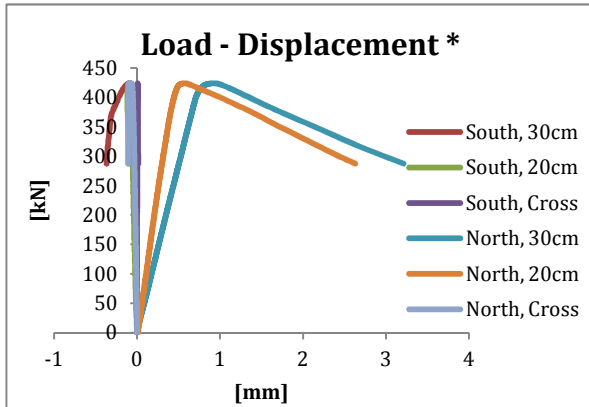
LWAC 1,0% Centric Loading, Prism B2

LWAC 1,0% Centric B2			
P_{peak} [kN]	f_{cp} [MPa]	P_{fail} [kN]	P_{change} [%]
724,32	32,192	723,92	-0,1

LWAC 1,0% Centric B2			
LVDT id.	ϵ_{peak} [‰]	ϵ_{fail} [‰]	ϵ_{change} [%]
South 30	1,7983	1,8180	1,1
South 20	1,9977	2,0682	3,5
South Cross	-0,6974	-0,9232	32,4
North 30	2,0673	2,0496	-0,9 ¹
North 20	2,0265	2,0775	2,5
North Cross	-0,4420	-0,5316	20,3

¹ Seems like the final failure crack takes form outside the north 30cm LVDT

C.b.11. Appendix LWAC with 1,0% steel fibre, Eccentric Loading, Prism B3



LWAC 1,0% Eccentric Loading, Prism B3

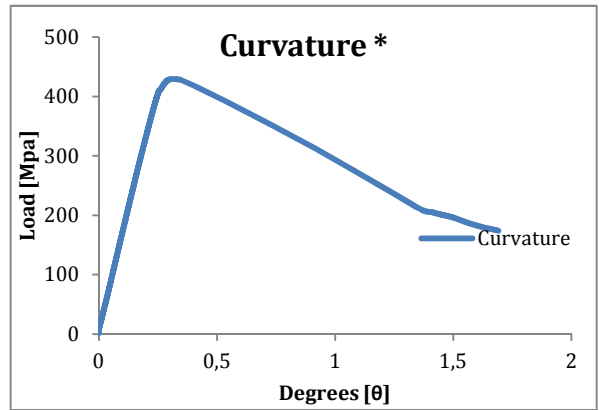
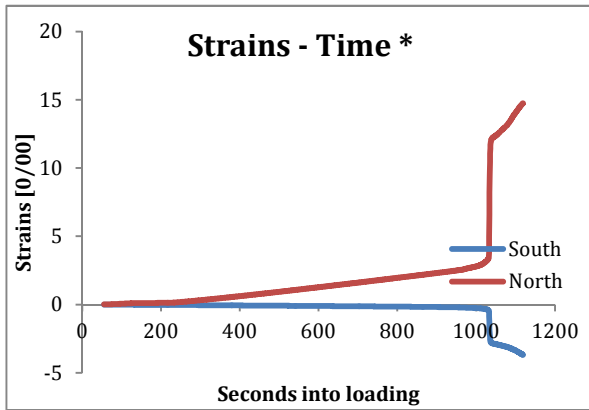
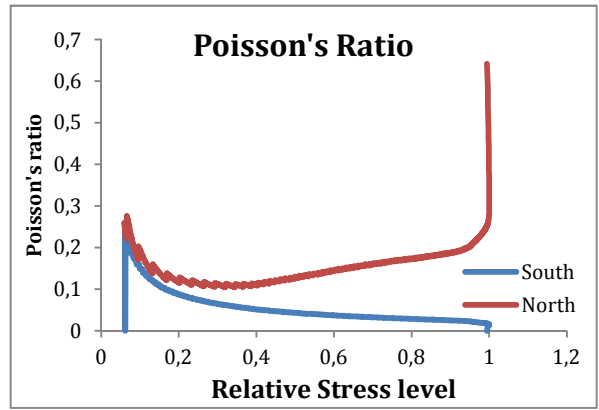
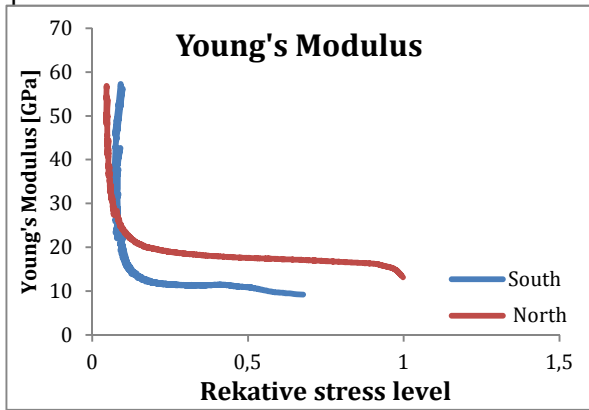
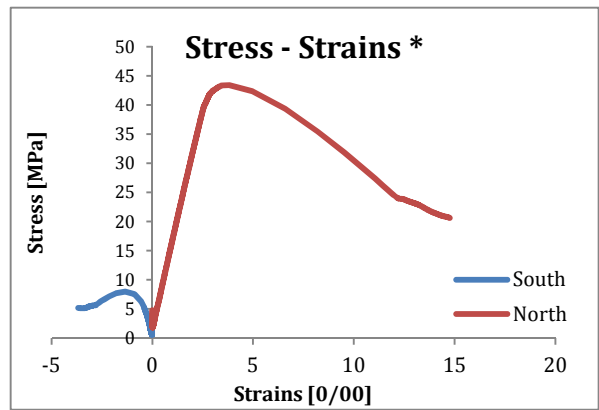
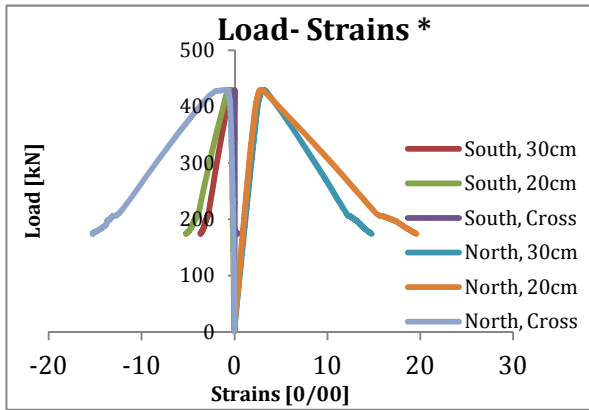
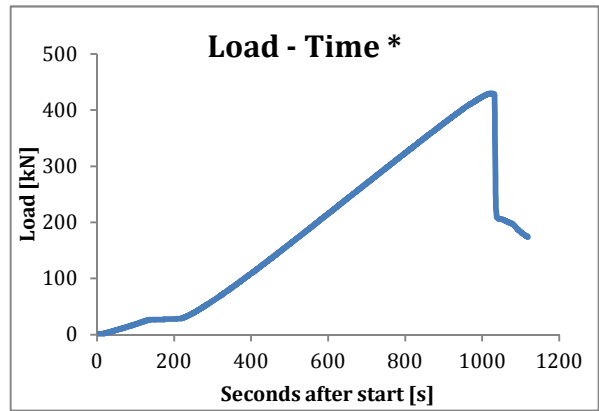
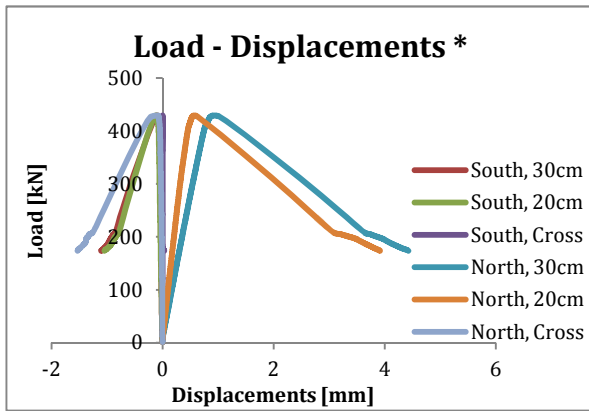
LWAC 1,0% Eccentric B3			
P_{peak} [kN]	f_{cp} [MPa]	P_{fail} [kN]	P_{change} [%]
424,0	-	382,36 ¹	-10

¹ Again, it was hard to starte the exact time of failure. The values presented in the table were “stopped” at 90% of peak load on the descending branch

LWAC 1,0% Eccentric B3			
LVDT id.	ϵ_{peak} [‰]	ϵ_{fail} [‰]	ϵ_{change} [%]
South 30	-0,2933	-0,9267	216,0
South 20	-0,4650	-0,5800	24,7
South Cross	0,0797	0,0930	16,7
North 30	3,0600	5,3800	75,8
North 20	2,8550	6,355	122,6
North Cross	-0,7820	-1,1020	40,9

¹ The exact time of failure was again hard to determine. The values presented in the table is therefor taken from 90% of peak load on the descending branch.

C.b.12. Appendix LWAC with 1,0% steel fibre, Eccentric Loading, Prism B4



LWAC 1,0% Eccentric Loading, Prism B4

LWAC 1,0% Eccentric B4			
P_{peak} [kN]	f_{cp} [MPa]	P_{fail} [kN]	P_{change} [%]
439,38	-	426,94	-2,8

LWAC 1,0% Eccentric B4			
LVDT id.	ϵ_{peak} [‰]	ϵ_{fail} [‰]	ϵ_{change} [%]
South 30	-0,3211	-0,4273	33,1
South 20	-0,5570	-0,7425	33,3
South Cross	0,0066	0,0000	-
North 30	3,0673	3,4300	11,8
North 20	2,8240	3,1785	12,6
North Cross	-0,8647	-2,1200	145,2

¹ Again, the final failure is hard to determine. The values of the “failure” presented in the table is taken from the first step of sudden drop in load bearing capacity and growth of strains. However, the strains continues growing and the load bearing capacity flattens out after this step. The failure might therefor be much later than assumed here!

Summary of strains for all LWAC prism in eccentric compression.

LWAC - Eccentric						
Fibre [%]	Prism identity	Prism face	Direction of LVDT	ϵ_{peak} [‰]	ϵ_{fail} [‰]	ϵ_{change} [%]
0,0	B3	North	Long. ¹	2,736 ³	2,785	1,8
			Cross ²	-0,986	-1,14	15,6
		South	Long.	-0,269	-0,289	7,4
			Cross	0,039	0,039	-
	B4	North	Long.	2,543	2,589	1,8
			Cross	-0,602	-0,743	23,4
		South	Long.	-0,336	-0,346	3,0
			Cross	0,013	0,013	-
0,5	B3	North	Long.	2,482	5,097	105,4
			Cross	-0,650	-9,140	1306,2
		South	Long.	-0,353	-1,497	324,1
			Cross	0,040	0,050	25
	B4	North	Long.	2,742	3,358	22,5
			Cross	-	-1,115	∞
		South	Long.	-0,382	-0,738	93,2
			Cross	-	0,013	-
1,0	B3 ⁵	North	Long.	2,958	5,868	98,1
			Cross	-0,769	-1,102	43,3
		South	Long.	-0,376	-0,753	100,3
			Cross	0,073	0,093	27,4
	B4 ⁶	North	Long.	2,946	3,304	12,2
			Cross	-0,865	-2,120	145,1
		South	Long.	-0,439	-0,585	33,3
			Cross	-	-	-

¹ "Long." refers to the strains in longitudinal directions

² "Cross" refers to the cross sectional- or lateral strains at the middle section

³ The longitudinal strains presented in the table have been averaged based on the data for both the 20- and 30cm LVDTs located at the same face, while cross sectional strains have been directly presented.

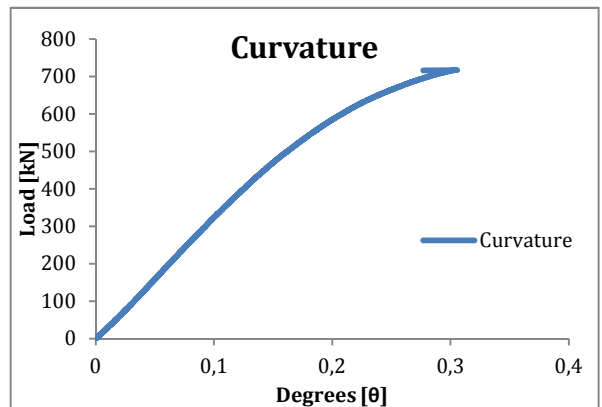
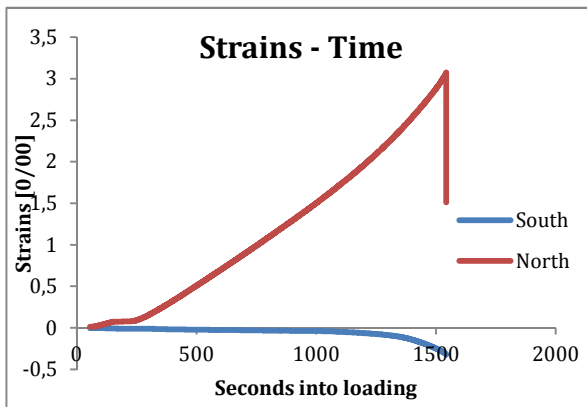
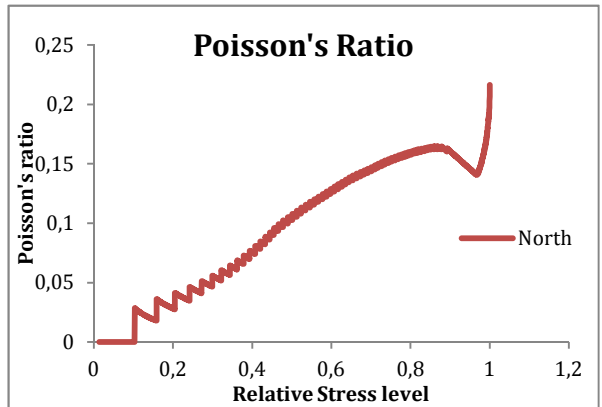
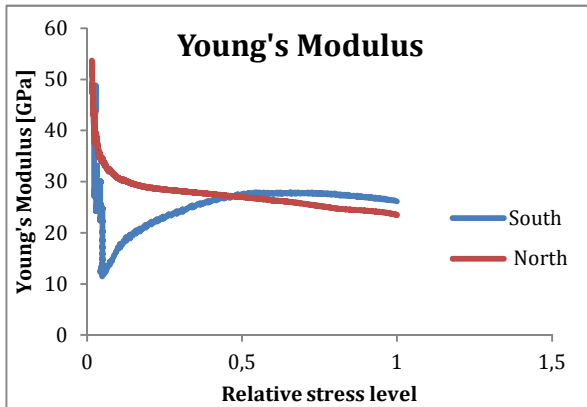
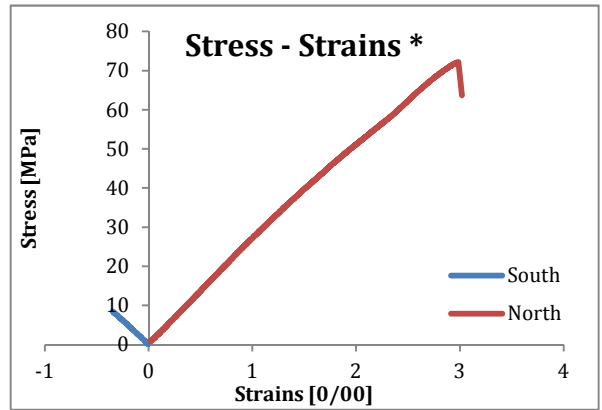
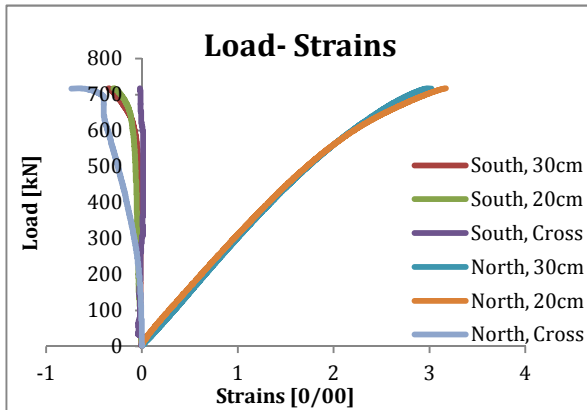
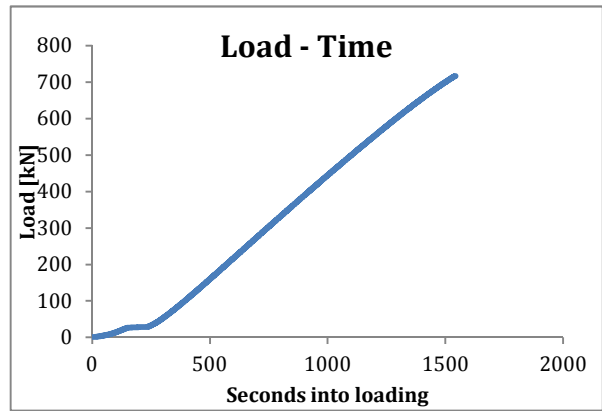
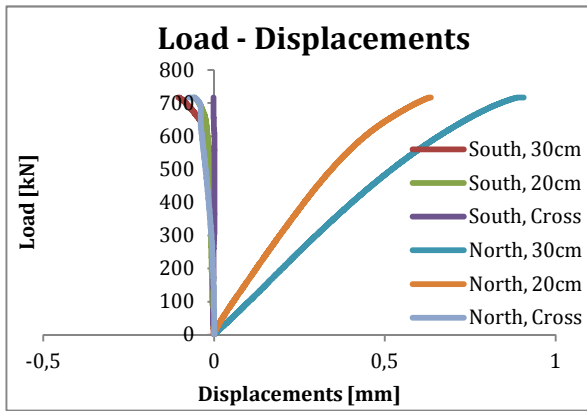
⁴ Recordings that did not seem likely to be correct was not included in the averaging of the values

presented in the table.

⁵ The values given for failure in the table have been taken from a load level of 90% on the descending branch. This is due to the fact that it was hard to establish the exact time of failure.

⁶ The strains in the table for the time of “failure” have been taken from a point where the load bearing capacity suddenly started dropping, and the strains started to grow at a very fast pace. However, at about 48% of the peak load bearing capacity the drop of capacity and the growth of strains stabilized. It might just be so that the failure did not occurred until at a very late stage. Se figure for Load-Strains Complete in the annex.

C.c.1. Appendix NDC with 0,0% steel fibre, Eccentric Loading, Prism B3

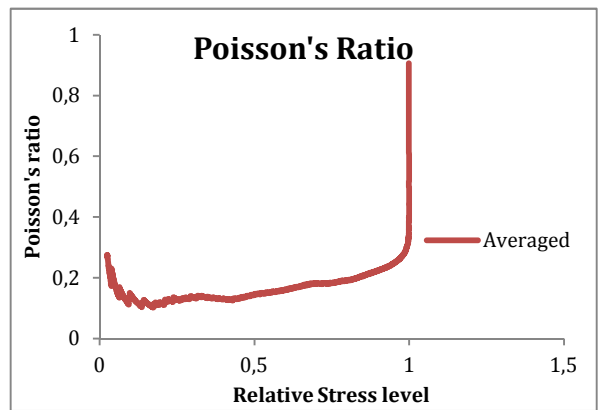
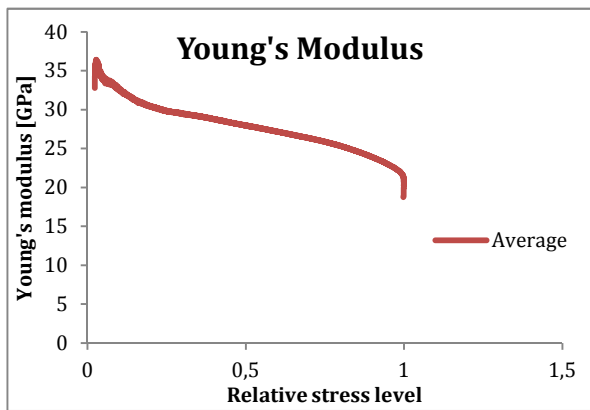
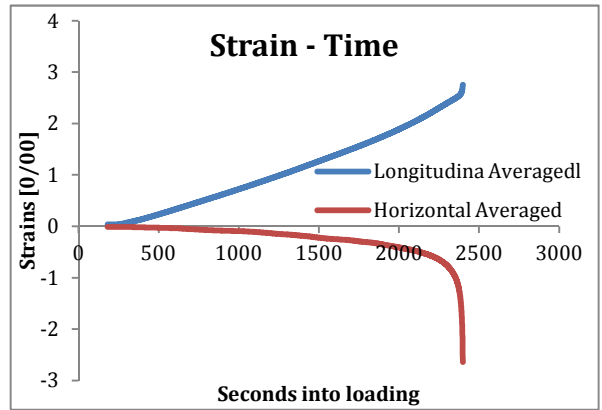
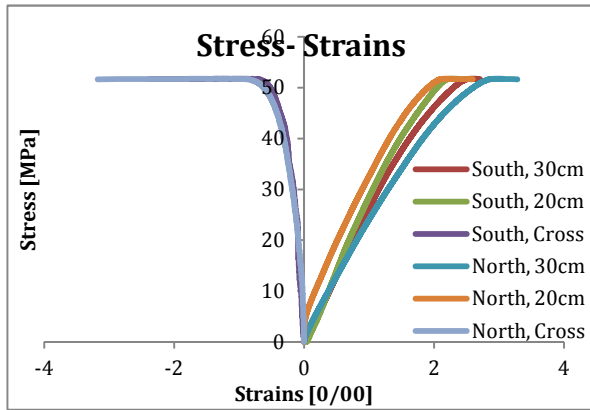
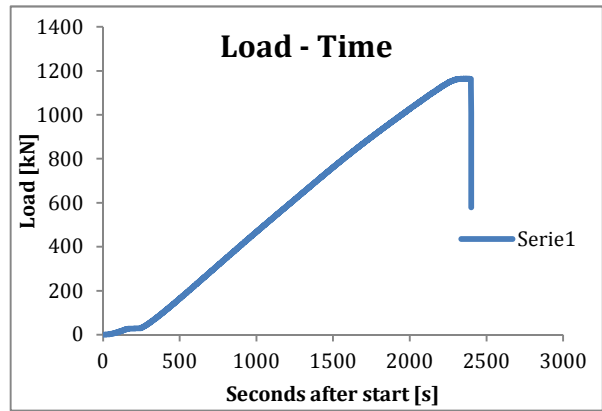
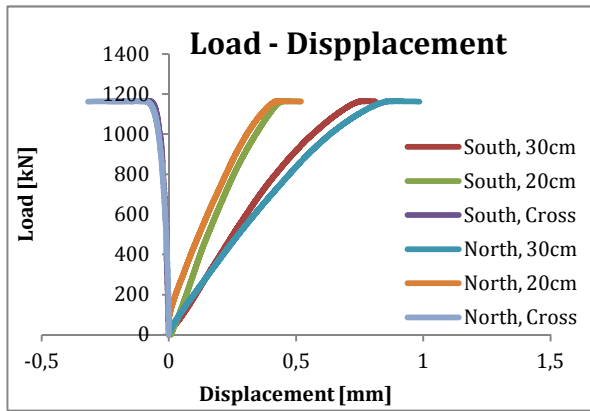


NDC 0,0% Eccentric Loading, Prism B3

NDC 0,0% Eccentric B3			
P_{peak} [kN]	f_{cp} [MPa]	P_{fail} [kN]	P_{change} [%]
717,03	-	717,03	0

NDC 0,0% Eccentric B3			
LVDT id.	ϵ_{peak} [‰]	ϵ_{fail} [‰]	ϵ_{change} [%]
South 30	-0,3493	-0,3493	-
South 20	-0,2971	-0,2971	-
South Cross	-	-	-
North 30	2,9853	2,9853	-
North 20	3,1723	3,1723	-
North Cross	-0,6661	-0,6661	-

7.1.1.1 C.c.2. Appendix NDC with 0,5% steel fibre, Centric Loading, Prism B1

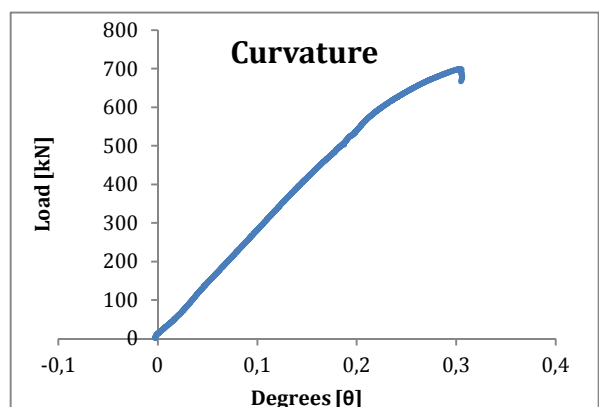
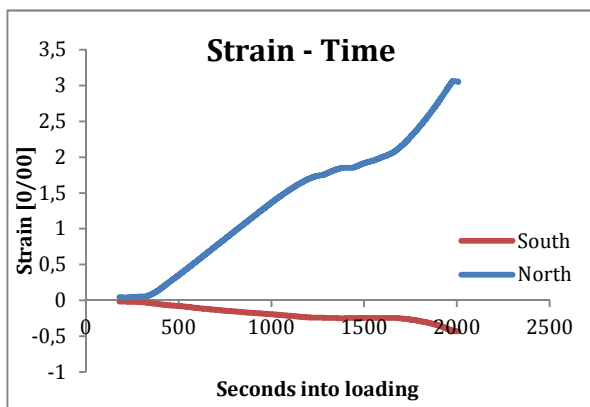
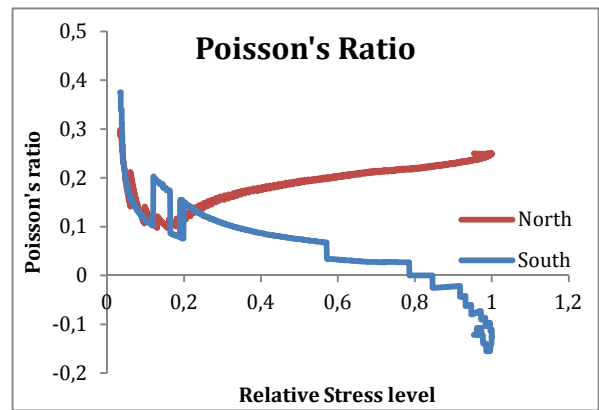
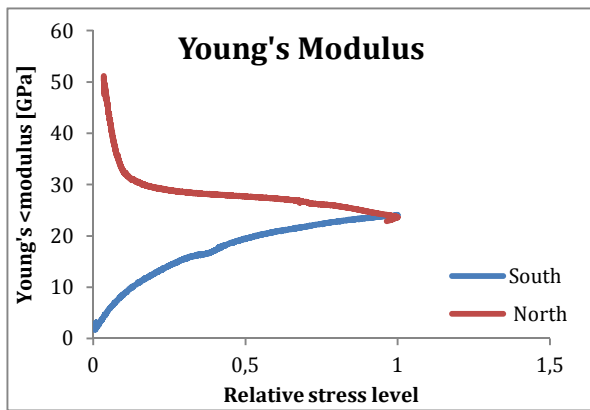
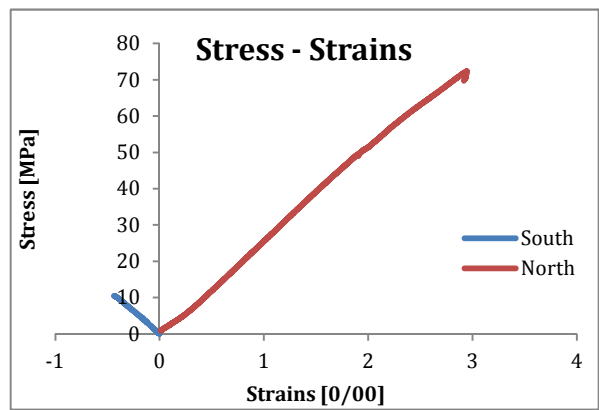
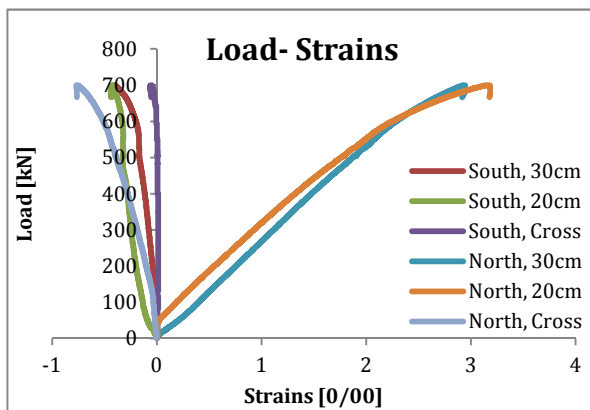
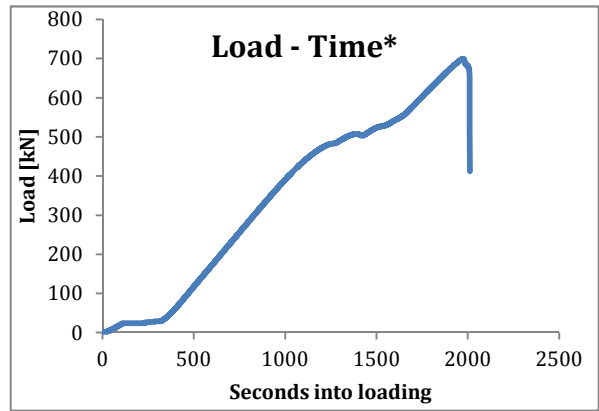
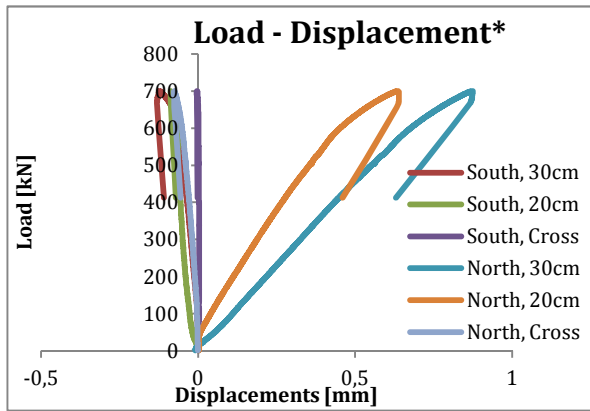


NDC 0,5% Centric Loading, Prism B1

NDC 0,5% Centeric B1			
P_{peak} [kN]	f_{cp} [MPa]	P_{fail} [kN]	P_{change} [%]
1164,7	51,76	1162,3	-0,2

NDC 0,5% Centric B1			
LVDT id.	ϵ_{peak} [‰]	ϵ_{fail} [‰]	ϵ_{change} [%]
South 30	2,6030	2,7007	3,8
South 20	2,3020	2,5175	9,4
South Cross	-1,0100	-2,391	136,7
North 30	2,9893	3,2070	7,3
North 20	2,2050	2,5945	17,7
North Cross	-1,2680	-2,8890	127,8

C.c.2. Appendix NDC with 0,5% steel fibre, Eccentric Loading, Prism B3

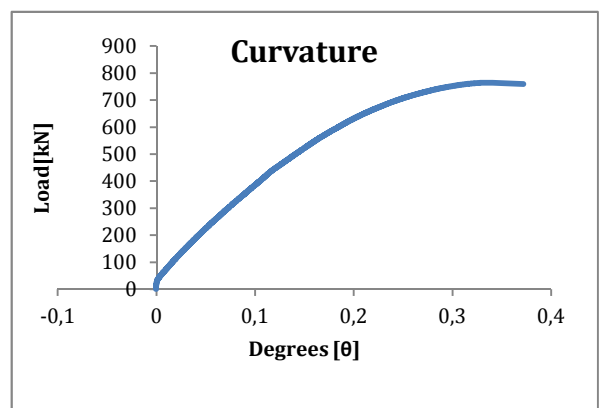
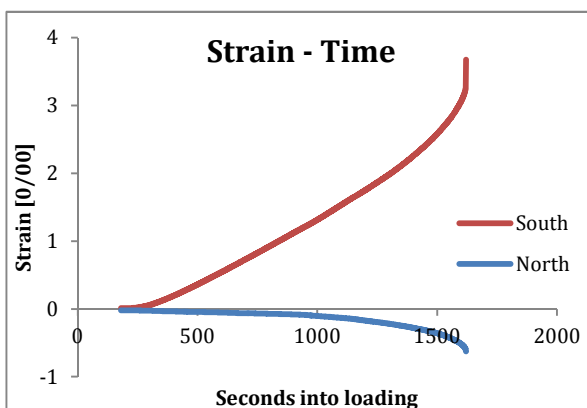
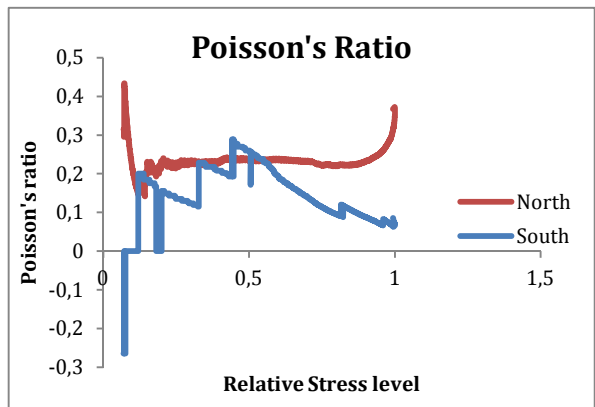
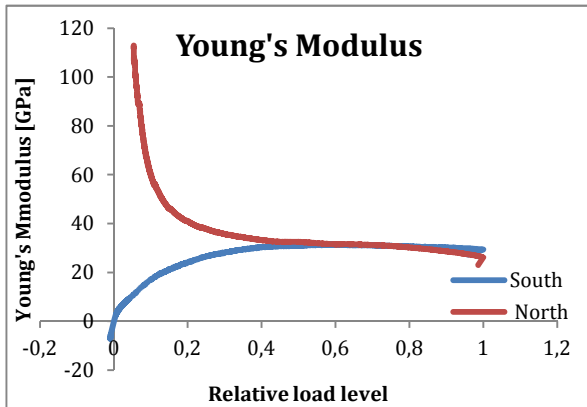
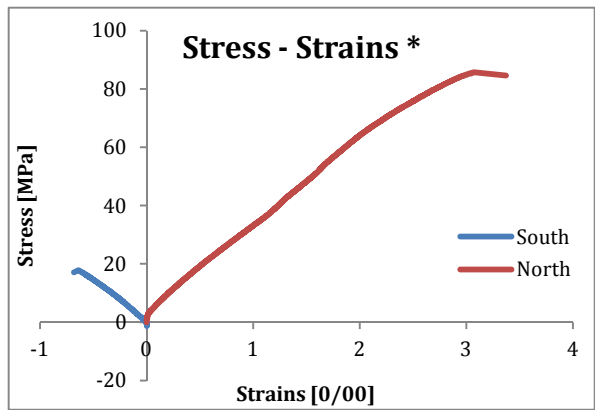
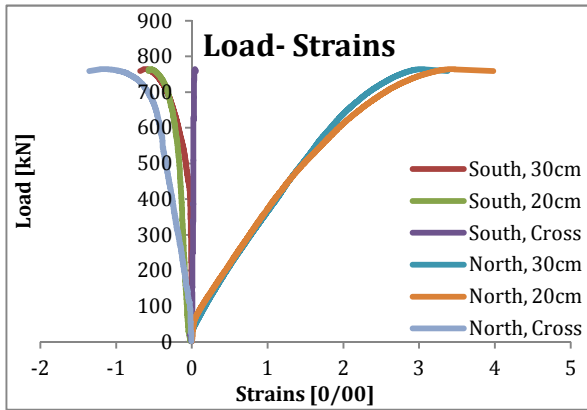
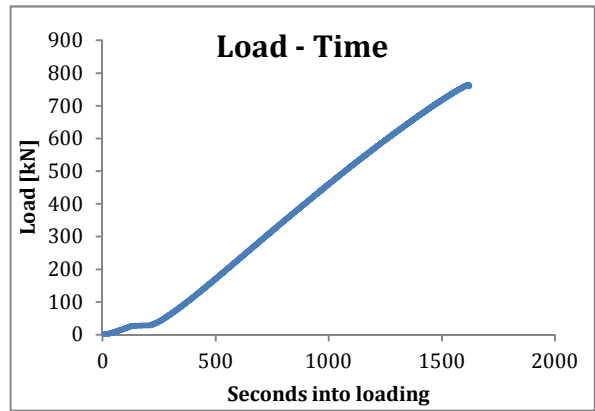
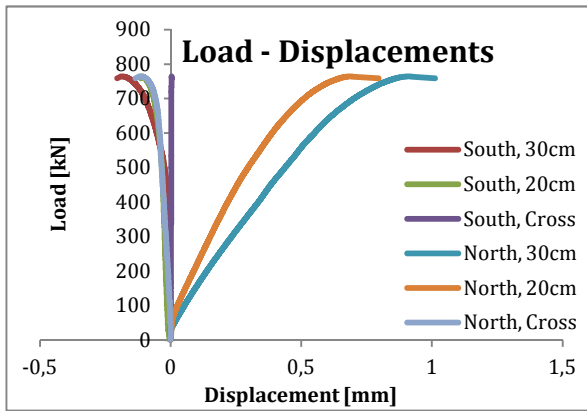


NDC 0,5% Eccentric Loading, Prism B3

NDC 0,5% Eccentric B3			
P_{peak} [kN]	f_{cp} [MPa]	P_{fail} [kN]	P_{change} [%]
699,85	-	667,09	-4,7

NDC 0,5% Eccentric B3			
LVDT id.	ϵ_{peak} [‰]	ϵ_{fail} [‰]	ϵ_{change} [%]
South 30	-0,4100	-0,4361	6,4
South 20	-0,4345	-0,4345	0
South Cross	-	-0,0531	-
North 30	2,9396	2,9176	0,1
North 20	3,1628	3,1783	0,5
North Cross	-0,7622	-0,7622	0

C.c.3. Appendix NDC with 0,5% steel fibre, Eccentric Loading, Prism B4

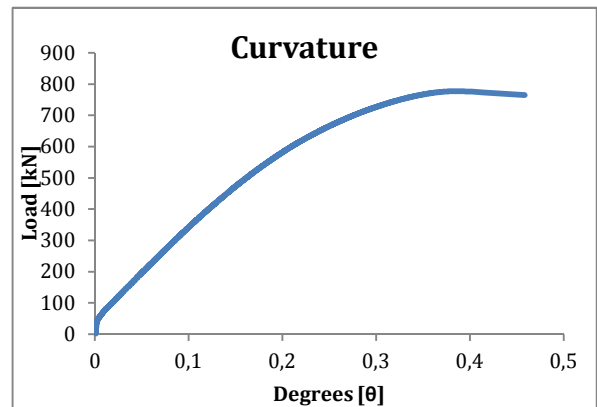
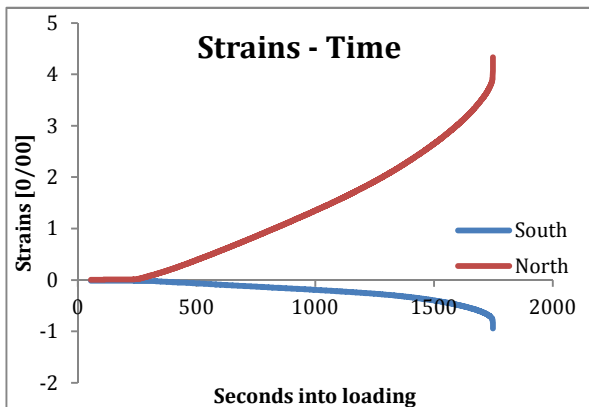
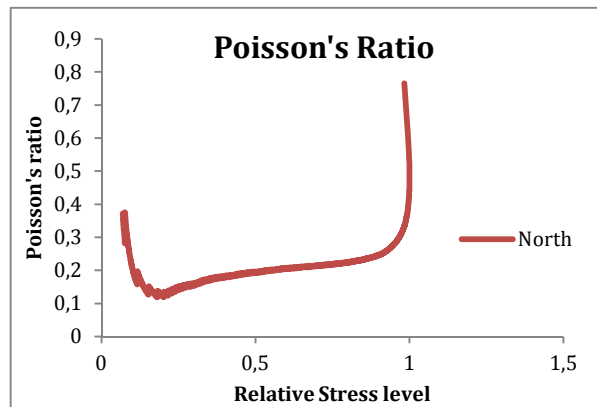
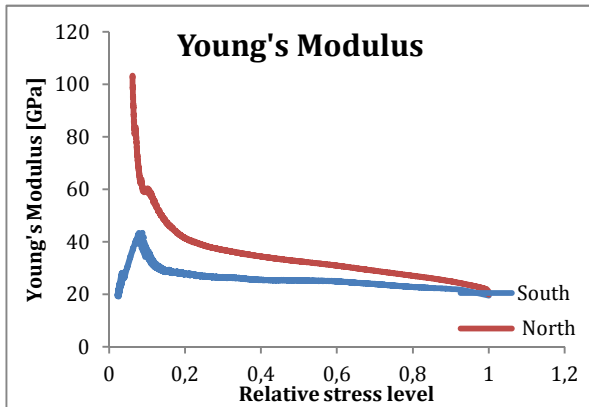
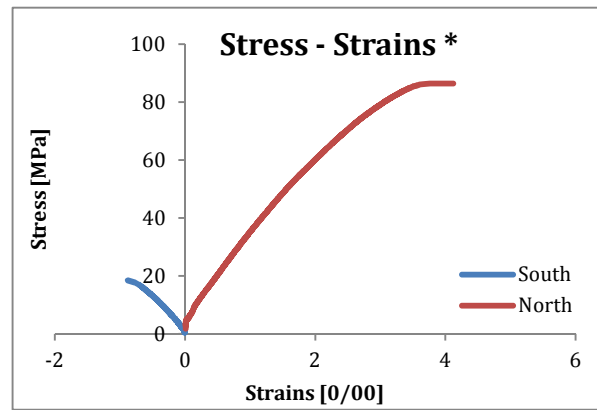
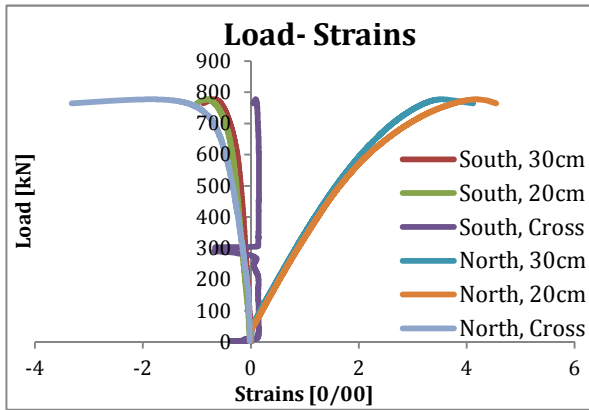
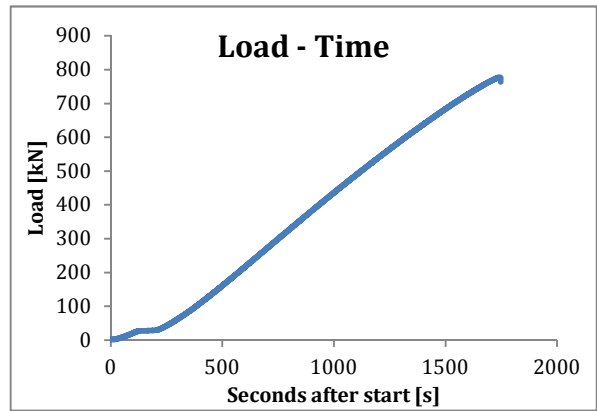
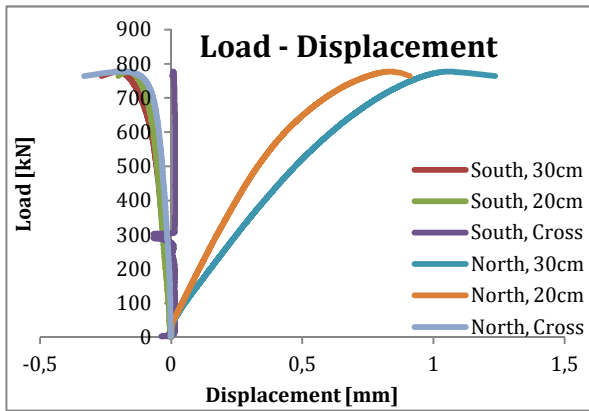


NDC 0,5% Eccentric Loading, Prism B4

NDC 0,5% Eccentric B4			
P_{peak} [kN]	f_{cp} [MPa]	P_{fail} [kN]	P_{change} [%]
764,13	-	759,2	-0,6

NDC 0,5% Eccentric B4			
LVDT id.	ϵ_{peak} [‰]	ϵ_{fail} [‰]	ϵ_{change} [%]
South 30	-0,6140	-0,6810	10,9
South 20	-0,5495	-0,5720	4,1
South Cross	0,0399	0,0532	33,3
North 30	3,0253	3,3733	11,5
North 20	3,4240	3,9795	16,2
North Cross	-1,1470	-1,3520	17,9

C.c.4. Appendix NDC with 1,0% steel fibre, Eccentric Loading, Prism B3

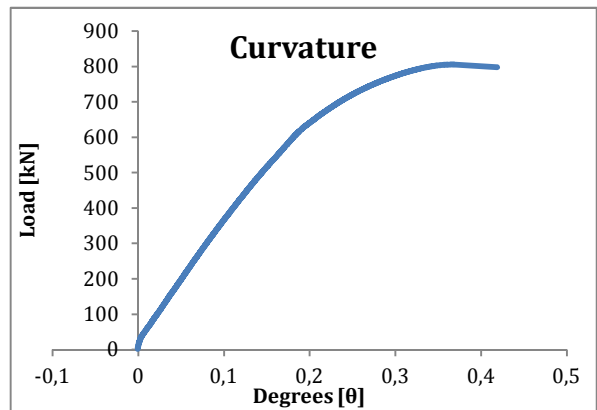
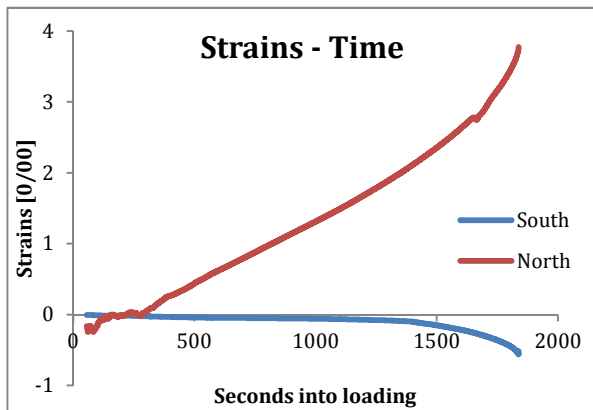
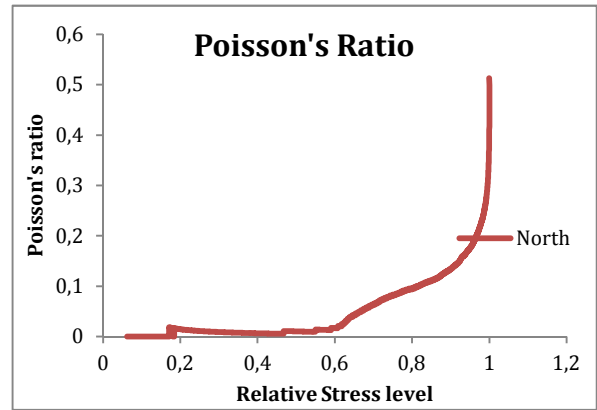
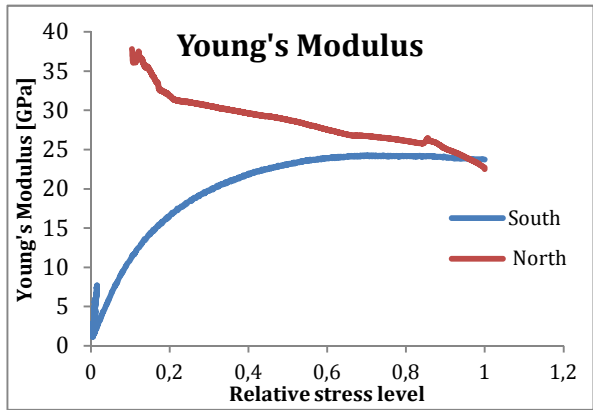
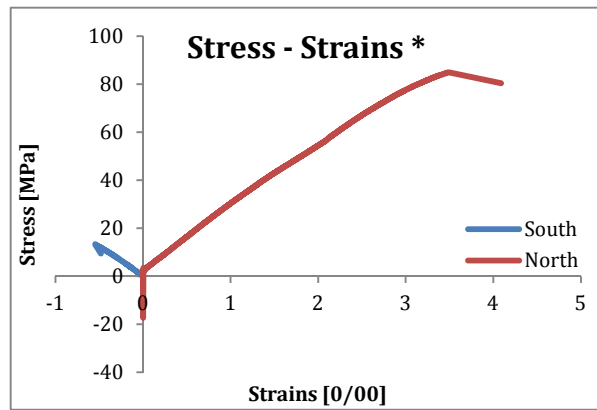
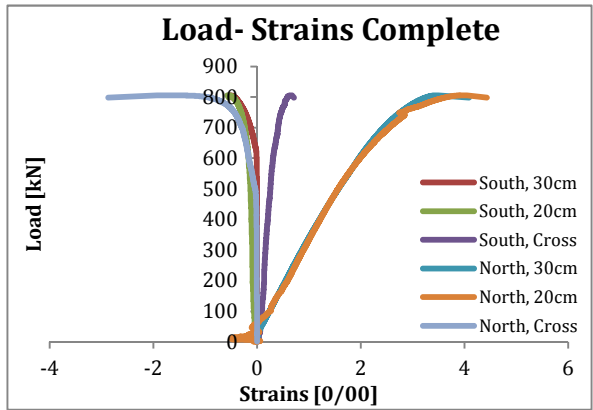
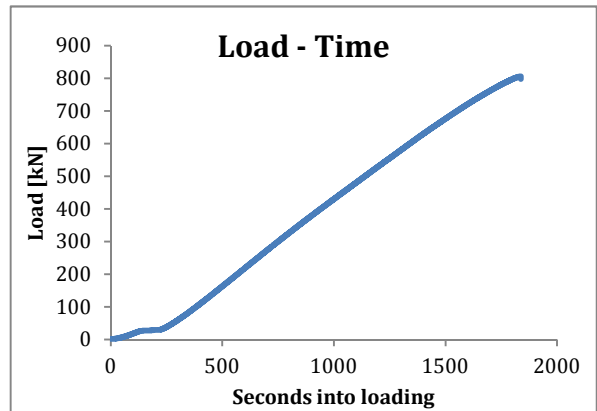
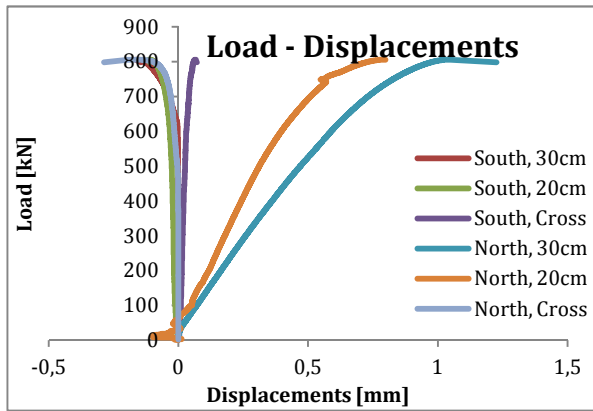


NDC 1,0% Eccentric Loading, Prism B3

NDC 1,0% Eccentric B3			
P_{peak} [kN]	f_{cp} [MPa]	P_{fail} [kN]	P_{change} [%]
777,34	-	764,45	-1,6

NDC 1,0% Eccentric B3			
LVDT id.	ϵ_{peak} [‰]	ϵ_{fail} [‰]	ϵ_{change} [%]
South 30	-0,6747	-0,8807	30,5
South 20	-0,8020	1,0065	25,5
South Cross	0,0864	0,0465	-46,8
North 30	3,5167	4,1200	17,2
North 20	4,1645	4,5475	9,2
North Cross	-1,806	-3,3180	83,7

C.c.5. Appendix NDC with 1,0% steel fibre, Eccentric Loading, Prism B4



NDC 1,0% Eccentric Loading, Prism B4

NDC 1,0% Eccentric B4			
P_{peak} [kN]	f_{cp} [MPa]	P_{fail} [kN]	P_{change} [%]
805,81	-	798,17	-1,0

NDC 1,0% Eccentric B4			
LVDT id.	ϵ_{peak} [‰]	ϵ_{fail} [‰]	ϵ_{change} [%]
South 30	-0,5270	-0,4817	-8,6
South 20	-0,5570	-0,5535	0,6
South Cross	0,6509	0,7107	9,2
North 30	3,4533	4,0867	18,3
North 20	3,9445	4,4295	12,3
North Cross	-1,6460	-2,8700	74,4

Summary of averaged strains for NDC prisms in eccentric compression

NDC - eccentric						
Fibre [%]	Prism identity	Side of prism	Direction	ϵ_{peak} [‰]	ϵ_{fail} [‰]	Change [%]
0,0	B3	North	Long.	3,079	3,079	-
			Cross	-0,661	-0,661	-
		South	Long.	-0,323	-0,323	-
			Cross	0,020	0,020	-
	B4 ¹	North	Long.	-	-	-
			Cross	-	-	-
		South	Long.	-	-	-
			Cross	-	-	-
0,5	B3 ³	North	Long.	3,051 ²	3,048	-0,1
			Cross	-0,762	-0,762	-
		South	Long.	-0,42	-0,435	3,6
			Cross	0,053	0,053	-
	B4	North	Long.	3,225	3,676	14,0
			Cross	-1,147	-1,352	17,9
		South	Long.	-0,582	-0,627	7,7
			Cross	0,039	0,053	35,9
1,0	B3	North	Long.	3,847	4,334	12,7
			Cross	-1,866	-3,318	77,8
		South	Long.	-0,738	-0,944	27,9
			Cross	0,087	0,047	-46,0
	B4	North	Long.	3,699	4,258	15,1
			Cross	-1,646	-2,870	74,4
		South	Long.	-0,532	-0,518	-2,6
			Cross	0,651	0,711	9,2

¹ No test was performed

² All longitudinal presented strains have been averaged on the recorded data from both the 20- and 30cm LVDTs at the same face, as long as the recordings seemed to be good.

³ The test showed elastic failure behaviour. See figure in Annex.

